Life Cycle Assessment (LCA) And Energy Modeling of a Solar Hybrid PV/T System

Ali Husain

Bachelor of Engineering

Mechanical Engineering

Department of Engineering

Macquarie University

Date 6/11/2017

Supervisor: Dr Nazmul Huda

ACKNOWLEDGMENTS

I would like to express my greatest gratitude and my thanks to the academic supervisor Dr. Nazmul Huda for his guidance, support and understanding throughout the thesis report process.

I would like to thank you for putting up with all my questions during the whole semester.

STATEMENT OF CANDIDATE

I, Ali Husain, declare that this report, submitted as part of the requirement for the award of Bachelor of Engineering in the Department of Mechanical Engineering, Macquarie University, is entirely my own work unless otherwise referenced or acknowledged. This document has not been submitted for qualification or assessment any academic institution.

Student's Name: Ali Husain

Student's Signature:

Date: 6/11/2017

ABSTRACT

The solar photovoltaic/thermal hybrid system is considered one of the most significant solar energy systems in terms of the production and efficiency. The feature of this system is the production of electricity and heat simultaneously. This projects aims to perform a life cycle assessment for solar photovoltaic/thermal hybrid system. Through this study it is possible to obtain the results of the environmental impacts of this system. The second aim of this thesis is to simulate the hybrid PV/T system for Australia and other places in order to calculate the annual energy output of the system such as, thermal energy, and electrical energy likewise, to calculate the daily hot water and electricity consumption of the PV/T system and the overall efficiency of the system. Moreover, This project also aims to investigate the performance for two types of solar hybrids PV/T collectors, water-based PV/T collector, and air-based PV/T collector.

Table of Contents

List of Figures

List of Tables

Chapter 1: Introduction

1.1 Energy Demand and Solar PV/T Hybrid System

The energy demand is increasing dramatically worldwide during recent years. According to (UN[1]), the world population is increasing gradually and it has reached approximately 7.3 billions in 2017 and it will be more than 10 billions in 2050. Before 200 years age the world population was less than 1 billion however, in only 100 years the population increased from 1.5 to 6 billions. Likewise, the world history can be divided into two main periods based on the population growth. The first period is the pre-modernity, and it was very slow growth of population, the second period is the modernity, the growth rate was faster than the first period due to the rising standards of living and better health care [1]. In addition, the demand for the natural resources is increasing with the increasing of the population size and this became a crisis and this crisis will develop negatively as the population increases. Moreover, the energy consumption is also rising gradually in many countries around the world. The world's biggest energy consumers are China and United States of America with 3,101 MTOE[2] and 2,196 MTOE respectively however the lowest countries that consume energy are African countries and some countries in Southeast Asia. In addition, according to the U.S (EIA[3]), the consumption of overall world of the marketed energy increased from 549 quadrillion to 629 quadrillion BTU[4] between 2012 and 2020 likewise, it is expected to rise to 815 quadrillion BTU in 2040. 1 million BTU is equivalent to 8 gallons of gasoline [2].

---

[1] United Nations
[2] Million Tones of Oil Equivalent
[3] Energy Information Administration
[4] British Thermal Units

Figure 1 shows the annual energy consumption per person by using millions of British Thermal units. According to the map in figure 1, Australia, Saudi Arabia, Canada, and United States of America consume between 250 to 400 millions BTU yearly per person. Kuwait, United Arab Emirates and Iceland Consume more than 400 millions BTU yearly per person. However, the Europe Union countries consume around 75 to 400 millions BTU yearly per person and South America's countries consume approximately 25 to 149 millions BTU yearly per person. Some countries consumes less than 10 millions BTU yearly per person yearly such as Haiti, Madagascar, Yemen, India and Nepal. Russia, japan, and New Zealand consume between 150 to 249 millions BTU yearly per person [2, 3].
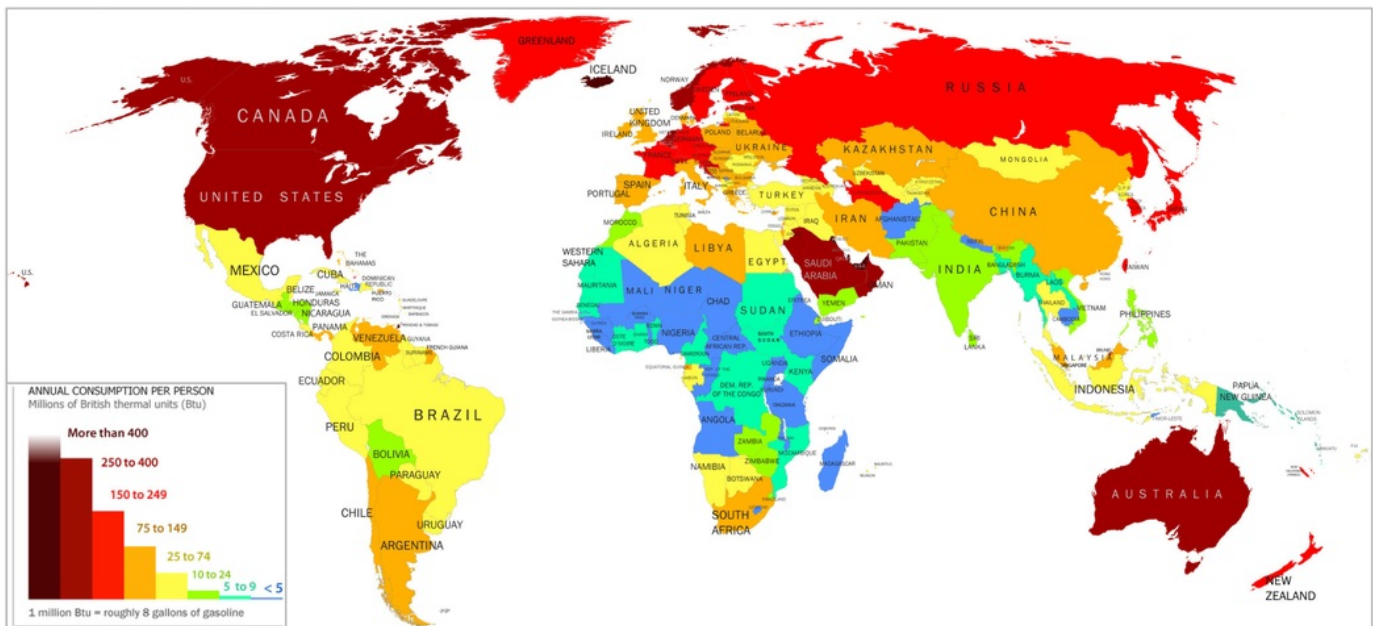
Figure 1: Annual World Energy Consumption Per Person (BTU) [3]

Therefore, one of the best resources to decrease the energy consumption is to use the renewable energy resources, as it is very clean energy compared that with other natural

resources. The renewable energy is considered the energy that can be generated from various natural resources for instance, wind, sunlight, and the geothermal heat. Likewise, many technologies can be discovered from using the sunlight resource such as, the solar photovoltaic PV technology, solar thermal collectors, and the solar hybrid PV/T[5] technology [4, 5]. Figure 39 in appendix A shows these technologies with details. Moreover, to take the advantages of the solar energy, using the solar hybrid PV/T system is considered one of the best systems that can convert the solar energy into electrical energy and also to thermal energy so it can provide the heat and hot water. This technology was used in many countries recently, as the panel of the solar PV/T must be installed in the roof of the building and one system will generate electricity and another system will generate heat, consequently, the solar PV/T system combines two technologies into one panel [4]. Moreover, it is clear that the solar PV system can generate electricity only while the PV/T can produce electricity and heat as shown the figure below.
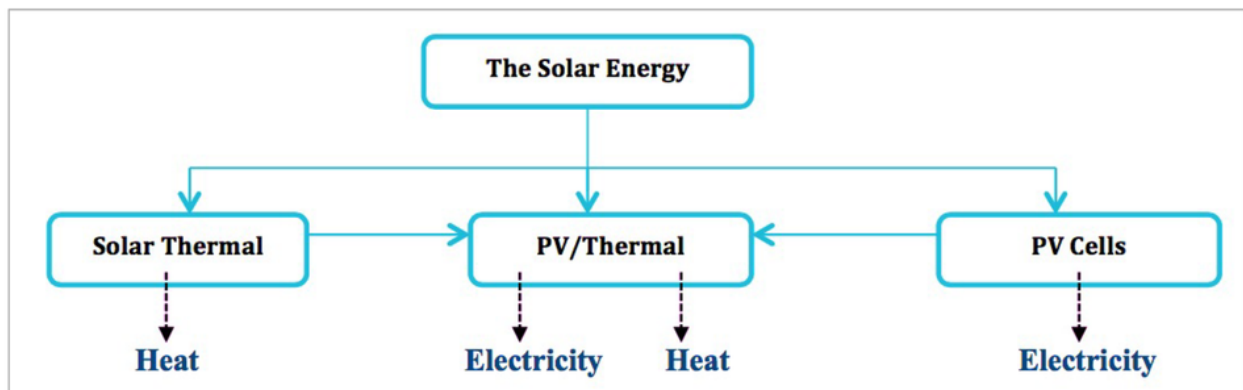
Figure 2: The Technologies of Solar Conversion

The PV/T hybrid system contains two main systems, the photovoltaic system, and the hybrid solar thermal collector system. Each of these two systems is consist of several

---

[5] Photovoltaic/Thermal

3

components such as, the photovoltaic system in consist of solar panel, solar photovoltaic cells and electrical cables while the thermal collector system has water pump, water tank, tubular heat exchanger and piping system. In addition, a small scale PV/T system was designed by Nike Leon at Macquarie University in 2015. This system is a 0.2 kWp[6] solar panel attached with heat copper pipes. Niko's aim from designing this system is to decrease the temperature of the solar panels because the ambient temperature in Australia is very high in summer. His system was consists of 2 main parts, the solar panels and the hot water system [6].

1.2   Project Goal

The Purpose of the project is to study and perform a life cycle assessment (LCA) for solar hybrid PV/T system. The LCA is one of the best management tools to evaluate the environmental performance and impacts in the system. The life cycle of the solar PV/T hybrid system will be divided into 7 phases from the raw material acquisition phase to the end of life phase. The LCA of solar hybrid PV/T system can be implemented by using GABI Software. Additionally, through the investigation of the LCA the environmental impacts will be identified for various materials, substances, and products of the solar hybrid PV/T system. Likewise, the environmental impacts of different materials can be compared to each other in order to compare the amount of green house gases (GHG) carbon emissions that generated from each raw material of each component of the solar hybrid PV/T system [7].

 In addition, the other aims of this project are to investigate the energy modeling of the solar hybrid PV/T system. For instance, the mathematical analysis of the flat plate PV/T collector will be discussed and examined. Also, TRNSYS software results will be used to investigate the energy modeling of the solar hybrid PV/T system. Moreover, this project also investigated the performance and design of solar PV/T collectors such as the air PV/T collectors and water PV/T collectors.

---

[6] Kilo Watt Peak

1.3 Project Planning

1.3.1 Project Scope

Activity Statement:

A. Investigation of life cycle assessment of solar hybrid PV/T system

    I.   Life Cycle Plan Model of Solar PV/T Hybrid System
    II.   Systems Inventory and Data Analysis
    III.   Life Cycle Framework Phases
    IV.   Environmental Impact Assessment
    V.   Results, data and calculations from Gabi Software
    VI.   Life Cycle Plan Model of Solar PV System
    VII.   Comparison Between PV and PV/T Systems

B. Energy modeling and experimental modeling of hybrid PV/T System

    I.   Development of Solar Hybrid PV/T System
    II.   Mathematical Analysis of Thermal and Electrical Energy
    III.   Energy Modeling and TRNSYS Tool

C. Performance and design of Solar PV/T Collectors

    I.   Performance and design of water PV/T collector
    II.   Performance and design of air PV/T collector
    III.   Comparison between water PV/T collector and air PV/T collector

1.3.2 Project Cost

This project was allocated budget of $400 however, because of the nature of this project, the original budget is zero dollars leaving a $400 surplus. Therefore, this project basically has no financial fee.

1.3.3 Project Timeline

Project Activity	Commencement (Week)	Duration (Week)	Weeks 1	2	3	4	5	6	7	B1	B2	8	9	10	11	12	13	14	15
Edit and Write Thesis Document	Week 1	14 Weeks	▓	▓	▓	▓	▓	▓	▓	▓	▓	▓	▓	▓	▓	▓			
Background Research	Week 1	1 Week	▓																
Literature Review	Week 1	1 Week	▓																
Life Cycle Assessment for Solar PV/T System	Week 2	8 Weeks		▓	▓	▓	▓	▓	▓	▓									
System Inventory and Data Analysis	Week 2	3 Weeks		▓	▓	▓													
Results and Data From GABI Software	Week 5	2 Weeks					▓	▓											
Environmental Impact Assessment	Week 5	3 Weeks					▓	▓	▓										
Life Cycle Assessment for PV System	First Week of Mid Semester Break	1 Week								▓									
Comparison Between PV/T and PV Systems	Second Week of Mid Semester Break	1 Week									▓								
Energy Modeling Investigation	Week 8	3 Weeks										▓	▓	▓					
Development of Solar Hybrid PV/T System	Week 8	1 Week										▓							
Mathematical Analysis of Thermal and Electrical Energy	Week 8	1 Week										▓							
Energy Modeling and TRNSYS Tool	Week 9	2 Weeks												▓	▓				
Performance and Design of PV/T Collectors	Week 11	1 Week														▓			
Finalise Thesis Document	Week 12	1 Week															▓		
Meeting with Supervisor	Week 2	11 Weeks		▓	▓	▓	▓	▓	▓	▓	▓	▓							
Poster, Abstract and Presentation	Week 13	3 Weeks															▓	▓	▓

Figure 3: Gantt Chart of Project

Figure 3 shows the Gantt chart of the project, as the project started in week 1, 31/7/2017 and finished in week 15, 21/11/2017. As with any thesis project, there have been changes in this project. In particular, according to the initial project plan, the

exergy analysis of the solar hybrid PV/T system was supposed to be studied and investigated in this project. However, it was canceled because after studying and verifying the details of the analysis accurately, it turned out that the exergy analysis is not directly related to the main topics of the project, the life cycle assessment or the energy modeling. Likewise, it was just an additional topic for the project. Despite this change, the thesis project was completed and finished on time. Additionally, table 46 in appendix B shows the project schedule in details.

Chapter 2: Background and Related Work

2.1 Global Electric Capacity of Solar Power Systems

Many countries in the world have used the solar power capacity as an alternative energy source. The photovoltaic technology growth is increasing gradually in the world since the 19th century. The photovoltaic capacity reached approximately 300 Giga watts (GW) between 2016 and 2017 and expected to increase more then 370 GW between2017 to 2018. The solar power technology supplies 1.8% of the total electricity consumption of the world [8]. According to the International Energy Agency (IEA), 303 Giga watt of the photovoltaic (PV) capacity has been installed worldwide in December 2016. In 2016 and 2017, China became the world's first photovoltaic market following by Japan and Germany while; Australia is the world's ninth photovoltaic market [9]. The figure below displays the results of the top 15 nations in the world for annual installed photovoltaic capacity in 2016.
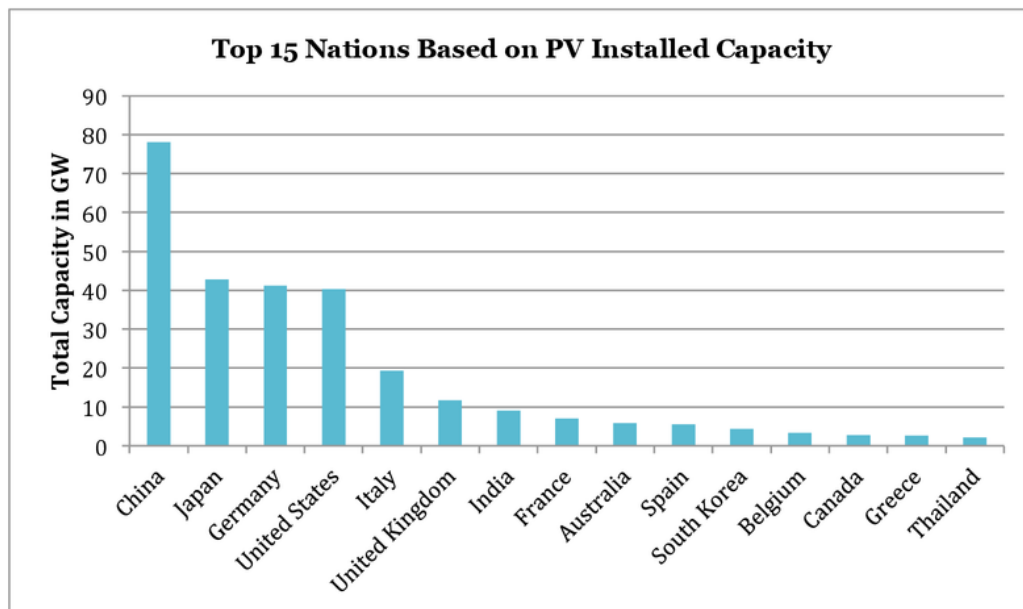
Figure 4: Top 15 Nations for Annual Installed PV Capacity in 2016.

Australia installed 5.9 GW of the photovoltaic capacity in 2016, which accounts for approximately 2% of the total world's installed photovoltaic capacity while China installed 78.1 GW and 26% of the total world's installed PV capacity. Japan, Germany, and United States installed 42.8 GW, 41.2 GW, and 40.3 GW respectively and these 3 countries account for 14.1%, 13.6%, and 13.3% of the total world. In addition, the 15 top countries mentioned in the chart above contribute 91.3% of the total world's installed PV capacity while the rest of the world contribute 8.7% only of the total world installed PV capacity in 2016.

2.2 PV and PV/T Systems

The solar PV systems consist of solar PV cells that convert the sunlight into electricity. These cells contain 2 layers of semi conducting materials such as, monocrystalline silicon or crystalline silicon. When the PV cells are exposed to the sunlight it will generate an electric field around the 2 layers, and then the electricity will be able to flow [10]. Moreover, there are many classifications of the solar panels such as, the monocrystalline cells, polycrystalline cells, and the thin film cells. The thin film cells provide the lowest coefficient of temperature comparing that with other solar cells. Also, manufacturing the PV system with the thin film solar cells requires a large surface area of solar panel in order to collect enough amount of electricity. While manufacturing the PV system with monocrystalline solar cells can harvest the same amount of electricity with small or medium solar panel.

Furthermore, the PV system in general is consists of solar panel system only which contains solar PV cells, solar panel, and electrical cables. While the PV/T hybrid system is consists of solar panel system and hot water system [4]. The hot water system is consists of 4 main components, the hot water tank, water pump, tubular heat exchanger and piping system. The aim of the piping system is to connect the water pump, how water tank and the tubular heat exchanger. There are some researches and studies conducted on life cycle assessment of the solar PV/T hybrid system by T.T

Chow [4], Clara Good [11] and Y. Tripanagnostopoulos et al. [12]. Also, some articles investigated the energy modeling of the solar PV/T hybrid system by Dilsal Engin et al. [13], Chao-Yang Huang et al. [14] and S. Baljit et al. [15].

In addition, some other studies conducted on the design, modeling and thermal performance of the solar PV/T collectors by Mohd Nazari Abu Bakar et al. [16] Jin Hee Kim et al. [17], F. Sarhaddi et al. [18] and Busiso Mtunzi et al. [19].

2.3 Solar PV/T Hybrid System

The solar PV/T hybrid system is a combination of 2 systems together, the PV system, and the thermal system. This system can generate electrical energy and heat simultaneously from one integrated component. Generally, the photovoltaic system can convert approximately 20% of the sunlight or sun radiation into electrical energy and the rest will be turned to heat. However the amount of electrical energy that generated from the PV/T system is higher than the amount of heat produced [20].

2.3.1 Types of Solar PV/T Hybrid Systems

- **Solar PV/T Liquid Collectors:** These types of collectors consist of PV module and piping system and channel to direct the water flow or other types of liquids. This piping system must be attached to the PV unit. The working fluid in this collector absorbs the heat that produced from the photovoltaic cells in the PV module. Assuming that the temperature of the working fluid is lower than the temperature of the PV cells, this type is called the heat pipe based PV/T system [12]. In this collector, the nanoparticles can be isolated in the fluid in order to create an appropriate fluid filter for the photovoltaic/thermal applications [21]. In addition, there are many companies manufactured the solar PV/T liquid collectors such as, PVTWINS company and Millenium Electric company. The PVTWINS Company

developed the autonomous PV/T water treatment units as well as they developed the PV/T swimming pool collectors. While Millenium Electric company developed the air collector by adding the function of hot water as well as the air reheating [20].

Figure 5: The Multi Solar Panel of Millenium Electric Company.

- **Solar PV/T Air Collectors:** This collector is called the air-cooled type. Which contains a hollow conductive metal. When air accesses the collector, it will cool the panel. There are many types of air based PV/T collectors. For instance, the singular pass and double pass PV/T. Moreover, many companies developed and, manufactured the air PV/T collectors such as, the Solar-Venti Company designed air-cooled PV/T collector in 2001. These collectors can be used in houses, garages, and storerooms [20].

- **Solar PV/T Concentrators:** In this type, the amount of PV cells can be decreased in order to use the multi junction PV cells. The multi junction PV cells can be used to produce more electricity comparing that the normal PV cells. Ina addition the Solar PV/T Concentrators has low performance due to the dispersion of the reflected radiation also, this collector absorb only particular components of the sun spectrum. Consequently, the MJ[7] cells will intersect with each other, so the performance of these cells will decrease [22]. In addition, there are 3 types of concentrator, the low, medium, and high concentrators [23].
  1. Low concentration PV systems

---

[7] Multi Junction Cells

- Flat Plate
- Compound parabolic collector (CPC)

2. Medium concentration PV systems
   - Linear parabolic reflector
   - Fresnel reflector

3. High concentration PV systems
   - Three-dimensional Fresnel lens

Furthermore, figure 6 shows the all the types of the solar hybrid PV/T system. Also, figure 100 in appendix A displays more details regarding the solar systems.
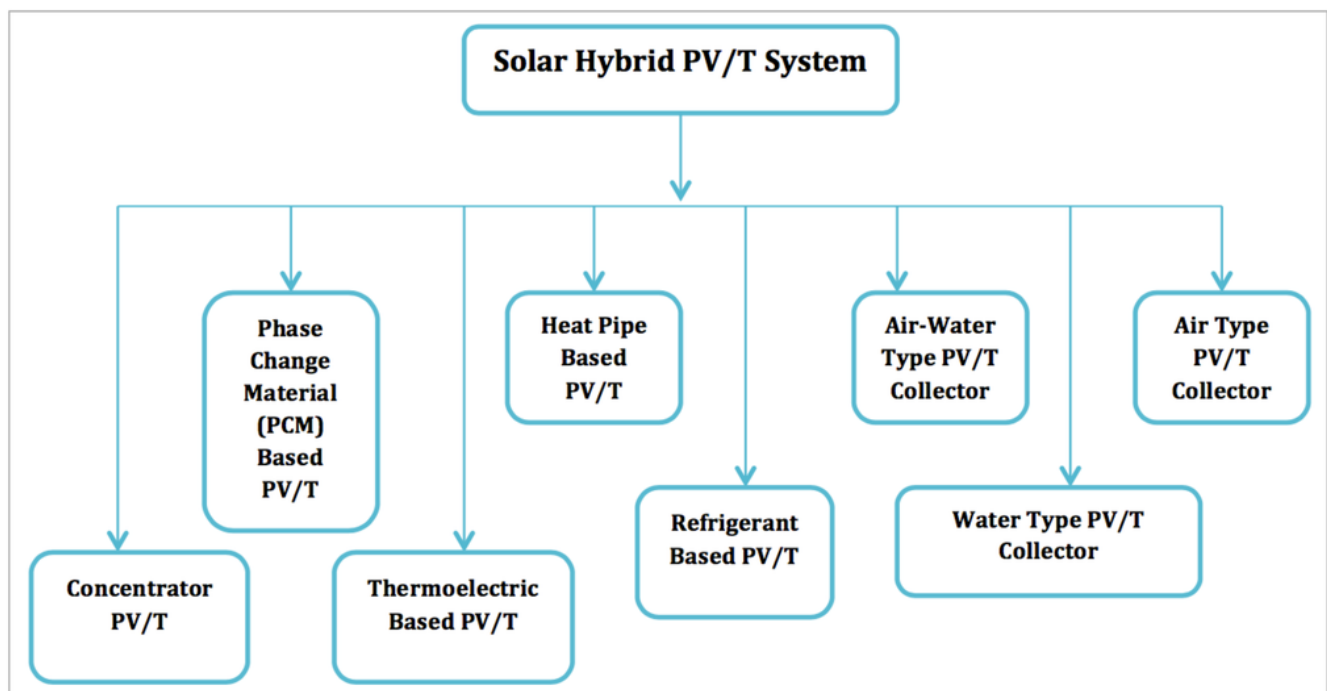
Figure 6: Classification of Solar PV/T Hybrid System [24]

2.3.2 Solar PV/T Hybrid System Components

The solar PV/T Hybrid system has two main subsystems; the solar panel system and the hot water system. Each of these subsystems contains several components and raw materials [25, 26].

The solar panel subsystem (PV system) has 3 main components:
- Solar panel (includes metal frame, fibre glass, insulation layer and black sheet).
- Solar photovoltaic (PV) cells
- Electrical cables

While the hot water subsystem (Thermal system) has 4 main components:
- Hot water pump
- Hot water tank
- Piping system
- Tubular heat exchanger

2.3.3 Characteristics of Solar PV/T Hybrid System Components

1- Solar PV Cells: When the sunlight reaches the solar PV cells and the electrical conductors are attached properly to the negative and positive sides, then it will from the required electrical current and the sunlight energy will be converted to electricity.
Materials Used: Cadmium telluride, crystalline silicon, copper indium selenium, poly silicon, and monocrystalline silicon [26].

2- Solar Panel: To generate the electricity flow by using the solar cells.
Materials Used: Aluminum and crystalline.

3- Metal Frame: Must be attached to the edges of the solar panel.
Material Used: Aluminum and copper.

4- Insulation layer: This layer is the bottom layer of the PV/T collector.
Material Used: Polyurethane (PUR) [27].

5- Glass: This glass must be placed on the top surface of the PT/T collector and it can be used to provide additional thermal insulation for the solar collector.
Materials Used: Glass Fibres.

6- Black Sheet (PVF): To protect the internal components of the PV/T collector.
Material Used: Polyvinyl Fluoride (PVF[8]) and crystalline.

7- Electrical Cables: To interconnect the solar panel with the Photovoltaic cells. These cables must be covered by insulation such as Polyurethane Insulation. Also, these cables must be weather resistant.
Materials Used: Polyurethane, copper wire and polyethylene.

8- Hot Water Pump: 12 Volt DC pump to move the water throughout the tubular heat exchanger, piping system, and form/ to the hot water tank. 2 water pump are required for the solar PV/T system. The water pump is consists of bearing, hub, fittings, seal impeller, back plate, bolts, housing, gasket, brass inlet and outlet Ryton (PPS[9]) impeller [6].
Materials Used: Steel for the hub, bearing, fittings, bolts, and back plate. Aluminum for housing, gasket, and seal, likewise, cast iron for impeller, Brass for the brass inlet and outlet and Ryton (PPS) impeller.

9- Tubular Heat Exchanger Unit: This unit consists of one copper header, six copper pipes, and bronzes connectors for both of the header sides. Likewise, it contains stainless steel and brass joints. Also, it consists of 4 to 6 titanium strips to support the solar panel as well as the 6 pipes [28]. The purpose of the heat exchanger is to transfer heat between two or more liquids particularly the liquid that circulates throughout the

---

[8] Formula: $(CH_2CHF)_n$
[9] Polyphenylene Sulphide

solar PV/T collector and also to extract the heat from the surface of the PV panel. The heat exchanger is also known as the heat extraction device [29].

Materials Used: Bronzes, copper, titanium, brass, and stainless steel.

10- Piping System: The purpose of the piping system is to connect the hot water pump with the hot water tank and the heat exchanger. This system consists of copper water connectors and polyethylene insulation layer [25].

Materials Used: Copper and polyethylene.

11- Hot Water Tank: Hot water storage unit to restore approximately 50 liter of hot water. The dimension of this tank is 0.7 m × 0.4 m diameter and the thickness of the cylinder is 0.005 m so the volume is 0.0879 m^3. Moreover, Niko Leon used the Dux Proflo 50 liter storage water heater, as the water tank for his solar thermal system and the dimensions was approximately the same. [6].

Material Used: Mild Steel cylinder and vitreous enamel.

Component	Dimension (Length × Height)	Thickness (mm)	Weight (kg)	Number of Pieces Required
Glass Fibre	1 m × 0.5 m	4.5 mm	(1 m×0.5 m×4.5 mm 2.5)= 5.625 kg	1
Metal Frame [Aluminum (1 kg) and Copper (0.5 kg)]			1 kg+0.5 kg= 1.5 kg Total (1.5×4=6kg)	4
Insulation layer (Polyurethane)	1 m × 0.5 m	30 mm (Each 50 mm thickness of the polyurethane weights 7.807 kg for 1m × 0.5 m)	4.684 kg	1
Black sheet	1 m × 0.5 m		3 pounds or 1.36 kg	1
Solar Panel System (1000W)	1 m × 0.5 m			1

Table 1: Specifications of Components of Solar Panel of PV/T Hybrid system [25-27]

2.4 Literature Review

Abu Bakar et al. [16] has shown the several improvements in the design of the PV/T solar collector. This solar collector can combine PV panel with the serpentine shaped copper (Cu) tube. The bi-fluid can be used to create better range of thermal applications. As that it can offer some selections in which the cold and hot water can be used based on the energy requirements. In addition, predicting the bi-fluid solar collector performance for the mass flow rates range of the liquid and the air can be done by using the design model of bi-fluid solar PV/T collector and the equations of 2-dimensional steady-state of the energy balance. Furthermore, Moradi et al. [30] reviewed the control parameters impacts on the performance of the PV/T collectors. Likewise optimizing the control parameters can develop and improve the PV/T performance. Therefore, these articles can be used to investigate the design and performance of the solar PV/T solar collectors in the project.

Ban Weiss et al. [31] shows how the installation of photovoltaic PV units on the roofs can decrease the need for the air conditioning and the heating of atmosphere. These units can convert the sunlight to the electricity needed. Furthermore, Carnevale et al. [32] has shown the life cycle assessment of the solar energy systems in general. The authors compared 2 types of solar energy systems, the photovoltaic system, and the water thermal heater system.

According to T.T Chow [4] many researches and studies have been done since 1970 in order to develop and improve the technology of the photovoltaic/thermal PV/T systems specifically, the development of the flat-plat PV/T collectors, the air type PV/T collector, and water type PV/T collector. This article can be used to compare the air type and water type solar PV/T collectors in terms of their energy performance analysis. Additionally, there are other researches been conducted on the efficiency and performance of the solar PV/T systems by both T.T Chow [4] and Dubey et al. [33].

Engin et al. [13] presented a prototype development and mathematical model in order to examine electrical and thermal efficiency of the hybrid PV/T system. The electrical efficiency can be improved by reducing the temperature of the PV module's cell with cooling. Additionally, the solar PV/T system was modeled and manufactured by using the thermal collector and this collector must be placed underneath the PV panel. Likewise, the input of the thermal collector is the extra solar radiation through the clear PV unit.

Hassani et al. [34], Sobhnamayan et al. [35] presented the exergy analysis for the solar PV/T systems. Firstly, Hassani et al. [34] presented the exergy analysis for 3 types of nano-fluids based solar hybrid PV/T system configurations. Likewise, they compared the performance of these configurations to a PV and PV/T systems however, this project will focus only of PV/T solar hybrid system. Moreover, Sobhnamayan et al. [35] investigated the exergy rate (η_{ex}) of the inlet and outlet water flow in the water collector likewise, the heat exergy rate can be analyzed by using Petela theorem and the irreversibility rate ($\dot{I}$) by the sum of losses of exergy rate $\sum \dot{Ex}_{loss}$ and sum of destruction of exergy rate $\sum \dot{Ex}_{des}$ for only liquid type solar PV/T collector. This article is typically related to the liquid type solar PV/T collector only, however, the project will focus on the exergy analysis for all types of solar PV/T collectors (liquid type, air type, liquid and air type). Therefore, this article will be useful for the liquid type solar PV/T collector.

Herrando et al. [36] Investigated and examined the suitability of the solar PV/T system in providing sufficient electricity as well as hot water for some domestic suburbs in London, United Kingdom. Additionally, a mathematical model was developed in order to simulate the PV/T solar system.

Othman et al. [37], Rawat et al. [38] presented some experimental investigations regarding the solar PV/T water collector system. Generally, the purpose of designing the PV/T solar system is to decrease temperature of the PV units as well as to keep the electrical efficiency at satisfactory level. The PV/T water collector system was

developed and designed at the MANIT[10] Bhopal in order to test its efficiency and performance. As a result, this article can be used to investigate the water collector performance and then this can be compared with the other types of solar collector such as air type collector and liquid-air type collector.

Tripanagnostopoulos et al. [12] presented financial aspects of the solar hybrid system and the cost payback time was estimated to that system. Likewise, these articles investigated the life cycle assessment of the solar PV/T system in order to implement the energy and environmental assessment.

Zhang et al. [39] article is regarding the research and development of the solar hybrid PV/T systems as well as the practical applications of this technology. This includes a theoretical analysis and experimental/modeling investigation of the solar PV/T system and also some economic analysis. The economic aspects of the solar PV/T systems will not be investigated in this project. In addition, the purposes of investigating the experimental/modeling study are to explore the actual performance of the solar PV/T system and its individual components. Other purpose is to compare the practical applications with the theoretical analysis of the solar PV/T systems and discover the relationship between them.

Zogou et al. [40] presented the performance evaluation of the heat pipe solar PV/T system also they focused on the essential part of the BI-photovoltaic/thermal system which is the liquid collector, that is important and must be discussed in this project. In addition, Yin et al. [41] have shown full design and performance of the building integrated roofing in order to collect the required solar energy through the PV/T solar system. Likewise, the performance analysis proved that the solar roofing system has plenty of advantages and it can harvest enormous solar energy comparing that with the traditional asphalt shingle roof.

---

[10] Maulana Azad National Institute of Technology

18

Chapter 3: Life Cycle Assessment (LCA)

3.1 Introduction

The Life Cycle Assessment (LCA) is considered the evaluation and collecting of all the inputs of outputs as well as the potential environmental impacts throughout a particular system lifespan. LCA also is a process regarding the full life cycle of a system. This cycle can be from stage 1 the raw material until the life end of the system (disposal). Moreover, the Life cycle assessment can be used to develop and plan environmental strategies as well as to develop a particular product. It can be used also in marketing and to compare different products and processing alternatives. Likewise, LCA follows the environmental laws and legislations [11, 42].

In this project the life cycle of solar hybrid PV/T system was investigated. Technically, this life cycle can be done by using software GABI[11] as it is one of the best methods to study and explore all the processes and stages of the life cycle of the solar hybrid PV/T system such as studying the raw materials phases from first stage, which is the extracting phase to the end life phase. Likewise, many results can be obtained GABI software for example the results of global warming potential, acidification potential, ozone layer depletion potential and results of primary energy demand. The LCC[12] results in GABI can be used in order to calculate the potential environmental impacts of the solar hybrid PV/T system. Many results can be compared to each other by using graphs and diagrams. These diagrams can be obtained from GABI software [11, 32].

Additionally, creating scenarios in GABI software is important for the processes of the system; also it is possible to consider different scenarios and then to compare them

---

[11] (Ganzheitliche Bilanz) In German means the holistic balance
[12] Life Cycle Cost

with each other. This can be for example to compare the transport processes such as the trucks and planes associated in the plan system.

3.2 Life Cycle Framework Phases

The LCA framework is consists of 4 phases:
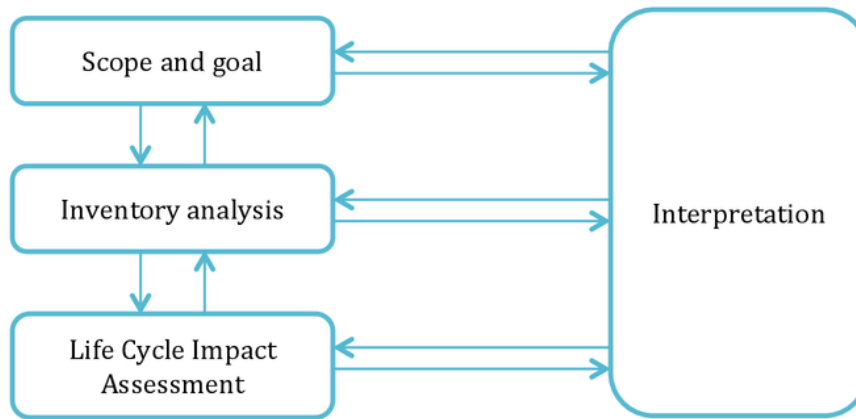
Figure 7: Life Cycle Assessment (LCA) Framework

I. **Goal and Scope Definition:** Contains all the general decisions required to perform and create the Life cycle assessment of the solar PV/T hybrid system. In this Phase the goal or purpose of the study can be defined as well as the defining the system boundaries, data quality and the impact categories [11, 42].

II. **Inventory Analysis (LCI[13]):** This phase is regarding the data collection, which includes all the collecting quantitative and qualitative data for every process in the solar hybrid PV/T system.

---

[13] Life Cycle Inventory.

III. **Life Cycle Impact Assessment (LCIA):** To identify and evaluate the quantity and amount of the potential environmental impacts of the system's products. There are four main steps to calculate the LCIA of the system, the classification, normalization, evaluation, and characterization. Additionally, the LCIA results such as, the global warming potential results, acidification potential of the solar PV/T system can be calculated by using many tools in Gabi Software categories [11, 42].

IV. **Interpretation:** To analysis the results from LCIA and determine the environmental hotspots in the solar hybrid PV/T system.

3.3 System Inventory and Data Analysis
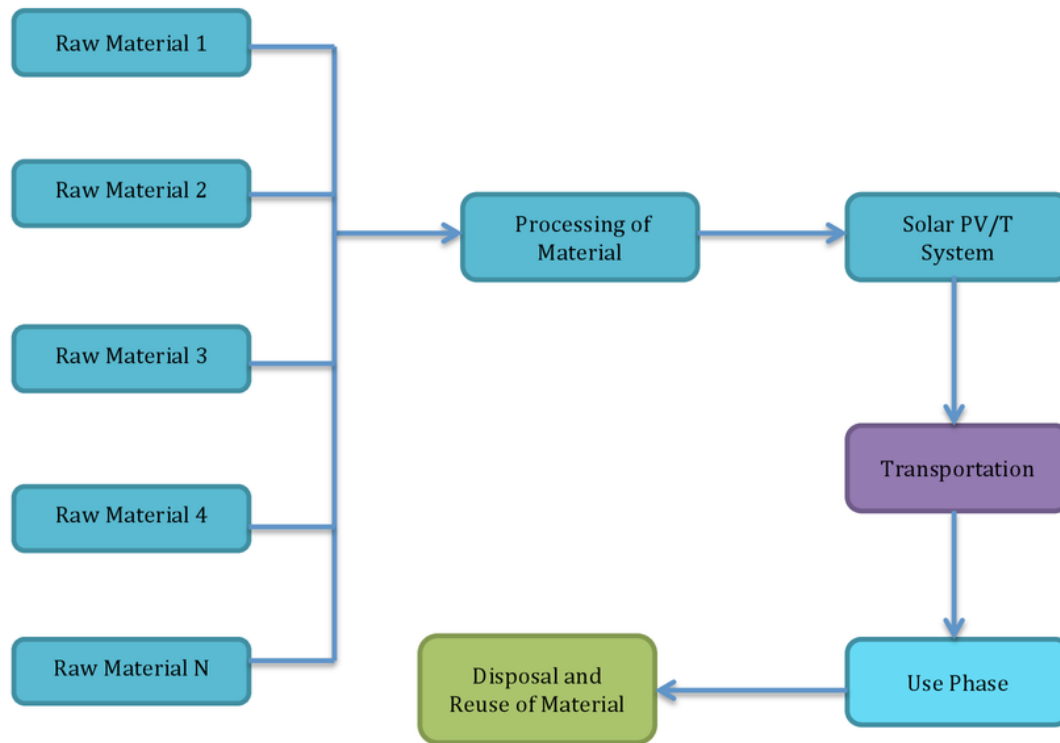
Figure 8: Holistic View of the Solar PV/T System

Section 3.3.1 to section 3.3.7 shows all the relevant data required to perform the life cycle analysis for the solar PV/T hybrid system. It displays the data for each phase starting from the raw material acquisition phase to the end of life phase of the solar PV/T hybrid system [20, 25, 42-46]. In addition, the materials required for each component in the solar PV/T system were specified in tables as shown below as well as the quantity required from each material [42-45].

3.3.1 Raw Material Acquisition Phase

Flow	Material	Amount / Unit	Objective	Nation
Input	Aluminum, Primary, at Plant	4 kg	Metal Frame	Europe
Input	Copper, Primary, at Refinery	2 kg	Metal Frame	Germany
Input	Polyvinyl Fluoride	1.36 kg or 3 pounds	Black Sheet	Australia
Input	Crystalline	0.05 mg	Black Sheet	Australia
Input	Polyurethane, Rigid Foam, at Plant	4.684 kg	Insulation Layer	Europe
Input	Glass Fiber, at Plant	5.625 kg	Glass Fibre Layer	Germany
Output	Materials for Production Phase	Total of 17.669 kg		

Table 2: Input and Output Flows of the Raw Material Acquisition Phase [42, 43, 45]

3.3.2 Material Processing Phase

Flow	Material	Amount / Unit	Nation
Input	Material for the Production Phase	17.669 kg	---
Input	Electricity mix (Production mix)	197,475 KJ	China
Output	Parts for Assembly	6 pieces	---

Table 3: Input and Output Flows of the Material Processing Phase [42]

3.3.3 Material Processing phase and Assembly Phase for the Main Components

Tables 4 and 5 summarized all the input and output flows of the raw material acquisition and processing of solar panel.

Flow	Material	Amount / Unit
Input	Aluminum Extrusion Profile	5 kg
Input	Crystalline	0.05 mg
Output	Solar Panel Parts	1 piece

Table 4: Input and Output Flows for Solar Panel Raw Materials [42, 47]

Flow	Material	Amount / Unit
Input	Solar Panel Parts	1 piece
Output	Solar Panel	1 Piece

Table 5: Input and Output Flows Associated with Solar Panel Production [42, 47]

Likewise, tables 6 and 7 summarized all the input and output flows of the raw material acquisition and processing of the piping system.

Flow	Material	Amount / Unit
Input	Copper, Primary, at Refinery	3.5 kg
Input	Polyethylene	190 mg
Output	Piping parts	4 pieces

Table 6: Input and Output Flows For Piping Raw Materials [42]

Flow	Material	Amount / Unit
Input	Piping parts	4 pieces
Output	Piping system	1 piece

Table 7: Input and Output Flows Associated with Piping System[42]

Tables 8 and 9 shows all the input and output flows of the raw material acquisition and processing of the Electrical Cables.

Flow	Material	Amount / Unit
Input	Polyurethane, Rigid Foam, at Plant	0.07 mg
Input	Copper wire (Cu; 0.6 mm)[metals]	78 g
Input	Polyethylene Low Density Granulate (PELD)	50 mg
Output	Electrical cables parts	20 pieces

Table 8: Input and Output Flows of Electrical Cables Raw Materials [42]

Flow	Material	Amount / Unit
Input	Electrical cables parts	20 pieces
Output	Electrical cables	20 pieces

Table 9: Input and Output Flows Associated with the Electrical Cables [42]

Tables 10 and 11 summarized all the input and output flows of the raw material acquisition and processing of the water pump.

Flow	Material	Amount / Unit
Input	Aluminum, primary, at plant	3.2 kg
Input	Cast Iron	2.4 kg
Input	Copper, Primary, at Refinery	1.25 kg
Input	Stainless Steel Hot Rolled Sheet	340 g
Input	Rubber, at plant	6.50 mg
Input	Brass	150 g
Input	Polyphenylene Sulphide	320 g
Input	Polyethylene Low Density Granulate (PELD)	70 mg
Output	Water Pump Parts	2 Pieces

Table 10: Input and Output Flows for Water Pump Raw Materials [42]

Flow	Material	Amount / Unit
Input	Water Pump Parts	2 Pieces
Output	Water Pump Systems	2 Pieces

Table 11: Input and Output Flows Associated with Water Pump Production [42]

25

Tables 12 and 13 shows all the input and output flows of the raw material acquisition and processing of the solar PV cells.

Flow	Material	Amount / Unit
Input	Cadmium Telluride	0.24 mg
Input	Crystalline Silicon	0.03 mg
Input	Copper Indium Selenium	0.075 mg
Input	Poly Silicon	1.90 mg
Input	Monocrystalline Silicon	0.044 mg
Output	Solar PV Cells Parts	20 pieces

Table 12: Input and Output Flows for Solar PV Cells Raw Materials [26, 42]

Flow	Material	Amount / Unit
Input	Solar PV Cells Parts	20 pieces
Output	Solar PV Cells	20 pieces

Table 13: Input and Output Flows associated with Solar PV Cell Production [42]

Tables 14 and 15 summarized all the input and output flows for the raw material acquisition and processing of the tubular heat exchanger.

Flow	Material	Amount / Unit
Input	Titanium	600 g
Input	Brass	20 g
Input	Stainless Steel Hot Rolled Sheet	1.6 kg
Input	Copper, Primary, at Refinery	9 kg
Input	Bronzes	80 g
Output	Tubular Heat Exchanger Parts	1 piece

Table 14: Input and Output Flows for Heat Exchanger Raw Materials [28, 42]

Flow	Material	Amount / Unit
Input	Tubular Heat Exchanger Parts	1 piece
Output	Tubular Heat Exchanger	1 piece

Table 15: Input and Output Flows of Heat Exchanger Production [28, 42]

Additionally, tables 16 and 17 shows all the input and output flows for the raw material acquisition and processing of the hot water tank.

Flow	Material	Amount / Unit
Input	Mild Steel Plate	18 kg
Input	Vitreous Enamel	0.656 mg
Output	Hot Water Tank Parts	1 Piece

Table 16: Input and output Flows for Tank Raw Materials [42]

Flow	Material	Amount / Unit
Input	Hot Water Tank Parts	1 piece
Output	Hot Water Tank	1 piece

Table 17: Input and Output Flows of Tank Production [42]

3.3.4 Solar PV/T System Assembly Phase

Table 18 shows the input and output flows of the assembly phase for solar PV/T system.

Flow	Material	Amount / Unit
Input	Parts for Assembly	6 pieces
Input	Electricity, Medium voltage, at grid	250,000 KJ

Flow	Material	Amount / Unit
	(Production Mix)	
Input	Solar Panel	1 piece
Input	Piping System	4 pieces
Input	Electrical Cables	20 pieces
Input	Water Pump	2 pieces
Input	Solar PV Cells	20 pieces
Input	Tubular Heat Exchanger	1 piece
Input	Hot Water Tank	1 Piece
Output	Solar PV/T Hybrid System	1 piece/ 63.207 kg

Table 18: Inputs and outputs Flows of Solar PV/T Hybrid System Assembly Phase [42]

3.3.5 Solar PV/T System Use-Phase

This table below shows the input and output flows of the use phase for one solar PV/T system.

Flow	Material	Amount / Unit
Input	Solar PV/T Hybrid System	1 piece/ 63.207 kg
Output	Solar PV/T Hybrid System	1 piece/ 63.207 kg

Table 19: Inputs and Output Flows of the Use Phase [42]

3.3.6 Solar PV/T System Disassembly Phase

Tabl2 20 shows the input and output flows of the disassembly phase of the solar PV/T system. These components shown in the table were disassembled into 7 parts as shown in the plan in figure 8. Then these 7 parts will be assembled again after the end of life phase.

28

Flow	Material	Amount / Unit
Input	Solar PV/T Hybrid System	1 piece/ 63.207 kg
Output	Solar Panel	1 piece
Output	Piping System	1 piece
Output	Electrical Cables	1 piece
Output	Water Pump	1 piece
Output	Solar PV Cells	1 piece
Output	Heat Exchanger	1 piece
Output	Hot Water Tank	1 Piece

Table 20: Input and Output Flows of Disassembly Phase [42]

3.3.7 End of Life Phase of Solar PV/T System

The end of life phase table shows how the materials will be recycled again and how each component of the solar PV/T system will be assembled after the end of life phase.

Flow	Material	Amount / Unit
Input	Solar Panel	1 piece
Input	Piping System	1 piece
Input	Electrical Cables	1 piece
Input	Water Pump Systems	1 piece
Input	Solar PV Cells	1 piece
Input	Heat Exchanger	1 piece
Input	Hot Water Tank	1 Piece
Output	Disposal [Municipal Incineration] [Municipal Solid Waste]	1.5 kg
Output	Disposal [Landfill]	2.65 kg
Output	Copper Scrap [waster for recovery]	2 kg

Output	Aluminum Scrap [waster for recovery]	4 kg
Output	Solar Panel	1 piece
Output	Piping System	1 piece
Output	Electrical Cables	1 piece
Output	Water Pump	1 piece
Output	Solar PV Cells	1 piece
Output	Heat Exchanger	1 piece
Output	Hot Water Tank	1 Piece

Table 21: Inputs and Outputs Flows Associated with End of Life Phase [42]

3.4 Life Cycle Plan Model of Solar PV/T Hybrid System

Figure 9 shows the life cycle plan model of the solar PV/T hybrid system. The boundaries represent the processes associated with the life cycle plan of the system. The blue arrows are the flows that link the processes together in order to complete the life cycle. These blue arrows represent all the materials and energy flows passing between the processes as well as to and from the system, likewise they define the input and output flows of the system. Moreover, the life cycle plan model of the solar PV/T hybrid system can be divided into 7 phases:

3.4.1 Raw Material Acquisition Phase

This phase contains the raw materials required to manufacture only the metal frame, black sheet, insulation layer, and the glass fibre. The total weight for these four components is 17.7 kg as shown in section 3.3.1.

3.4.2 Material Processing Phase

This phase is regarding the assembly process of the four components, metal frame, black sheet, insulation layer, and the glass fibre. Approximately, 198 KJ required to assembly the four components together after manufacture the solar panel and the PV cells in the next phase.

3.4.3 Material Processing phase and Assembly Phase for the Main Components

There are 7 main components in the solar PV/T hybrid system; solar panel, PV cells, electrical cables, hot water pump, hot water tank, piping system and the tubular heat exchanger. Each of these components requires a particular process and raw materials to manufacture and assemble it. The first stage is to get the raw materials for each component, and then the second stage is to process and assemble these raw materials together to manufacture the component. The raw materials for each component are displayed in tables in section 3.3.3.

3.4.4 Solar PV/T System Assembly Phase

This phase is the assembly stage where all the 7 main components as well as the metal frame, insulations layer, black sheet and fibre glass were assembled together as one system. There is electricity required to assemble all this components together as shown in the Life Cycle Plan Model. The total weight of the system is 63.2 kg including all its components.

3.4.5 Solar PV/T System Use-Phase

This Phase is regarding the utilization stage of the solar PV/T hybrid system. Transport process such as cargo plane is required to deliver the system to the store.

3.4.6 Solar PV/T System Disassembly Phase

After the use phase, the following phase is the disassembly phase of the solar PV/T system. At this phase all the 7 main components of the system must be disassembled into 7 parts as shown in life cycle plan model.

3.4.7 End of Life Phase of PV/T System

In order to complete the life cycle of the solar PV/T hybrid system, the end of life phase is required. In this stage all the 7 main components will be recycled again as well as the metal frame raw materials such as, aluminum and copper.

Figure 9: Life Cycle Plan Model of Solar PV/T Hybrid System
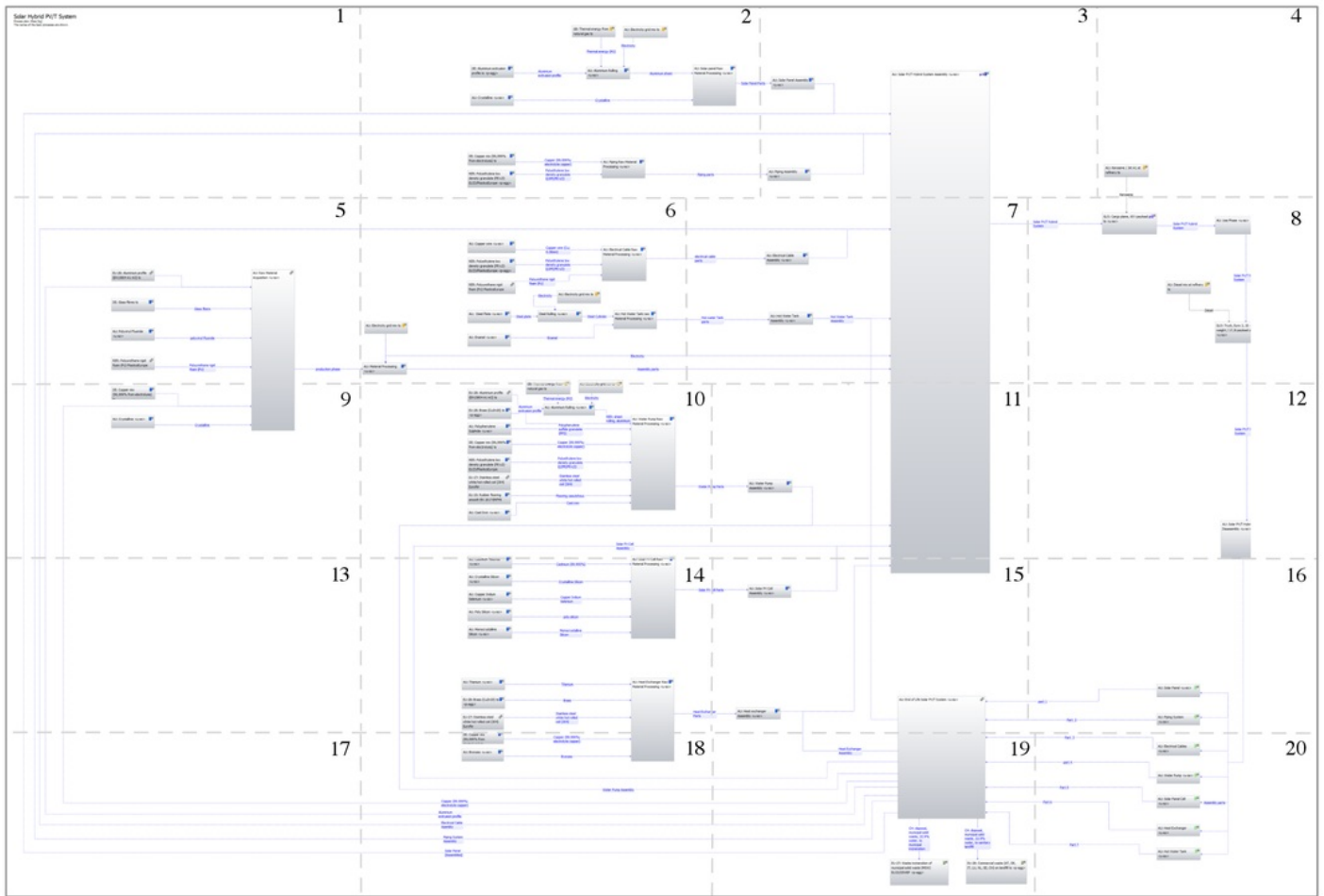
Figure 10: Life Cycle Plan Model of Solar PV/T Hybrid System (Divided into 20 Parts)

Solar Hybrid PV/T System
Process plan: Mass [kg]
The names of the basic processes are shown.

Selection: Solar Hybrid PV/T [...]
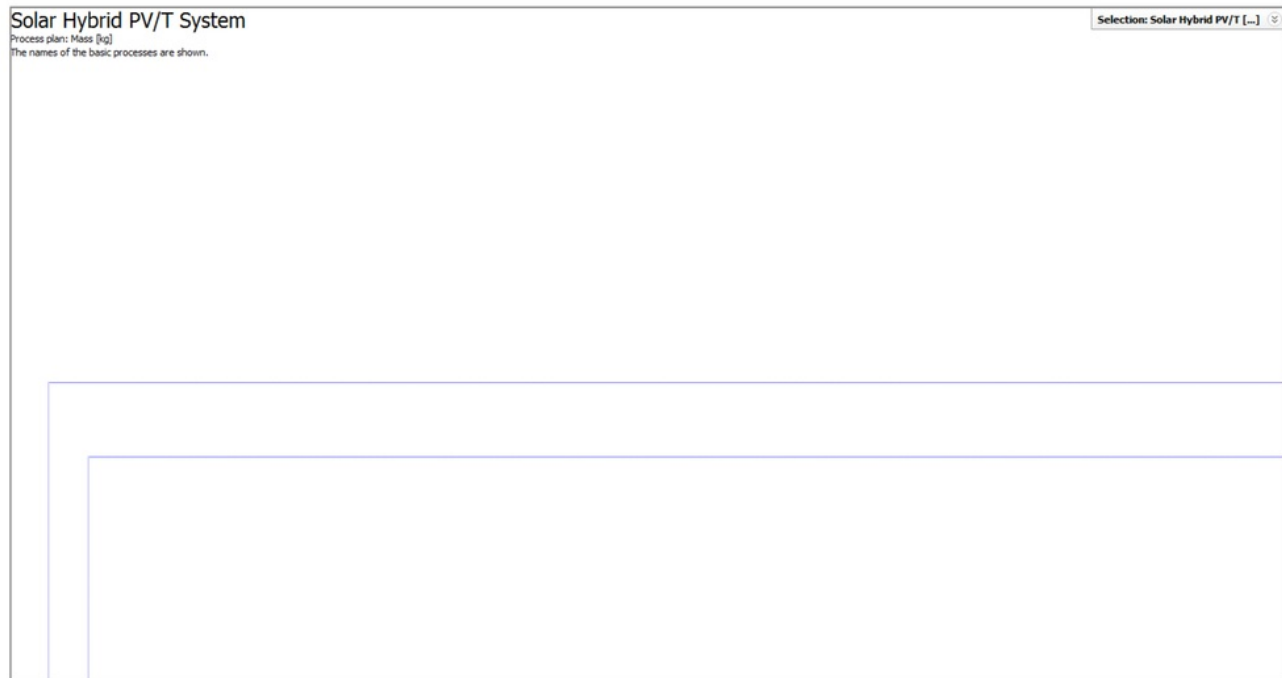
Figure 11: Life Cycle Plan Model of Solar PV/T System (Part 1)

Selection: Solar Hybrid PV/T [...]

GB: Thermal energy from natural gas ts

AU: Electricity grid mix ts

Electricity

Thermal energy (MJ)

DE: Aluminium extrusion profile ts <p-agg>

Aluminium extrusion profile

AU: Aluminium Rolling <u-so>

Aluminium sheet

AU: Solar panel Raw Material Processing <u-so>

Solar Panel Parts

AU: Crystalline <u-so>

Crystalline

DE: Copper mix (99,999% from electrolysis) ts

Copper (99.999%; electrolyte copper)

AU: Piping Raw Material Processing <u-so>

RER: Polyethylene low density granulate (PE-LD) ELCD/PlasticsEurope <p-agg>

Polyethylene low density granulate (LDPE/PE-LD)

Piping parts

Figure 12: Life Cycle Plan Model of Solar PV/T System (Part 2)
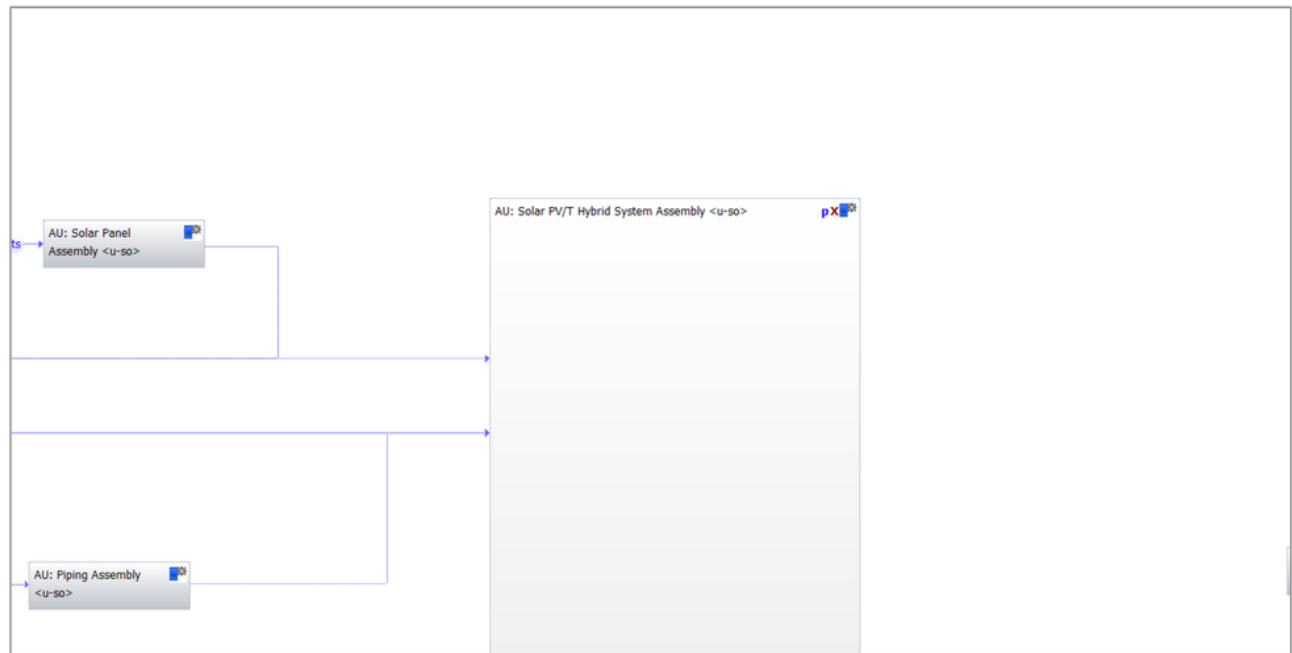
Figure 13: Life Cycle Plan Model of Solar PV/T System (Part 3)
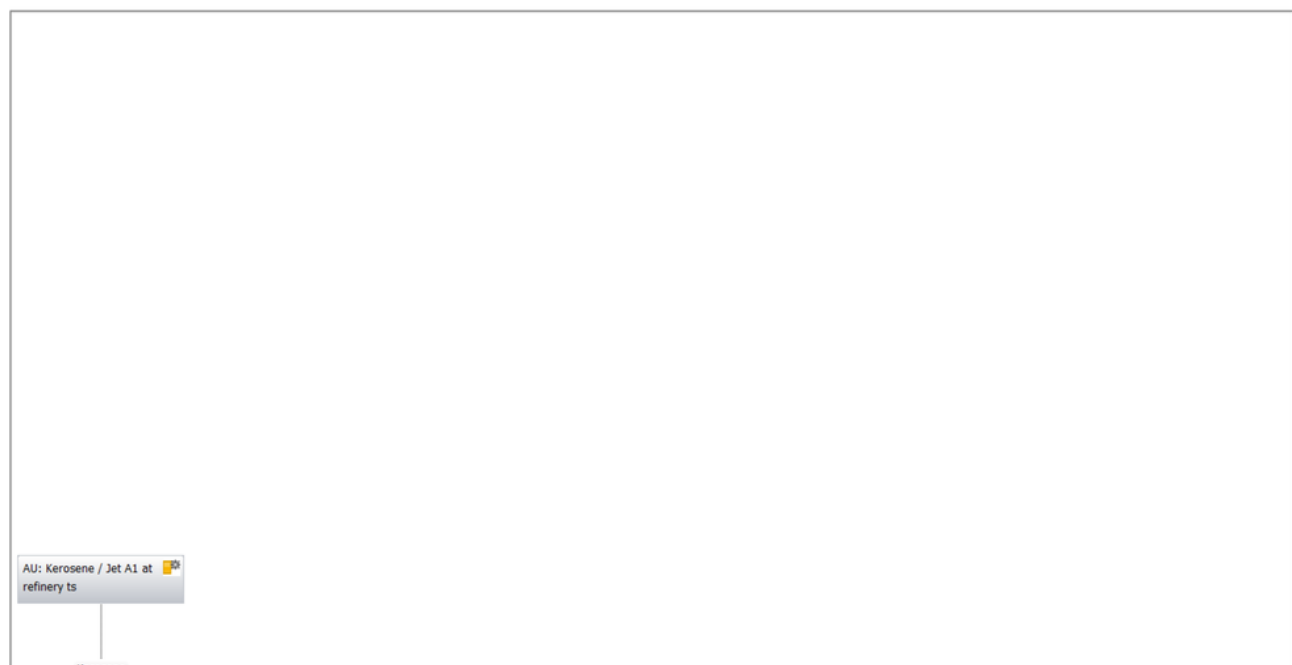
Figure 14: Life Cycle Plan Model of Solar PV/T System (Part 4)

36
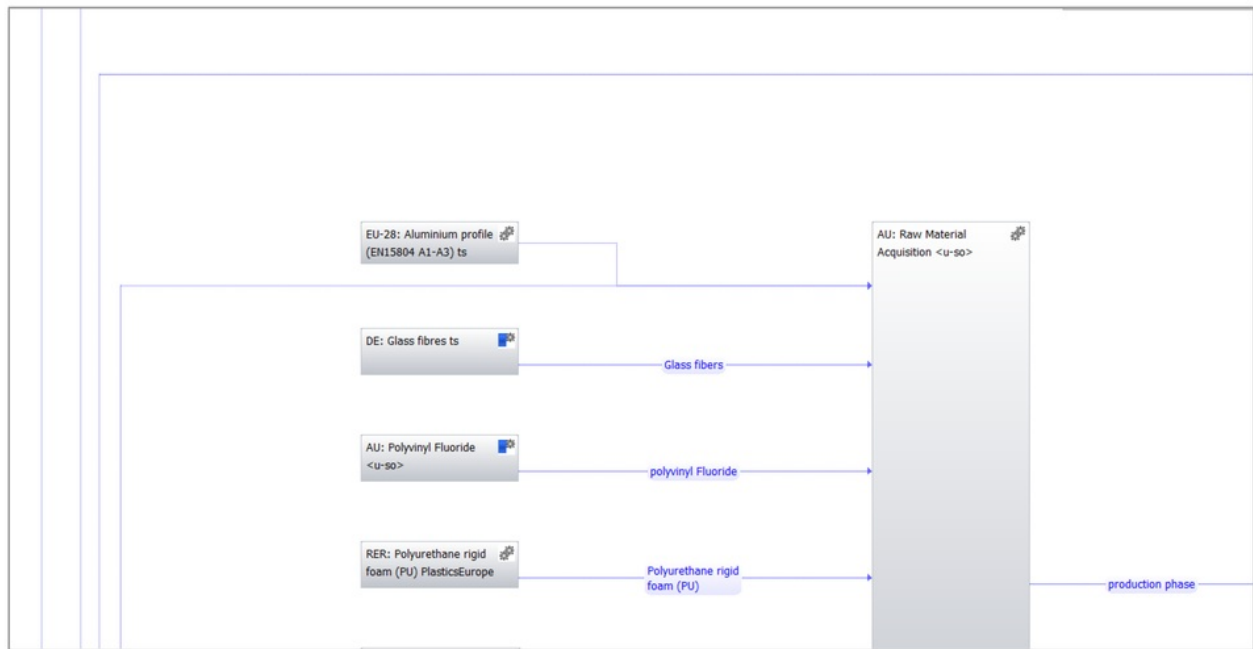
Figure 15: Life Cycle Plan Model of Solar PV/T System (Part 5)
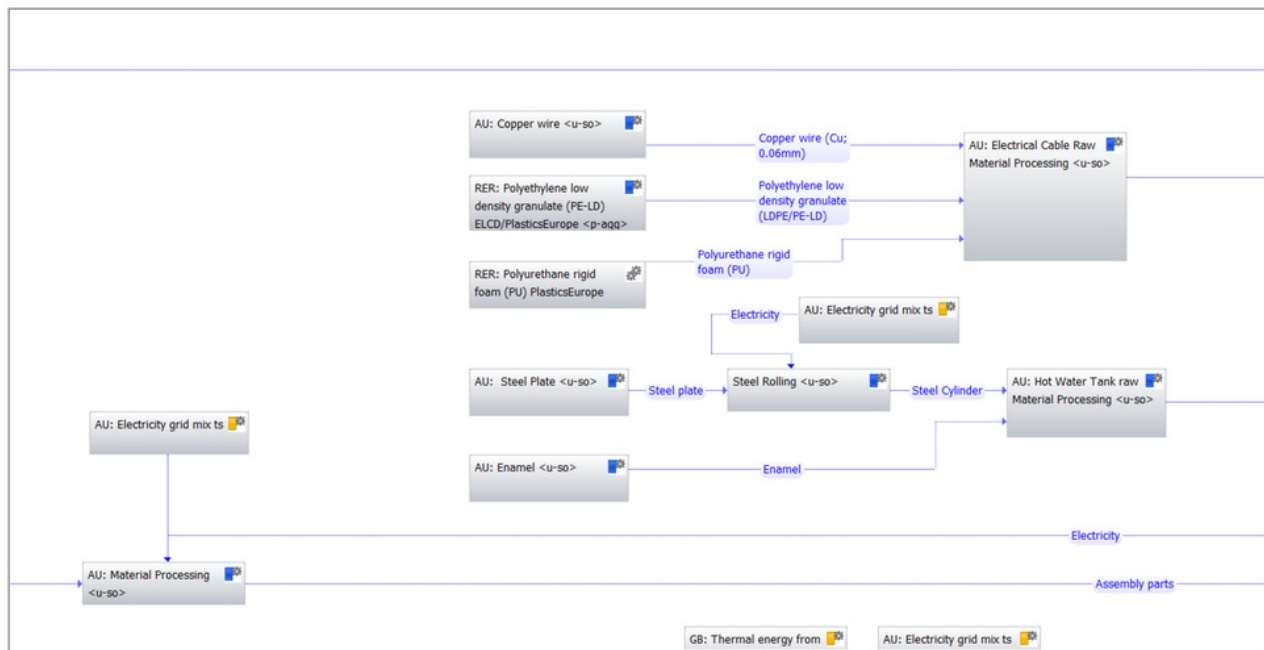
Figure 16: Life Cycle Plan Model of Solar PV/T System (Part 6)
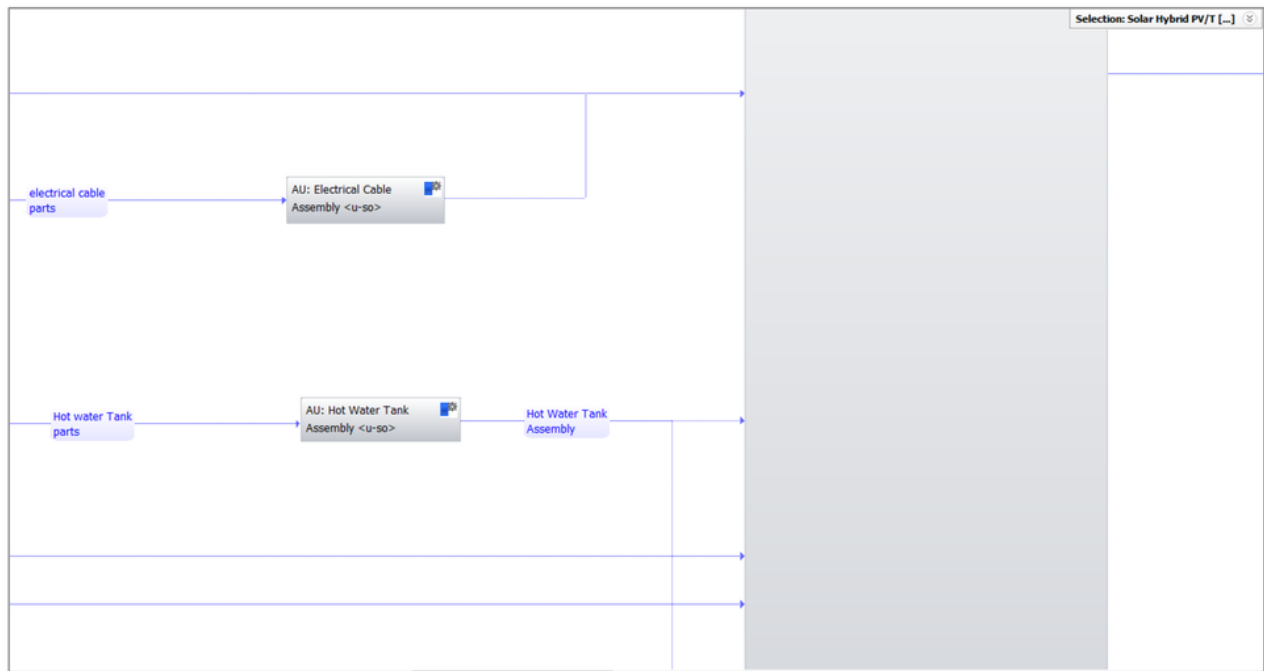
Figure 17: Life Cycle Plan Model of Solar PV/T System (Part 7)
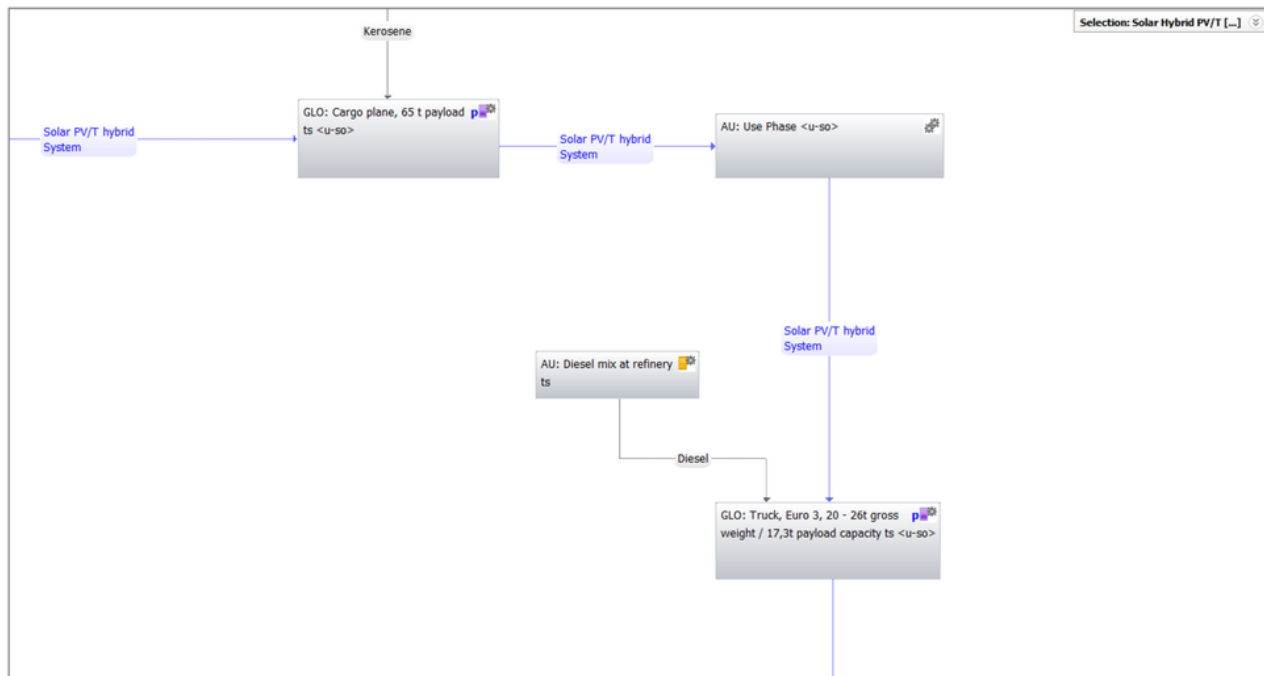
Figure 18: Life Cycle Plan Model of Solar PV/T System (Part 8)
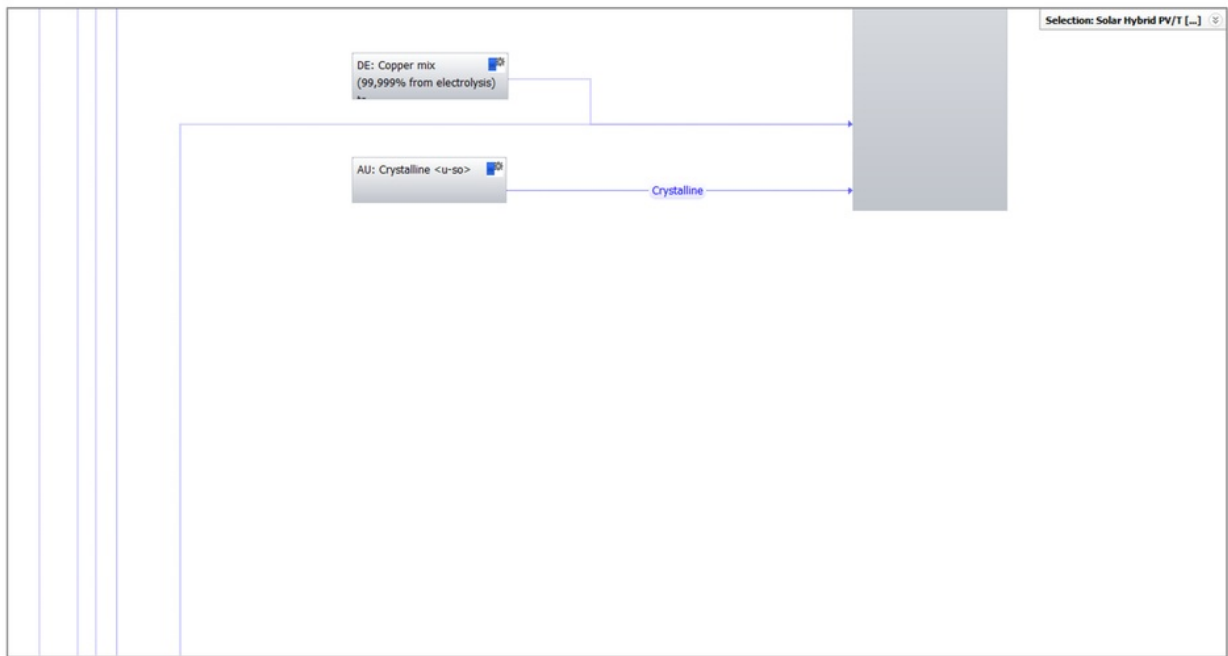
Figure 19: Life Cycle Plan Model of Solar PV/T System (Part 9)
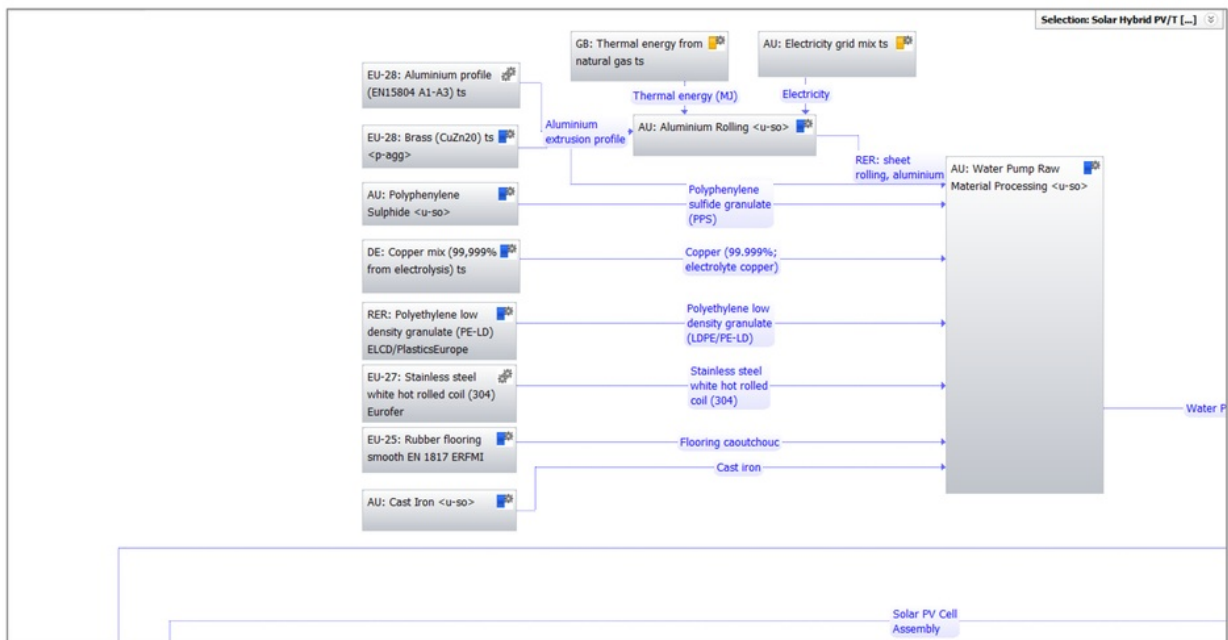
Figure 20: Life Cycle Plan Model of Solar PV/T System (Part 10)

39
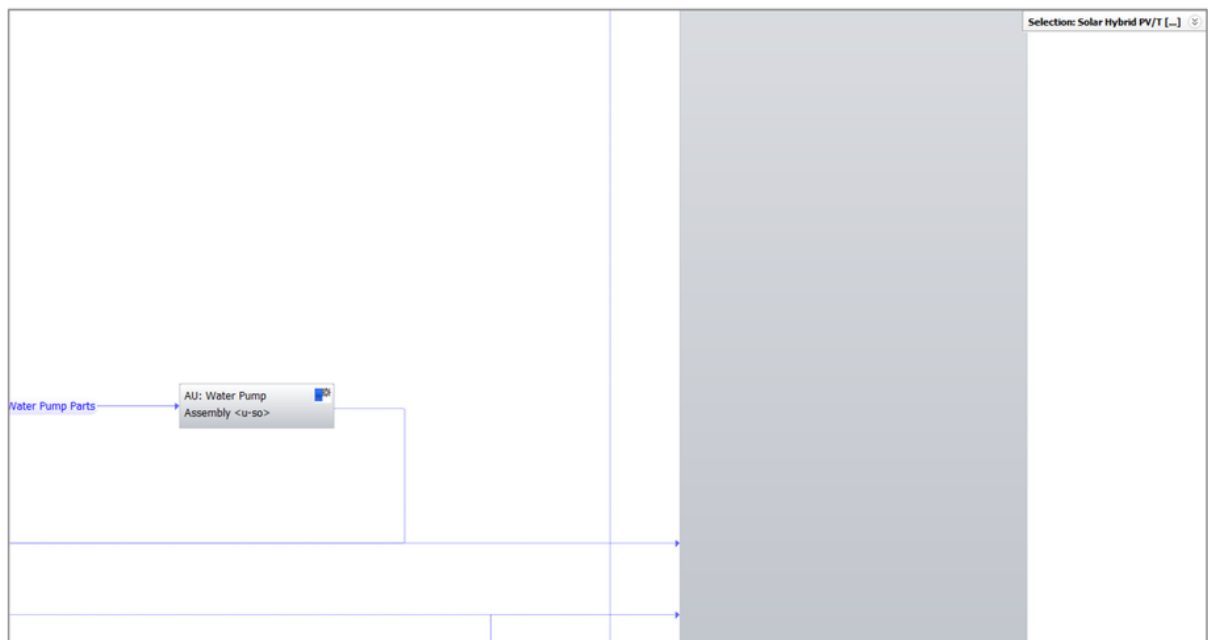
Figure 21: Life Cycle Plan Model of Solar PV/T System (Part 11)
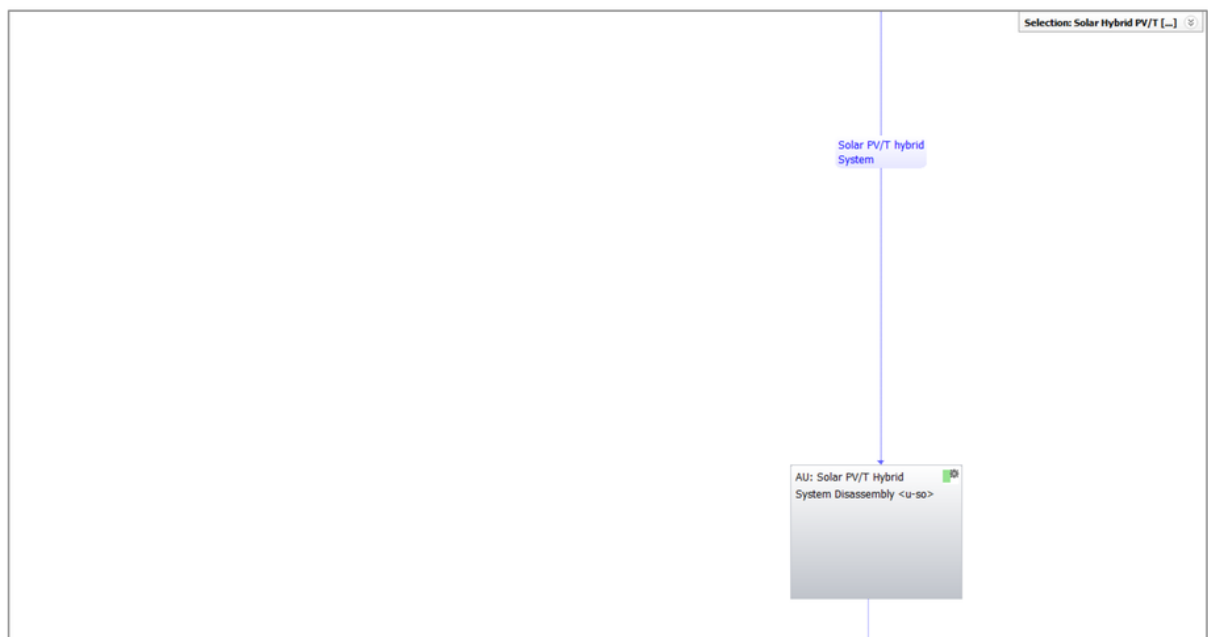
Figure 22: Life Cycle Plan Model of Solar PV/T System (Part 12)
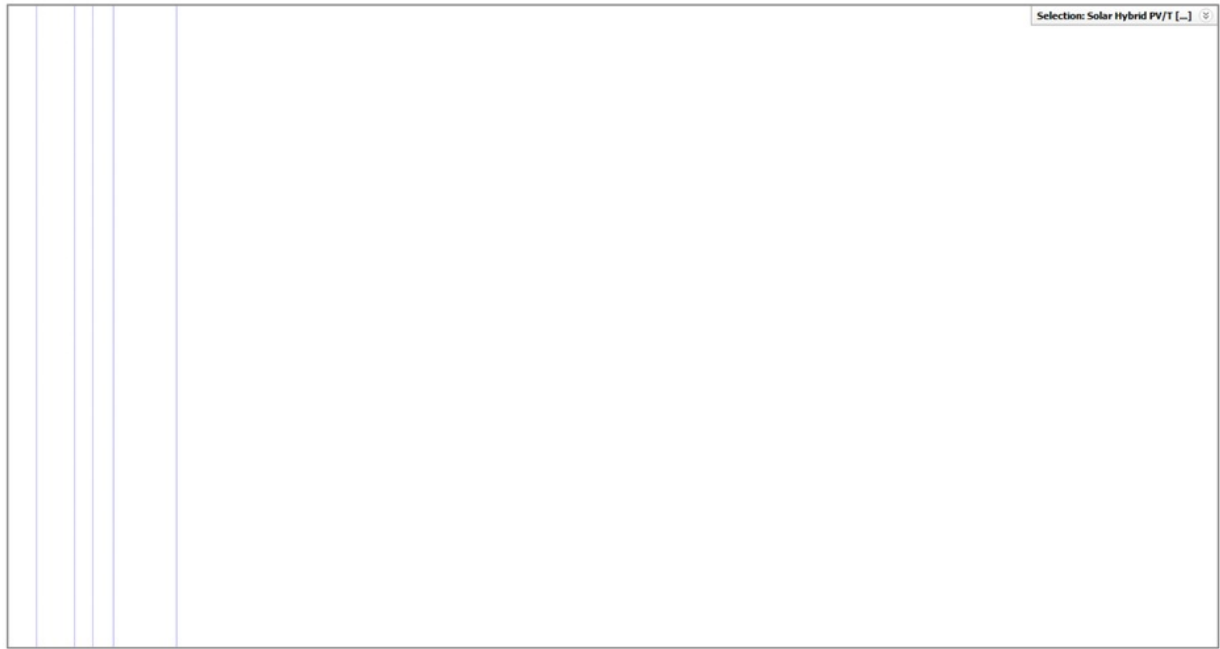
Figure 23: Life Cycle Plan Model of Solar PV/T System (Part 13)
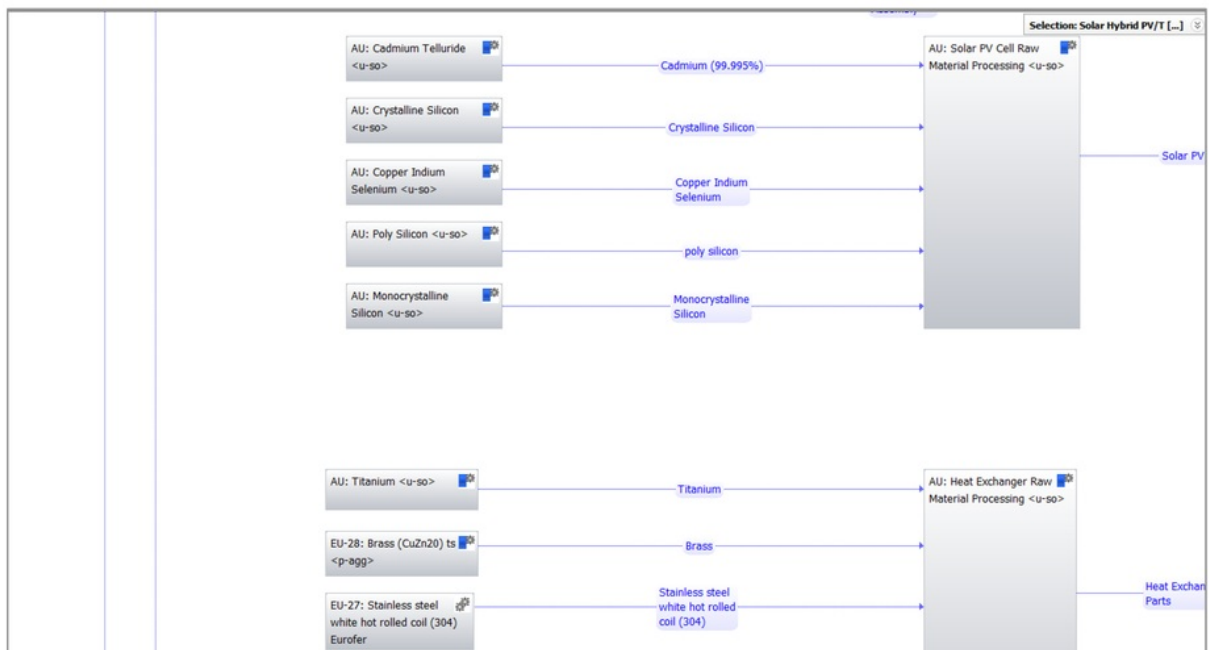
Figure 24: Life Cycle Plan Model of Solar PV/T System (Part 14)

41
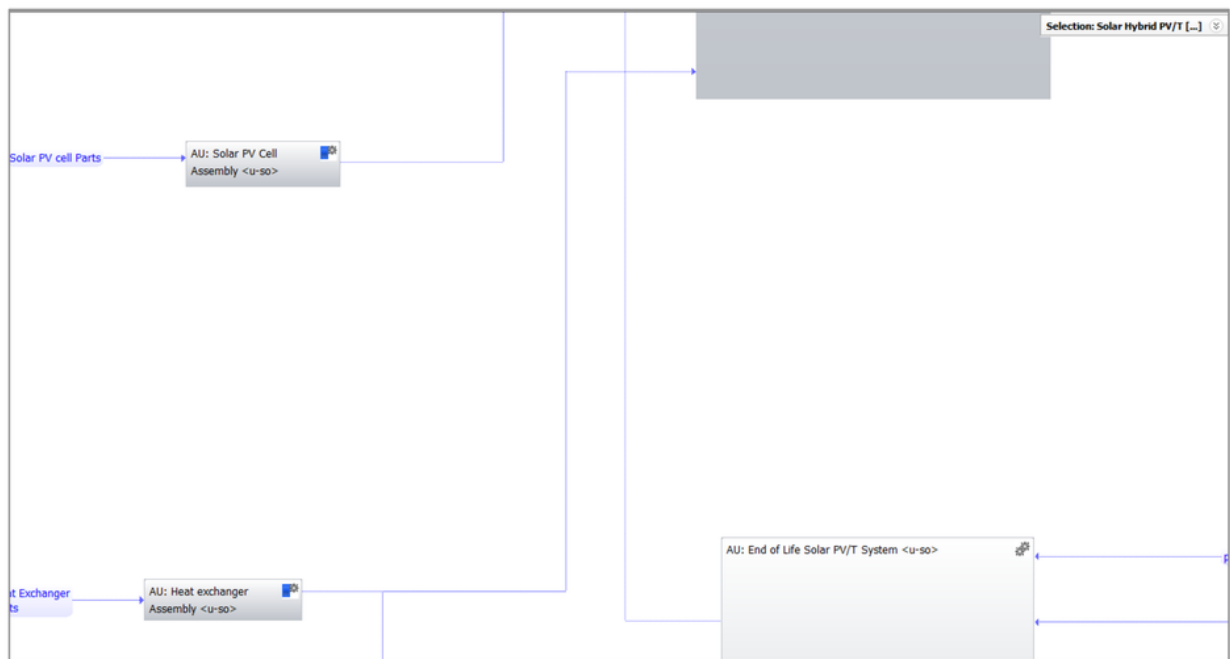
Figure 25: Life Cycle Plan Model of Solar PV/T System (Part 15)
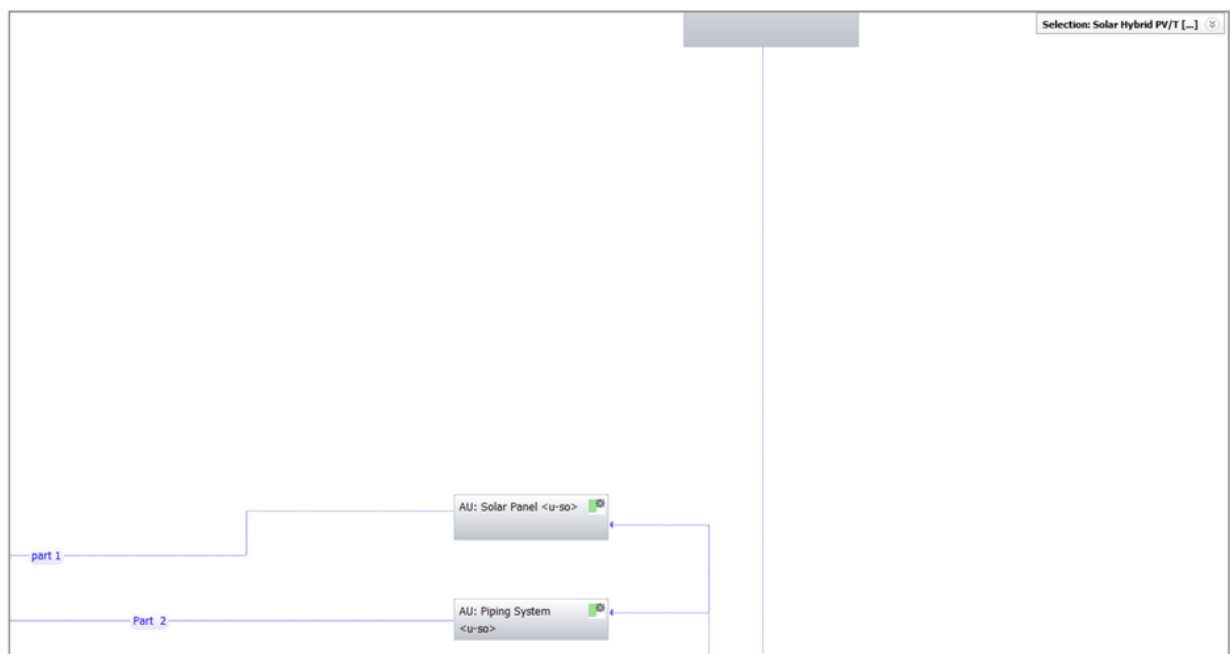
Figure 26: Life Cycle Plan Model of Solar PV/T System (Part 16)

42
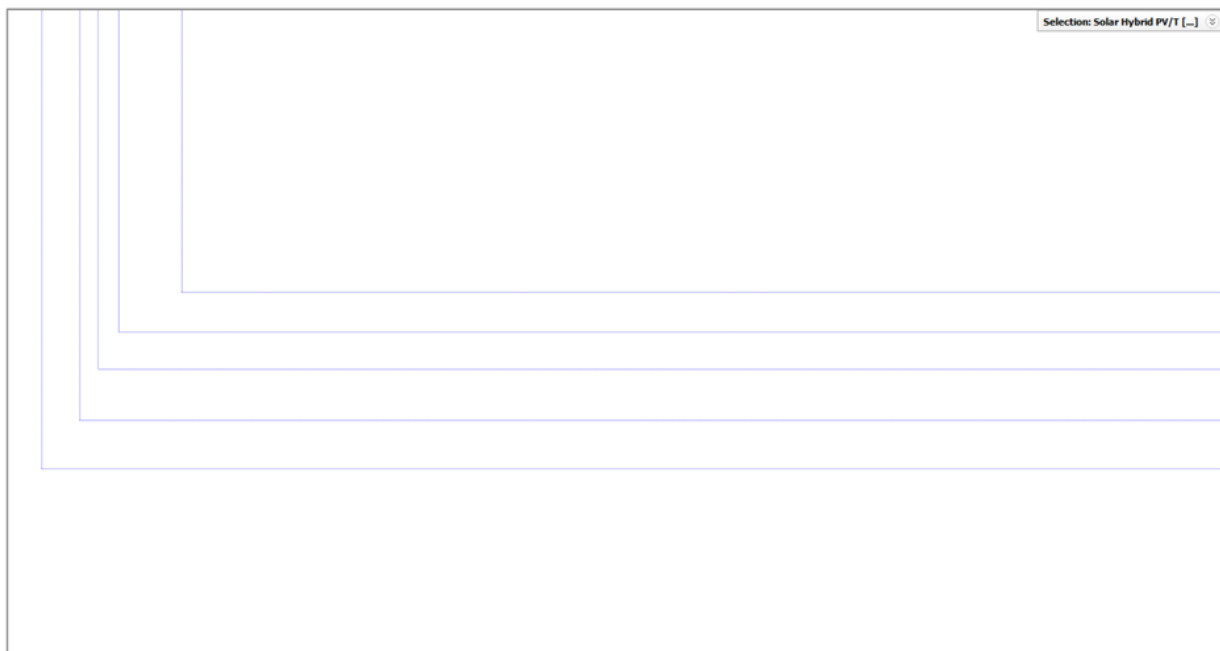
Figure 27: Life Cycle Plan Model of Solar PV/T System (Part 17)

Figure 28: Life Cycle Plan Model of Solar PV/T System (Part 18)
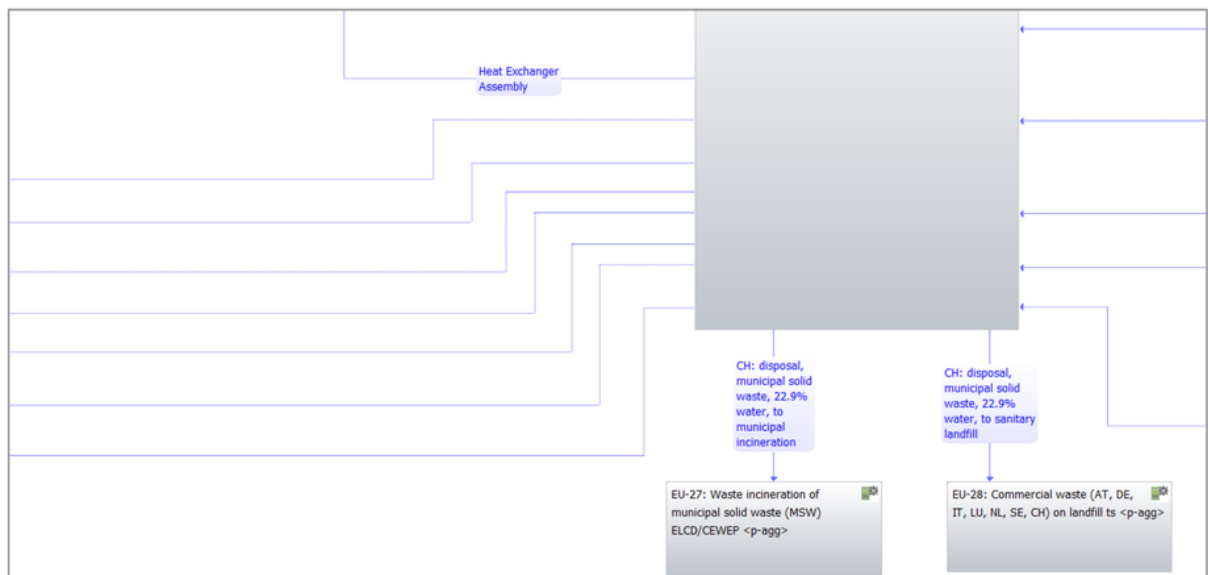
Figure 29: Life Cycle Plan Model of Solar PV/T System (Part 19)
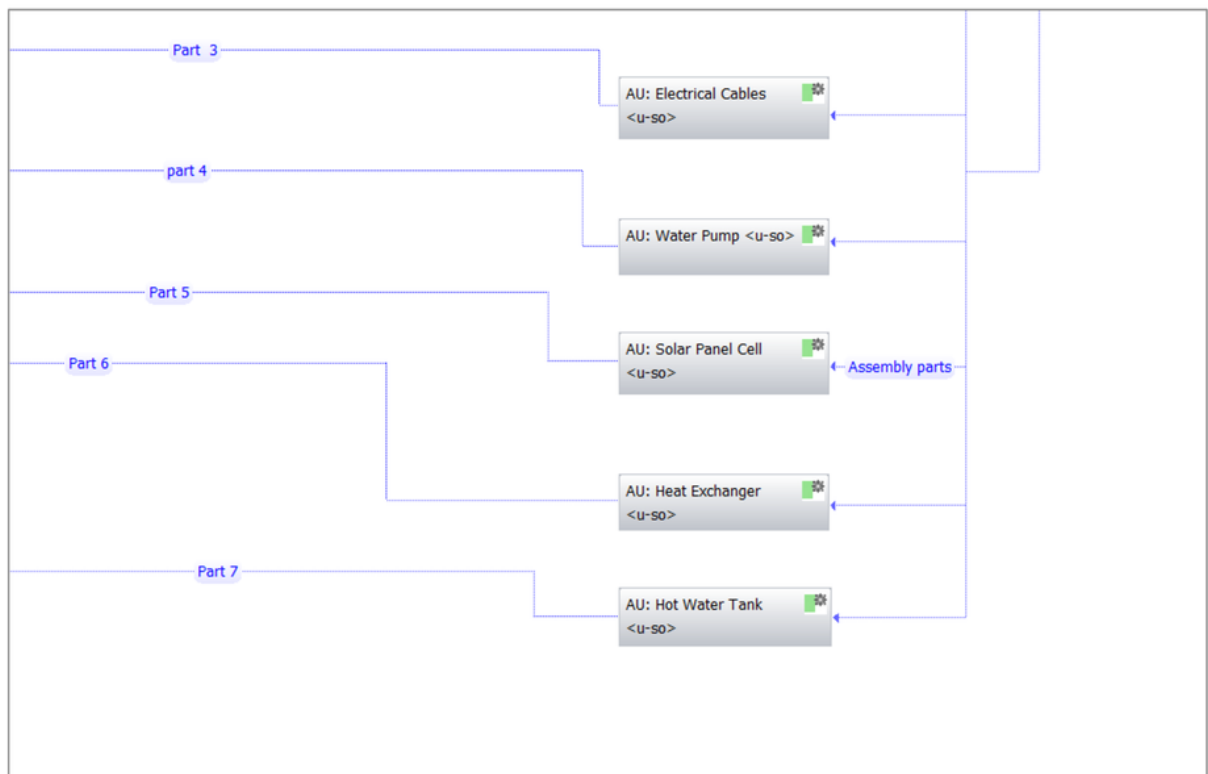
Figure 30: life Cycle Plan Model of Solar PV/T System (Part 20)

44

3.5 Environmental Impact Assessment

This section shows the results of the environmental impact assessment for solar hybrid PV/T system according to the CML[14] 2001 to January 2016 assessment methodology.

3.5.1 Global Warming Potential

The global warming potential (GWP) is the relative measure of the amount of heat that trapped by the emissions of the green house gases (GHG) in the air. The GWP can be measures in kilograms CO_2[15]. Worldwide the global temperature has been increased dramatically in the last 100 years. According to Karl and Arguez journal article, the temperature will increase approximately 10 degrees Fahrenheit or 261 Kelvin in the next century [48]. Additionally, the cause of the global warming is when the emissions of CO_2 and the other air pollutants absorb the sunlight as well as the solar radiation in the atmosphere. Therefore, these emissions and pollutants will trap the heat and then the earth planet will be warmer [7].
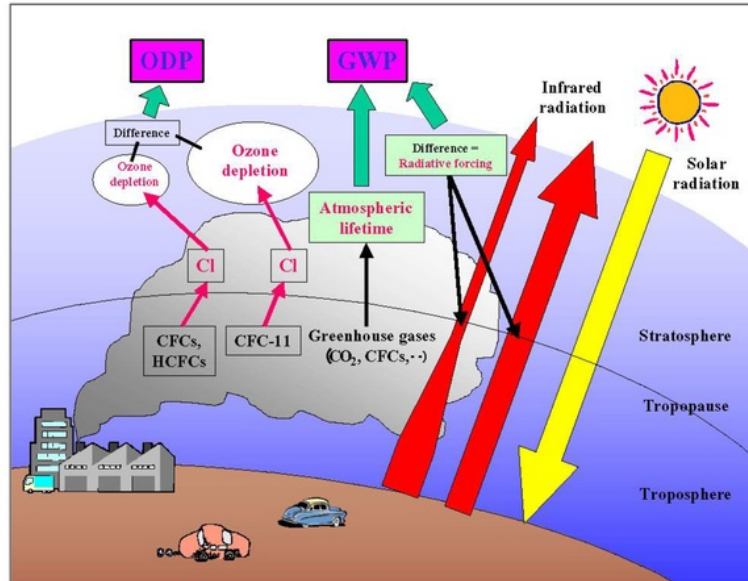
Figure 31: Global Warming Potential and Ozone Depletion [49]

---

[14] Chain Management Life Cycle Assessment
[15] Carbon Dioxide

45
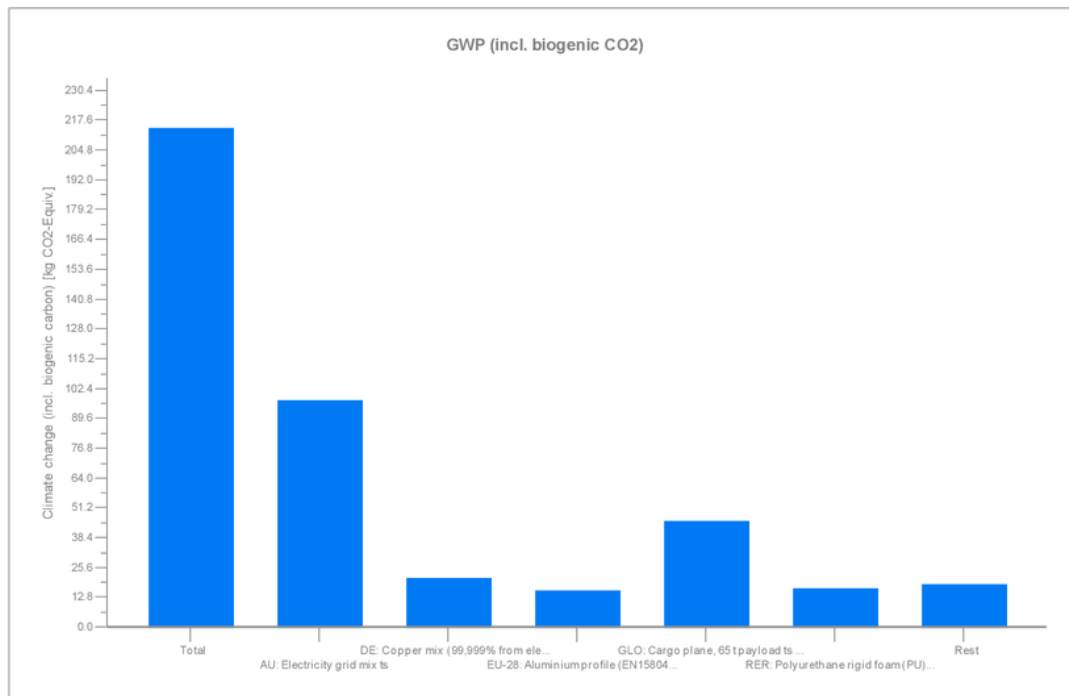
Figure 32: Global Warming Potential of PV/T System (includes Biogenic CO_2)

The chart above shows the global warming potential (includes biogenetic CO_2) of the solar PV/T hybrid system life cycle plan. The blue bars displays all the processes and materials in the life cycle plan of the solar PV/T hybrid system. Such as, the raw materials of the system, the transportations, and the electricity for assembly processes and for rolling processes. In addition, the amount of carbon dioxide that generated from the electricity grid mix is 97 [Kg CO_2 – Equiv.], which considered the highest result in the chart comparing that with other processes. Likewise, for the copper mix and aluminum profile are 20.5 [Kg CO_2 – Equiv.] and 17 [Kg CO_2 – Equiv.] respectively also, for the cargo plane and the insulation (polyurethane rigid foam) are 45 [Kg CO_2 – Equiv.] and 18 [Kg CO_2 – Equiv.] respectively. While the rest processes generated approximately 19 [Kg CO_2 – Equiv.] [42]. Consequently, 45% of the total amount of carbon dioxide was generated from the electricity grid mix. This electricity was used in the material processing phase and solar PV/T system assembly phase. Moreover, this table below shows the LCA results of the global warming potential (GWP 100 years)

46

according to the 2001 to January 2016 assessment methodology. These results are only the results of the elementary flows, which include the results of flows, resources, and emissions to air and inorganic emissions to air. This table does not include the non-elementary flows results such as the results of the valuable substances, ecoinvent and production residues in life cycle. The only negative values in this table is the resources results as the negative values indicate there was input of the carbon dioxide (CO_2) in the input side [42].

	Flows	Resources	Emissions to Air	Inorganic Emissions to Air
Diesel Mix At refinery	0.02	-0.00346	0.0234	0.018
Electricity Grid Mix	97.7	-1.63	99.3	96.2
Kerosene / Jet A1 At Refinery	4.98	-0.0208	5	3.62
Copper Mix (99,999% from electrolysis)	0.621	-0.0302	0.652	0.631
Copper Mix	20.9	-1.01	21.9	21.2
Glass Fibres	8.31	-0.755	9.07	8.59
Waste Incineration of Municipal Solid Waste	1.12	1.68×10^{-5}	1.12	1.12
Commercial Waste	3.74	-0.01	3.75	0.898
Aluminium Profile	15.5	-0.363	15.8	14.3
Cargo Plane, 65t Payload	45.5	---	45.5	45.5
Truck	0.183	---	0.183	0.183
Polyethylene	8.04×10^{-7}	---	8.04×10^{-7}	6.33×10^{-7}
Polyurethane	16.8	---	16.8	13.2
Solar Hybrid PV/T System	Total = 215	Total = -3.83	Total = 219	Total = 205

Table 22: Global Warming Potential (GWP 100 years) [Kg CO_2 – Equiv.]
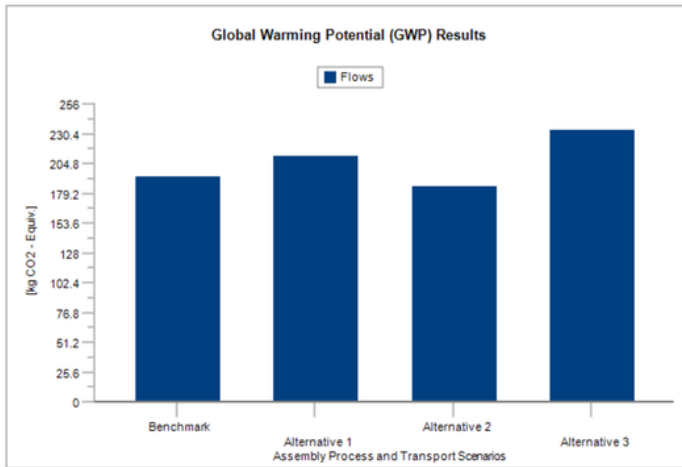
Figure 33: Global Warming Potential Results of Solar PV/T System 1
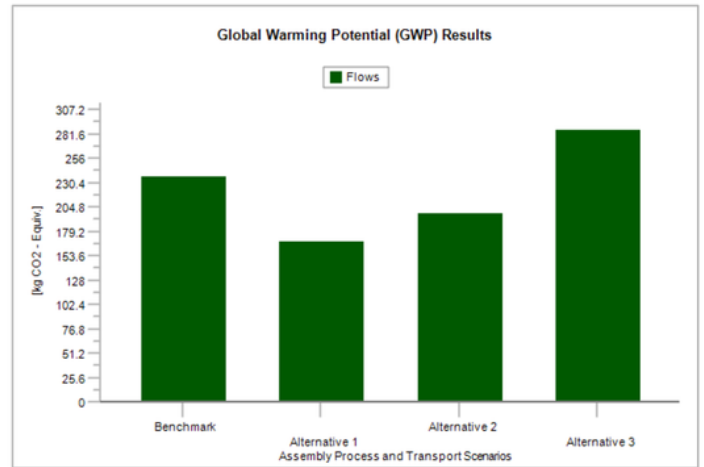
Figure 34: Global Warming Potential Results of Solar PV/T System 2

These charts above show the global warming potential results of 2 Solar PV/T Systems according to the CML 2001 to January 2016 assessment. The results in each chart are displayed for 4 different scenarios. According to Solar PV/T system 1, the truck distances for the scenarios benchmark, alternatives 1 are 80 km and 50 km respectively, and 0 km for both alternatives 2 and 3. Also, the truck utilisation by mass is 0.85 for all the scenarios and the capacity plane utilisation is 66% for all the scenarios. Likewise, the plane distances for benchmark and alternative 2 are 1250 km and 2500 km respectively but for alternative 1 and 3 the distances are 3750 km for both of them. In addition, the electricity required to assemble the solar PV/T system was divided into 3 steps; step A, B and C. For scenario alternative 1 the electricity required for step A, B and C are 15 MJ, 10 MJ and 80 MJ respectively. For scenarios benchmark and alternative 3 the electricity required for step A, B and C are 30 MJ, 70 MJ and 100 MJ respectively. Also, for scenario alternative 2 the electricity required are 20 MJ, 25 MJ and 70 MJ for step A, B and C respectively. Therefore, for benchmark scenario the total electricity required to assemble the solar PV/T system is 200 MJ and for scenarios alternative 1, 2 and 3 are 105 MJ, 145 MJ and 200 MJ respectively. As a result, according to the solar PV/T system 1, the amount of carbon dioxide is approximately 193 [Kg CO_2 – Equiv.] and for scenario benchmark and 192 [Kg CO_2 –

48

Equiv.] for scenario alternative 2. Likewise, for scenario alternative 1 and 3 the amounts of CO2 are 217 and 242 [Kg CO_2 − Equiv.] [42].

For solar PV/T system 2, the truck and plane distances were slightly different from the distances of solar PV/T system 1. The truck distances for the scenarios benchmark, alternative 1, 2 and 3 are 100 km, 80 km, 40 km and 0 km respectively and the plane distances for scenarios benchmark, alternative 1, 2 and 3 are 3750 km, 1250 km, 2500 km and 6200 km respectively. Additionally, the results of electricity input in solar PV/T system 2 are the same in solar PV/T system 1. So the result of the flows in scenario benchmark is 241 [Kg CO_2− Equiv.] for solar PV/T system 2. The scenario alternative 3 was the highest result in the chart with 295 [Kg CO_2− Equiv.] due to the increased distance travelled by the plane in this particular scenario. Moreover the amount of CO2 in alternative 1 and 2 are considered the lowest in this chart, for alternative 1 was approximately 167 [Kg CO_2− Equiv.] and 218 [Kg CO_2− Equiv.] for alternative 2 [42].

3.5.2 Ozone Depletion Potential

The ozone depletion potential (ODP) is considered the quantity of the destructive impacts of the gases on the ozone layer in the stratosphere. It can be measured in R11[16] equivalent or CFC 11. Likewise, the R11 has the highest potential amongst all the chlorocarbons because it contains 3 atoms of chlorine in each molecule. In addition, the ozone layer is generally can prevent the UV[17] radiation to reach the surface of the earth and also prevents the heat from reaching the earth. Moreover, the ozone layer depletion can also cause cancers or tumors in humans and some animals and also can affect the photosynthesis of the plants, which can negatively affect the growth of these plants [7, 50].

---

[16] Trichlorofluoromethane
[17] Ultraviolet
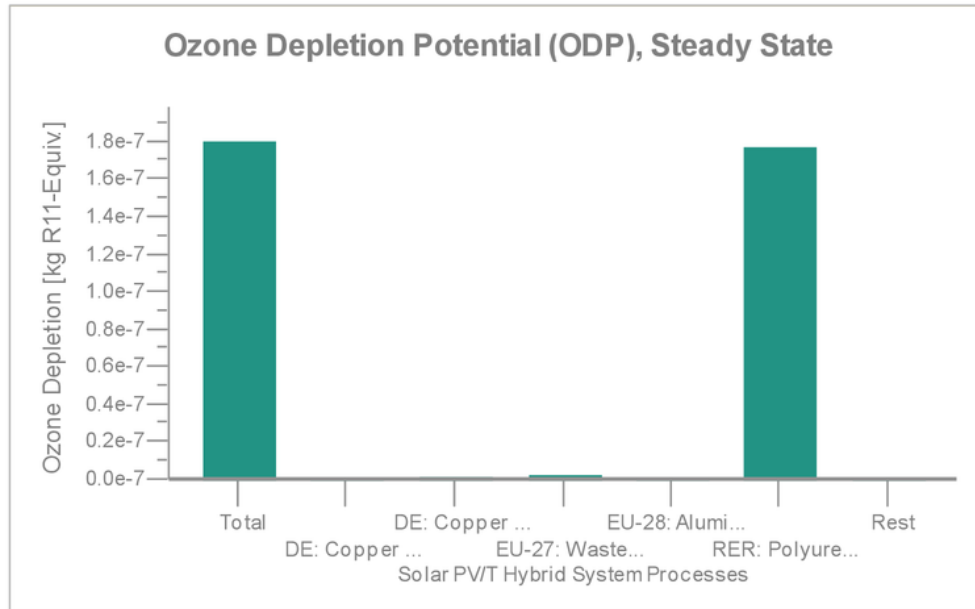
Figure 35: Ozone Depletion Potential (ODP) [kg R_{11} eq]

This chart above displays the results of the ozone depletion potential in kg R11 equivalent. According to the chart, all the processes and materials in the solar PV/T hybrid system plan model have very low results except for one process, which is the polyurethane (insulation). The polyurethane generated 1.77×10^{-7} kg R_{11} which equal to 98.3% of the total results of the all processes in the system. This material was used to manufacture the insulation layer of the solar panel. The other processes only contribute 1.67% of the total results. For instance, the copper mix process (second bar) generated 0.000221×10^{-7} kg R11 while the waste incineration of municipal waste generated 0.0224×10^{-7} kg R11 and the aluminium profile 0.00173×10^{-7} kg R11 [42].

3.5.3 Human Toxicity Potential (HTP)

The human toxicity potential (HTP) is considered the potential harm of a chemical element that released into the environment. This potential is basically depend on two

main factors, the component's inherent toxicity, and the component's potential dose. This potential can weight the toxic emissions in the atmosphere and some of them can cause cancer for humans. This potential can be measured in (CTUh[18]). In addition, the U.S Environmental Production Agency (TRI[19]) listed more than 250 chemicals that can cause cancers for humans. Likewise, they presented the results of cancer and non-cancer human toxicity potential (HTP) of 330 components. [51].

Moreover, the cancer and non-cancer HTP values of the solar PV/T hybrid system processes were plotted in two charts. The first chart (light green) shows the results of the emissions that can cause cancer of humans while the second chart (bright green) shows the results of the non-cancer emissions.
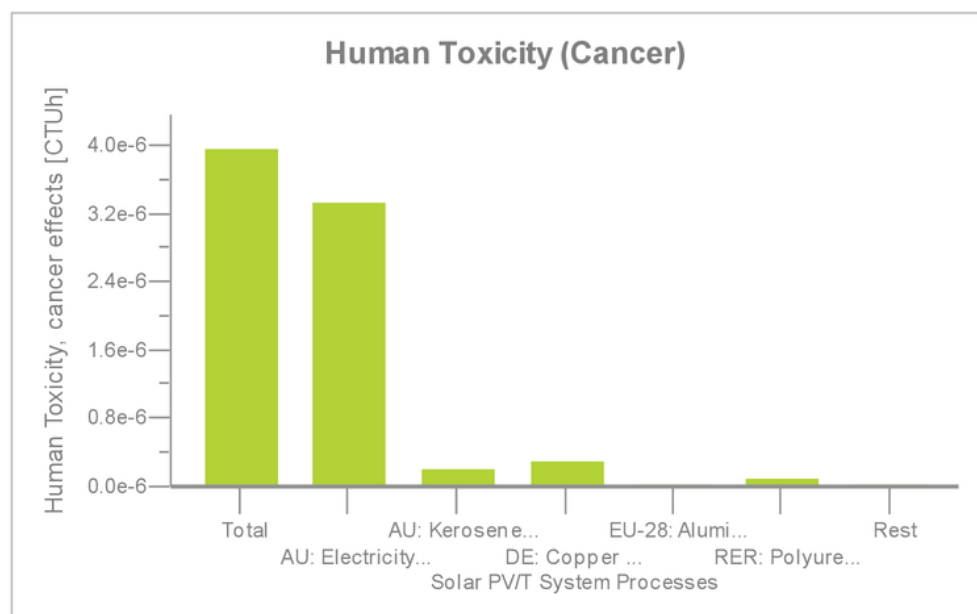
Figure 36: Human Toxicity (Cancer) [CTUh]

According to the figure 36, the total emissions of all the processes and materials associated with the solar PV/T system are equal to 3.97×10^{-6} CTUh. Likewise, the

---

[18] Comparative Toxic Units for Human
[19] Toxics Release Inventory

amount of emissions generated from electricity grid mix that used to assemble the raw materials and the seven main components of the solar PV/T system is equal to 3.33 $\times 10^{-6}$ CTUh and this result is the highest result in this chart comparing that with the other processes of the solar PV/T system. The amount of emissions of the other processes is very low, ranging from 0.29×10^{-6} CTUh to 0.0189×10^{-6} CTUh.
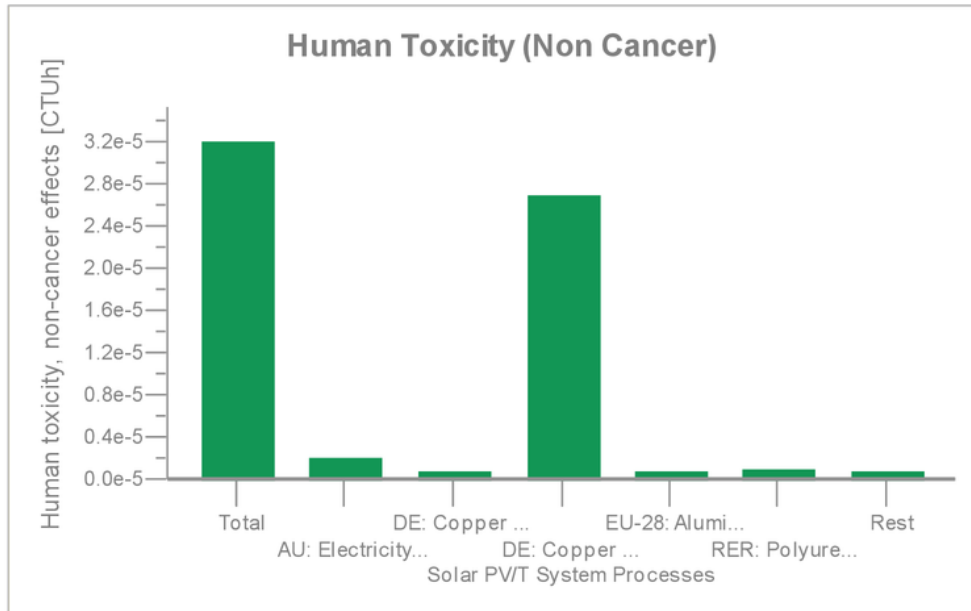
Figure 37: Human Toxicity (Non Cancer) [CTUh]

Moreover, according to the human toxicity non-cancer chart, the amount of emissions generated from the copper that used to manufacture the water pumps, and heat exchanger is 2.69×10^{-5} CTUh. While, the emissions generated from the copper to manufacture the metal frame is 0.08×10^{-5} CTUh . Additionally, the emissions generated from electricity grid mix is 0.2×10^{-5} CTUh and the lowest amount of emissions produced by other materials such as, cast iron, stainless steel, brass and monocrystalline silicon, and the amount is 0.079×10^{-5} CTUh.

52

3.5.4 Ionising Radiations

The ionising radiations are related to the electromagnetic waves and particles and it can be measured by (U235[20] eq). These radiations have a negative effect on humans, such as, causing burns in the skin and sometimes cancer [52]. The chart below displays the results of radiation emissions of solar PV/T system processes and raw materials. The amount of radiations generated from the aluminum profile to manufacture the metal frame and water pump is 2.8 (U235 eq). Likewise, the amount of radiation produced from the fiberglass and copper is 0.42 (U235 eq) and 0.93 (U235 eq) respectively.
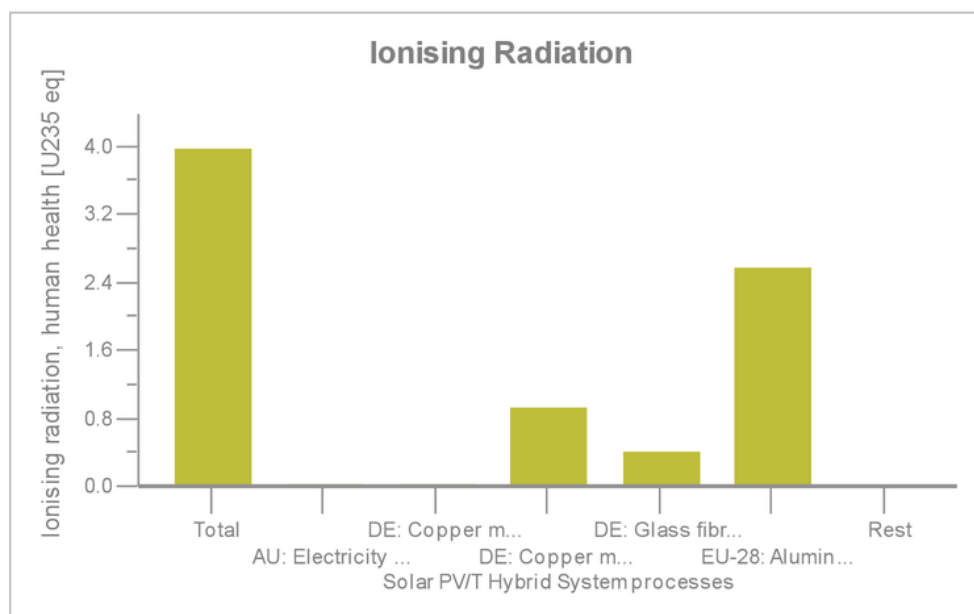
Figure 38: Ionising Radiation [U235 eq]

---

[20] Uranium-235

53

3.5.5 Photochemical Ozone Creation Potential (POCP)

The photochemical ozone creation potential is regarding the photo-oxidant formation and hydrocarbon emissions. Also, it is the results of the reactions between VOCs[21] and NO_x[22]. Likewise, the ozone formation is from VOCs, nitrogen oxides, and carbon monoxide (CO). This formation depends on the concentrations of pollutants and the meteorological circumstances. Additionally, the photochemical ozone creation potential can be measured by (kg NMVOC[23] eq) [53].
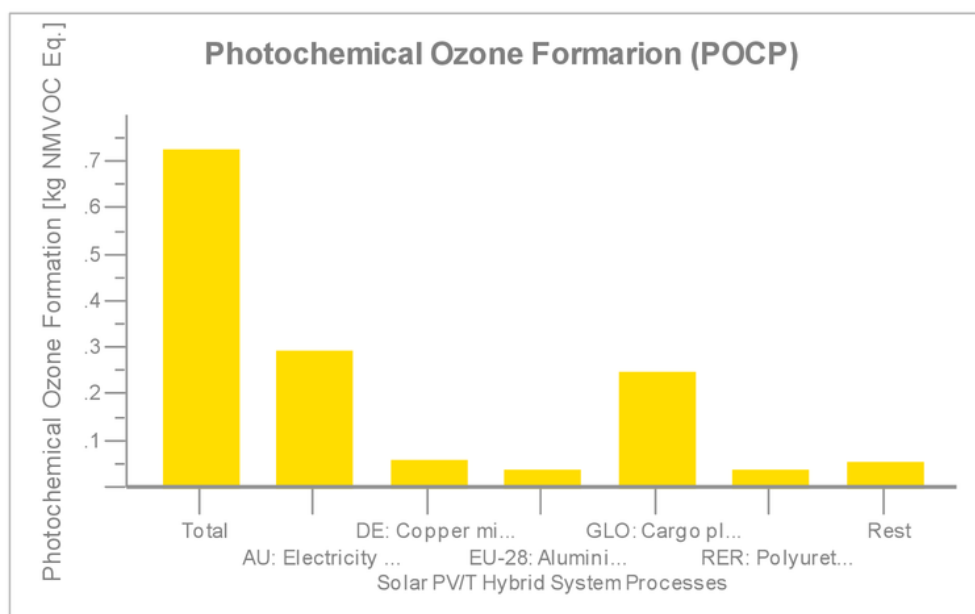
Figure 39: Photochemical ozone Formation

This figure above shows the results of the photochemical ozone formation of the solar PV/T system processes and materials. 0.293 (kg NMVOC eq) was generated from the electricity gird mix, and 0.248 (kg NMVOC eq) from the cargo plane process. These two amounts of emissions were the highest in the photochemical ozone formation

---

[21] Volatille Organic Components
[22] Nitrogen Oxides
[23] Non Methanic Volatile Organic Components

chart. The emissions of the other processes of the solar PV/T system range from 0.0359 to 0.0578 (kg NMVOC[24] eq).

3.5.6 Acidification Potential (AP)

This potential is regarding the acidic gases that are released into the atmosphere or the acidic gases that formed due to the non-acid components reactions. These acidic gases have negative impacts on the plants as well as on the soils when they absorb the acid rain. For example, it can cause leaf damage to the plants and also it can decrease the availability of plant nutrients in the soil and thus will affect plants growth. In addition this potential can be measured by (mole of H+[25] equivalent) or by (kg SO2[26] .Eq). [54].
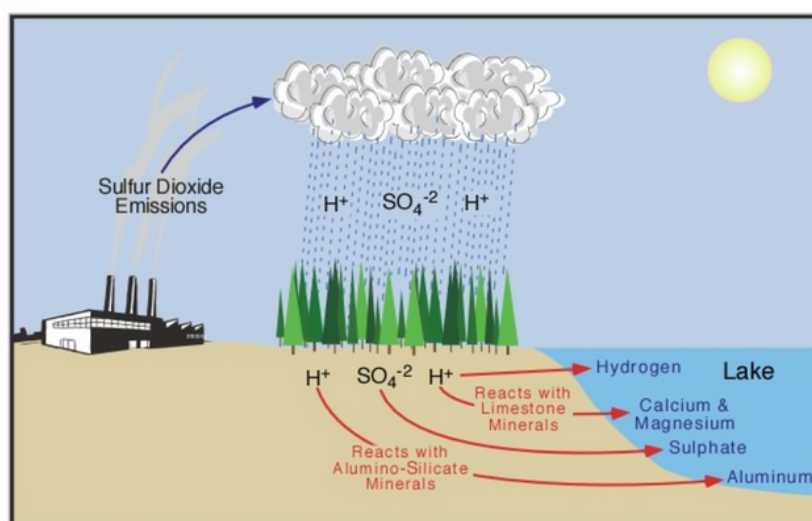
Figure 40: Lake Acidification [55]

Additionally, the acidification potential can be expressed in terms of the H+ potential of the Sulfur Dioxide. Where, V_a and V_{SO_2} are the acidification potentials of component

---

[24] Non Methanic Volatile Organic Components
[25] Cationic Form of Atomic Hydrogen
[26] Sulfur Dioxide

(a) and component SO2 respectively. Likewise, M_a and M_{SO_2} are the masses of substance (a) and substance SO2 [54].

$$AP_a = \left.\frac{\dfrac{V_a}{M_a}}{\dfrac{V_{SO_2}}{M_{SO_2}}}\right.$$

Furthermore, the table below shows the results of the life cycle assessment of the acidification potential (according to the CML 2001 to January 2016 assessment methodology) for the solar hybrid PV/T system's processes and raw materials. Additionally, this table only shows the elementary flows of the system (the input and output flows). Likewise, all these values were measured by (kg SO2 .Eq).

	Flows	Emissions to Air	Emissions to Fresh water	Emissions to Industrial Soil
Diesel Mix At Refinery	0.000118	0.000118	4.45×10^{-12}	7.73×10^{-18}
Electricity Grid Mix	0.429	0.429	8.91×10^{-8}	1.86×10^{-13}
Kerosene / Jet A1 at Refinery	0.0276	0.0276	1.86×10^{-9}	1.86×10^{-15}
Copper Mix	0.113859	0.113859	8.233×10^{-7}	4.85×10^{-14}
Glass Fibre	0.0554	0.0554	8.39×10^{-8}	5.98×10^{-14}
Aluminium Profile	0.0747	0.0747	2.77×10^{-7}	1.59×10^{-14}
Commercial Waste	0.000892	0.000892	3.35×10^{-7}	3.67×10^{-16}
Cargo Plane, 65 t Payloads	0.13	0.13	0	0
Truck	0.0011	0.0011	0	0
Polyethylene	3.83×10^{-8}	3.83×10^{-8}	0	0
Polyurethane Rigid Foam	0.0702	0.0702	0	0
Solar Hybrid PV/T System	Total = 0.913	Total = 0.913	Total = 1.61×10^{-6}	Total = 3.1310^{-13}

Table 23: Acidification Potential of Solar PV/T Hybrid System [kg SO2 .Eq]
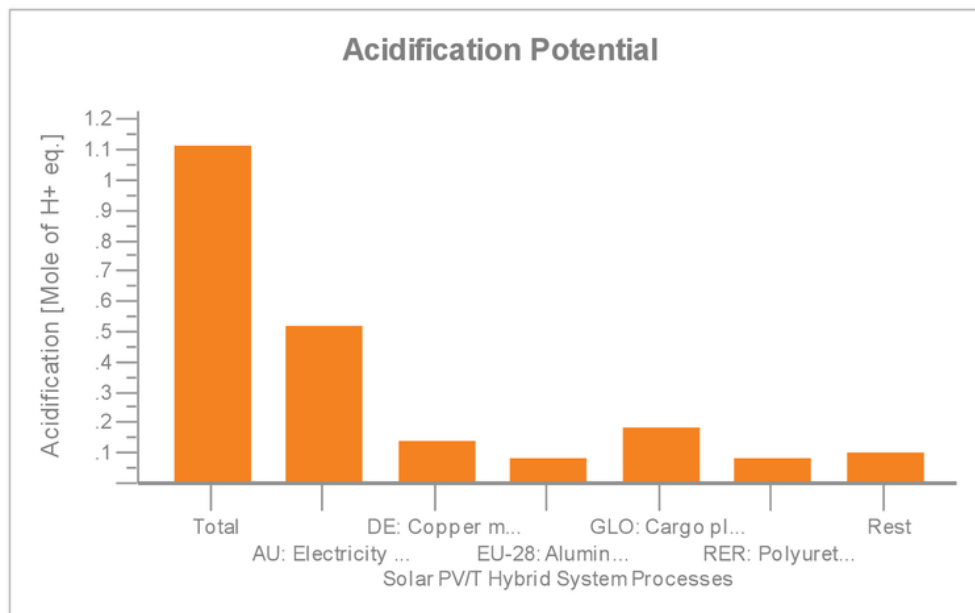
Figure 41: Acidification Potential [Mole of H+ eq.]

Figure 41 shows the acidification potential results of all the processes and materials associated with the solar PV/T hybrids system. According to the chart, all the processes and materials in the solar PV/T hybrid system generated 1.12 mole of H+ (Cationic Form of Atomic Hydrogen). The amount of emissions generated from electricity grid mix process is equal to 0.519 mole of H+, which account for 46.3% of the total emissions that generated from the solar hybrid PV/T system. Likewise, the cargo plane, aluminum profile, copper, and polyurethane emitted 0.186, 0.0854, 0.139, and 0.0828 mole of H+ respectively. The aluminum profile was used to manufacture the metal frame and water pump and the copper mix to manufacture the heat pump, heat exchanger, and the pipes. In addition, the emissions of the other processes and materials contribute 9.2% of the total emissions that generated from the PV/T system.

3.5.7 Eutrophication Potential (EP)

The eutrophication can be defined as the nutrients enrichment at particular place. This potential can cause growth for some photosynthetic organisms and fertilization

57

for the soil and the lakes through some emissions such as, phosphate (PO_4^{-3}), and ammonium (NH_4^+), nitrite (NO_3^-), nitrous oxide (N_2O) [56]. The eutrophication potential can be divided into to two regions, aquatic or terrestrial. There are many factors contribute to the eutrophication potential. For example, the waste water, air and water pollutants and the fertilizing in agriculture. The fertilization consists of some nutrients such as, Potassium (K), Phosphorus (P), and Nitrogen (N). These nutrients are necessary for the growth of the plants [57]. The air pollutants in the water cause a rapid growth of the algae and this rapid growth prevents the sunlight to reach the bottom of the lakes, leads to reduce the production of oxygen in the water as well as the photosynthesis. As a result, lack of oxygen causes the death of many aquatic plants and other organisms. [58]. Additionally, the eutrophication also leads to loss of food and habitat for many aquatic plants and organisms in the lakes and waterways as shown in figure 43 [59]. Figure 42 describes how the air pollution, waste water and fertilization negatively affect the lakes and waterways.
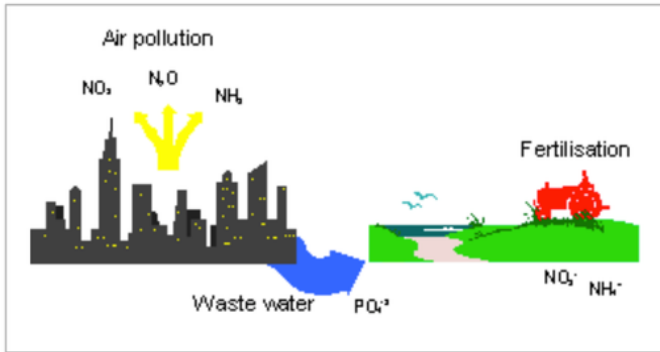
Figure 42: Eutrophication Potential [58]
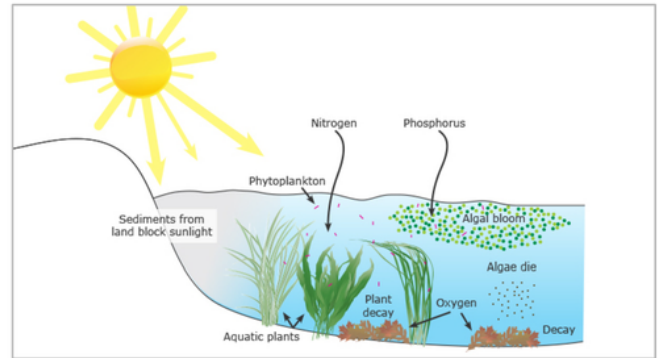
Figure 43: Eutrophication and Basic Nutrients [59]

In addition, the eutrophication potential can be calculated by using the formula below. Where EP_i is the eutrophication potential of the species (i) and is the species emissions. By using this formula the eutrophication potential in this situation can be measured in kg of phosphate (PO_4^{-3}) equivalent [56].

$$EP = \sum_i EP_i \times B_i$$

58

Moreover, figure 44 shows the terrestrial eutrophication potential results for the solar hybrid PV/T system. The terrestrial eutrophication potential can be measured by mole of nitrogen equivalent (Mole of N eq.). The electricity mix grid process was used to assemble the raw materials as well as the 7 main components of the solar hybrid PV/T system. This electricity process generated 1.15 mole of nitrogen equivalent. This process produced the largest amount of nitrogen compared to other processes of the PV/T system. The cargo plane that used to transport the solar hybrid PV/T system generated 0.988 mole of nitrogen equivalent While, The amount of nitrogen generated from the aluminum profile to manufacture the metal frame is 0.128 mole of nitrogen equivalent. The polyurethane that used to manufacture the insulation layer generated 0.143 mole of nitrogen equivalent and the copper mix generated 0.209 mole of nitrogen equivalent. This copper was used to manufacture the water pump and heat exchanger. The emissions of other processes and materials contribute 6.34% of the total emissions of nitrogen that generated from the PV/T system.
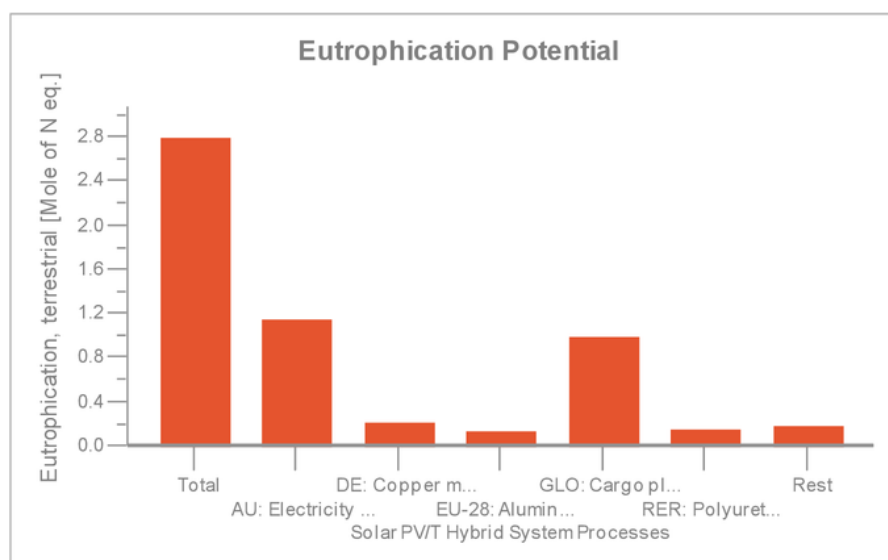
Figure 44: Eutrophication Potential (Terrestrial) [Mole of N eq.]

There are two types of aquatic eutrophication potential, the seawater (marine), and the fresh water. The chart in figure 45 displays the results of marine eutrophication potential of the solar hybrid PV/t system. This particular type can be measured by (kg of nitrogen equivalent). The amount of nitrogen emissions generated from electricity grid mix process is 0.105 kg of nitrogen and from the cargo plane is 0.0901 kg of nitrogen. The emissions of these two processes contribute approximately 75% of the total emissions that generated from the solar hybrid PV/T system. Additionally, the amount of nitrogen emissions that generated from the polyurethane is 0.0185 Kg of nitrogen and from the aluminum profile is 0.0118 kg of nitrogen. The aluminum profile was used to make the metal frame and the hot water pump. Also, the copper that used to make the tubular heat exchanger and the hot water pump generated 0.02 kg of nitrogen. Consequently, the total amount of nitrogen that generated from the solar hybrid PV/T system is equal to 0.262 kg of nitrogen.
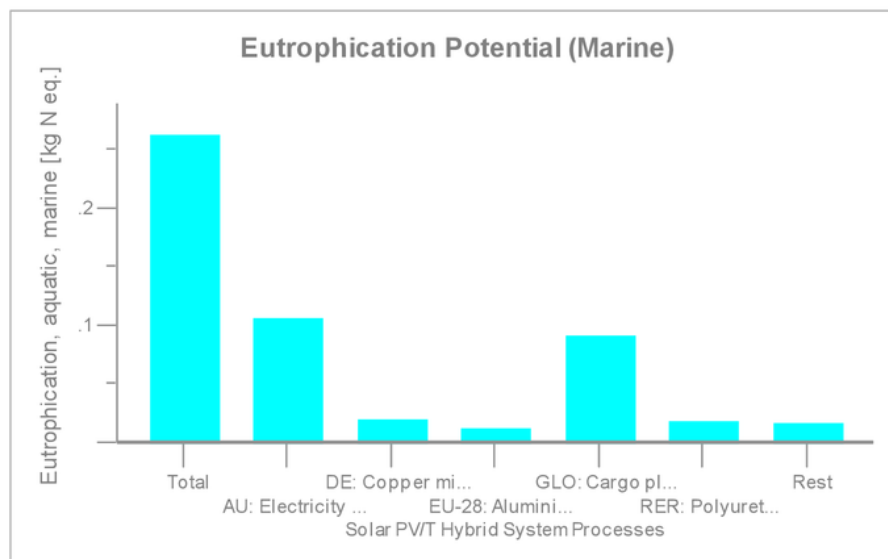
Figure 45: Eutrophication Potential (Aquatic, Sea Water) [kg N eq.]
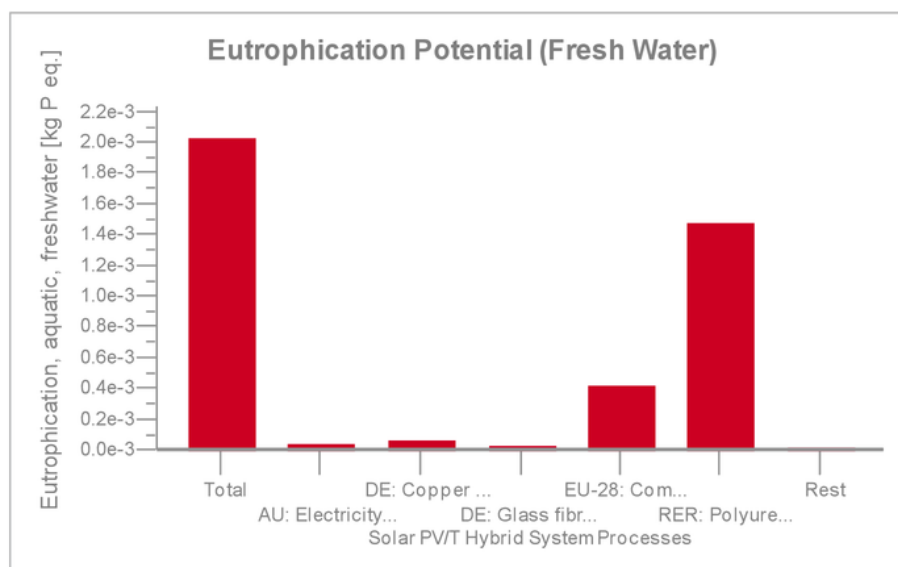
Figure 46: Eutrophication Potential (Aquatic, Fresh Water) [kg P eq.]

Furthermore, the difference between the fresh water eutrophication potential and marine eutrophication potential is the measuring unit. The fresh water eutrophication potential must be measured by kg of phosphorus equivalent [60]. Table 24 summaries the chart in figure 46 that shows the phosphorus emissions for all the raw materials and processes of the solar hybrid PV/T system.

Raw Material / Process of the Solar PV/T System	Phosphorus Emission Quantity [kg P eq.]	Relative Contribution
Electricity Mix Grid	0.0374×10^{-3}	1.85%
Copper Mix	0.0532×10^{-3}	2.63%
Glass Fibre	0.0258×10^{-3}	1.27%
Commercial Waste (Landfill)	0.419×10^{-3}	20.72%
Polyurethane	1.47×10^{-3}	72.70%
Rest	0.0165×10^{-3}	0.81%
Solar PV/T System	Total = 2.022×10^{-3}	

Table 24: The phosphorus Emissions of Solar Hybrid PV/T System

61

Table 24 indicates that the highest amount of phosphorus emission was generated from the polyurethane foam. This material was used to manufacture the insulation layer for the solar panel.

3.5.8 Eco Toxicity Potential

The eco toxicity is the study of the ecotoxicology field that refers to the chemical and ecological stressors that affect the ecosystems such as, the fresh water ecosystem. This field consists of both toxicology and ecology. Likewise, the study of toxic effects is considered one of the branches of the eco toxicology. These effects basically caused by the artificial and natural pollutants that can affect the plants, animals, and bacterium. It also have some impacts on the substructure of the organism for example, it can cause some diseases to animals such as the hepatotoxicity. There are many environmental toxicants that can affect the organisms such as Phosphates (PO_4^{-3}), oil (oil spilling) or petroleum hydrocarbon, pesticides and some metals. Additionally, the production of some metals such as aluminum and copper can also cause some artificial pollutants [61]. The eco toxicity potential can be measured in (CTUe)[27].
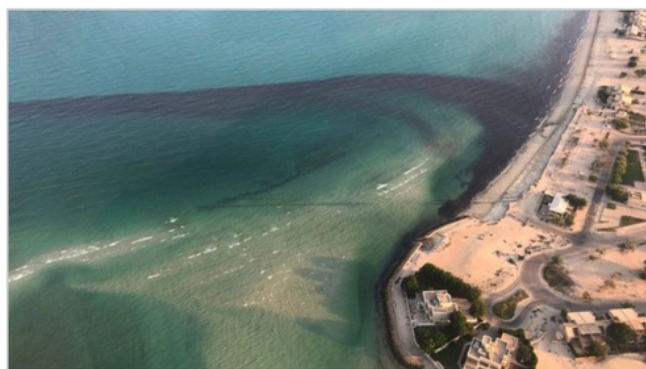
Figure 47: Oil Spilling in Kuwait City, Kuwait [62]
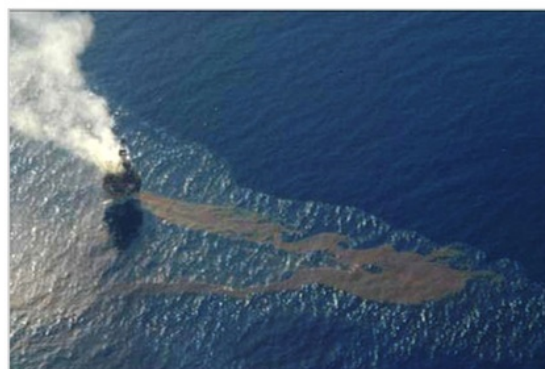
Figure 48: Oil Spilling in Timor Sea Near Australia [63]

---

[27] Comparative Toxic Units for Aquatic Eco toxicity

Moreover, figure 49 displays the results of the eco toxicity potential of the solar hybrid PV/T system. The amount of emissions that generated from the whole system is 132 CTUe in the fresh water. Table 25 shows eco toxicity potential results of all the materials and processes of the hybrid PV/T system.

Raw Material / Process of the Solar PV/T System	Aquatic Eco Toxicity Emissions (Fresh Water) [CTUe]	Relative Contribution
Electricity Mix Grid	36.3	27.50%
Kerosene / Jet A1 at Refinery	3.37	2.55%
Copper Mix (For Production of Metal Frame)	2.27	1.72%
Copper Mix (For Production of water pump and Heat Exchanger)	80.34	60.86%
Polyurethane	8.33	6.31%
Rest	1.24	0.95%
Solar PV/T System	Total = 132	

Table 25: Aquatic Eco Toxicity Emissions of Solar Hybrid PV/T System
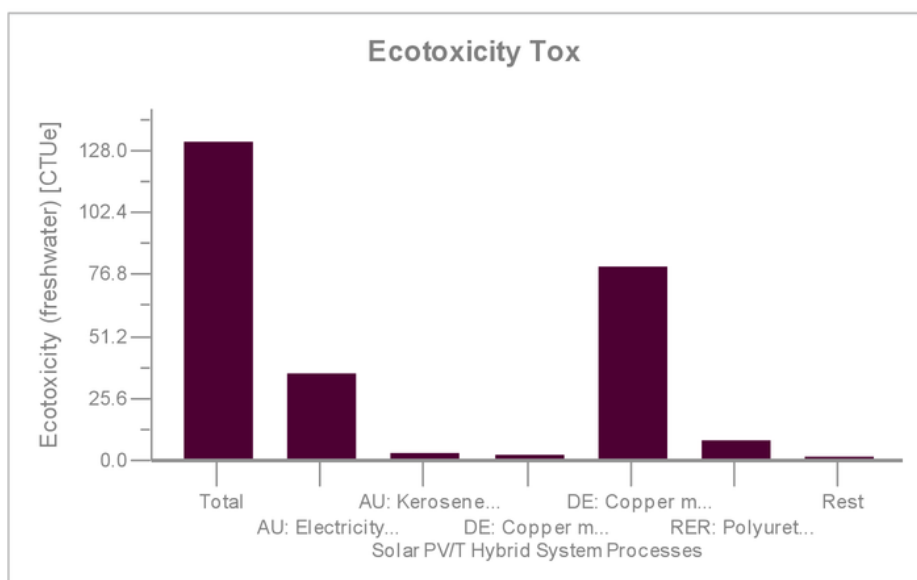
Figure 49: Eco Toxicity Potential of Hybrid PV/T System Processes and Materials [CTUe]

3.6 Life Cycle Plan Model of PV System

The figure below shows the life cycle plan model of the solar PV system. The only difference between the solar PV system and solar hybrid PV/T system is that the PV system does not contain the thermal part that contains the water pump, tank, heat exchanger, and piping system. Moreover, the life cycle plan model for PV system can also be divided into 7 phases exactly as the PV/T system was divided from the raw material acquisition phase to the end of life phase.
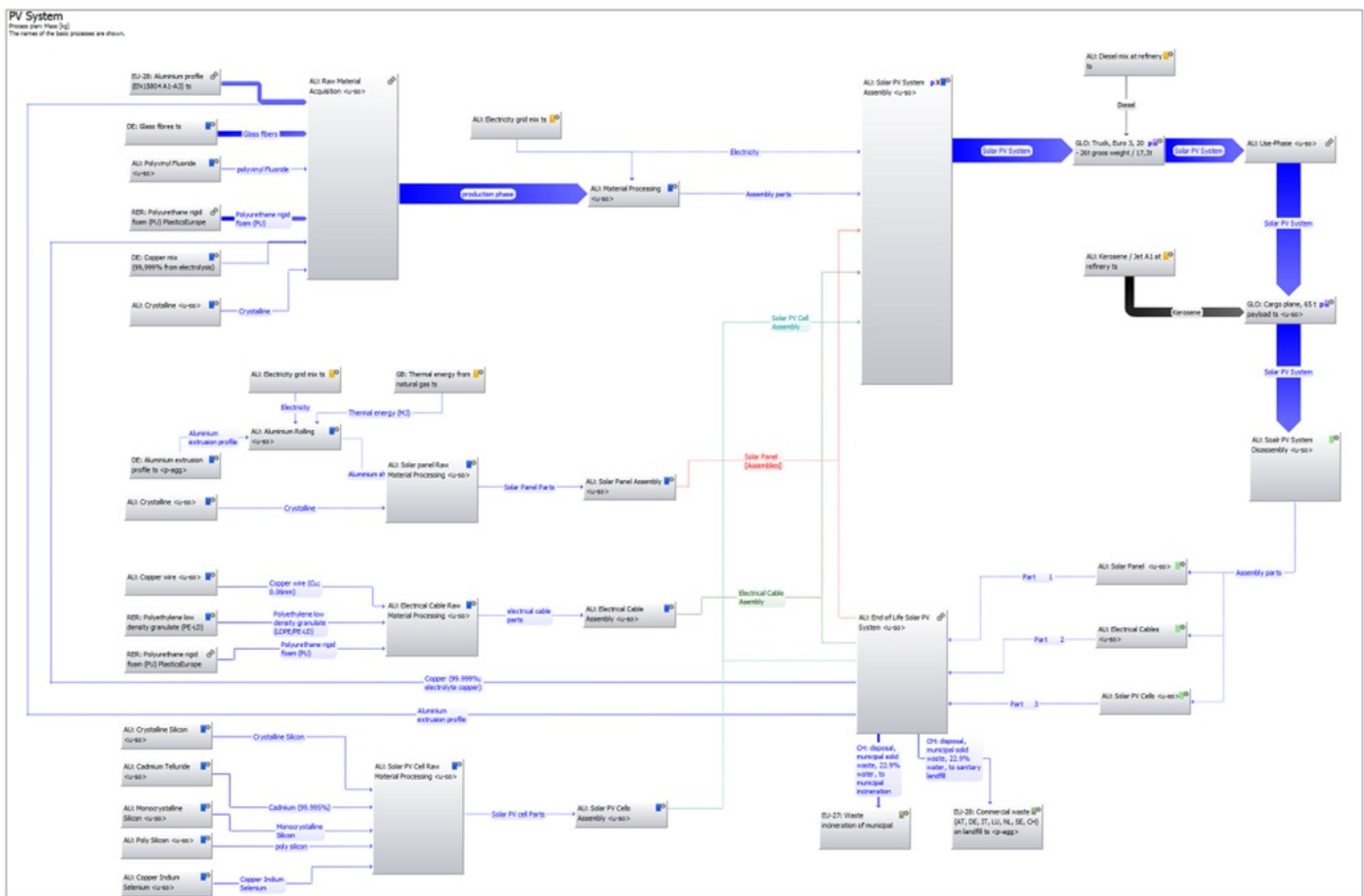
Figure 50: Life Cycle Plan Model of Solar PV System

Figure 51: Life Cycle Plan Model of Solar PV System (Divided into 6 parts)

PV System

Process plan: Mass [kg]
The names of the basic processes are shown.
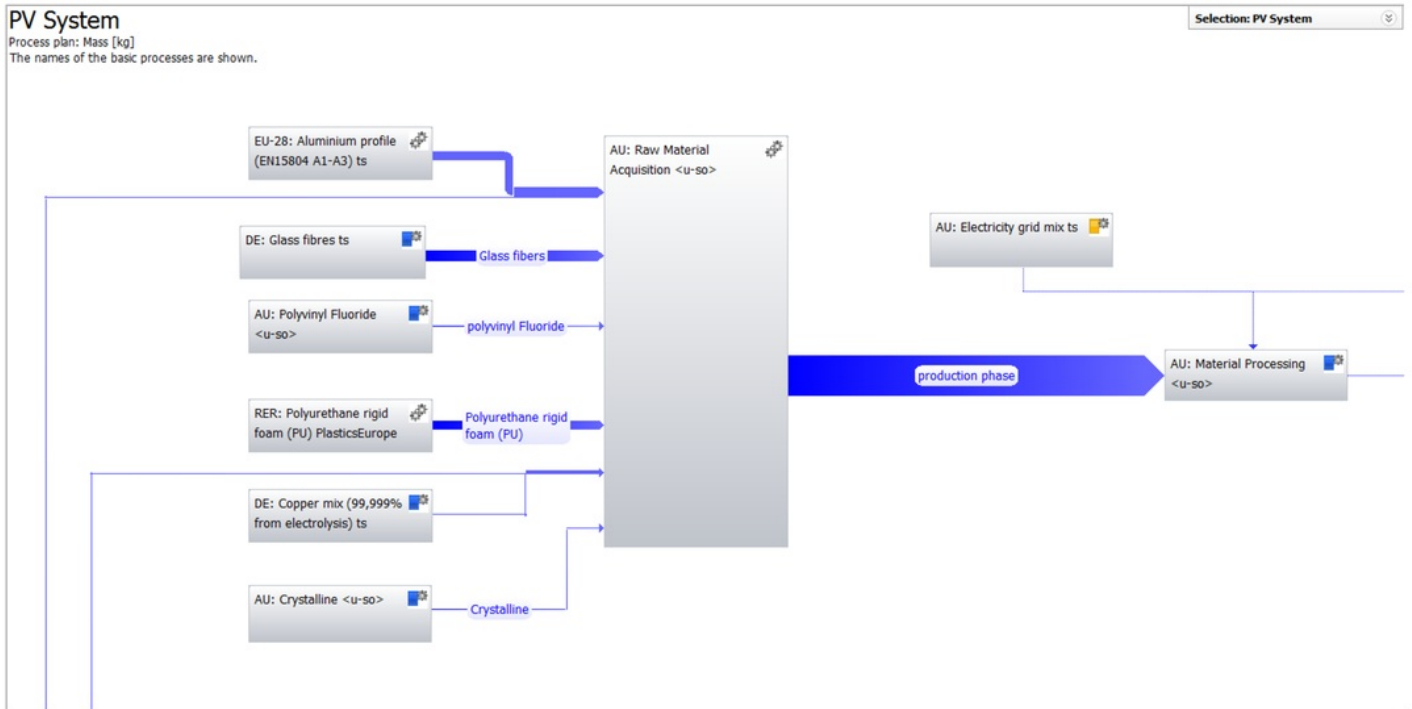
Figure 52: Life Cycle Plan Model of Solar PV System (Part 1)
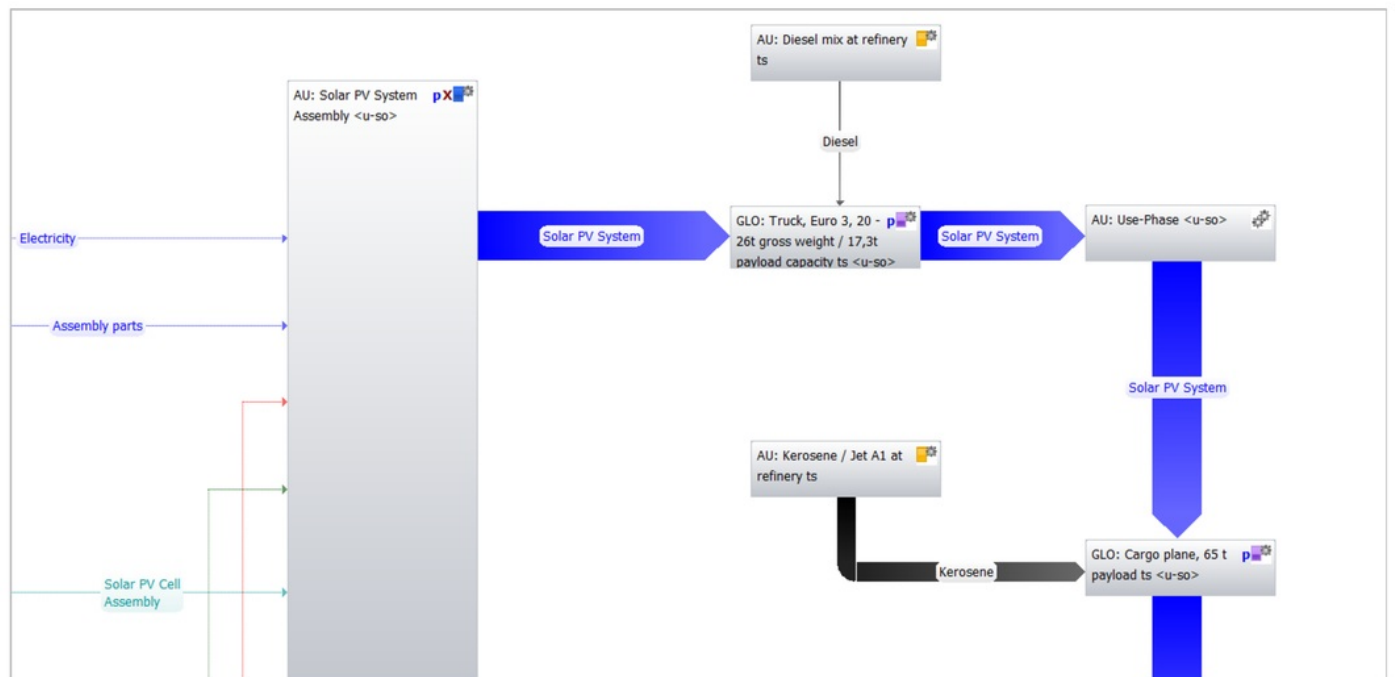
Figure 53: Life Cycle Plan Model of Solar PV System (Part 2)
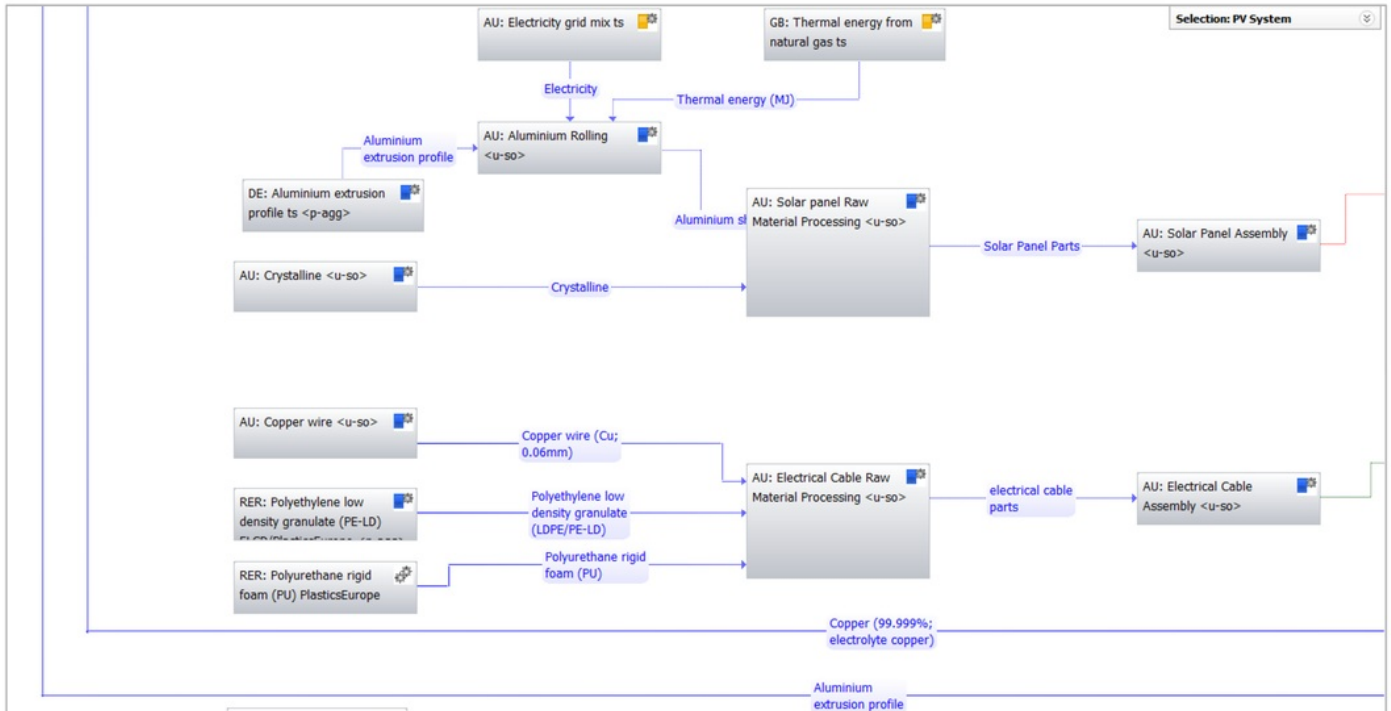
Figure 54: Life Cycle Plan Model of Solar PV System (Part 3)
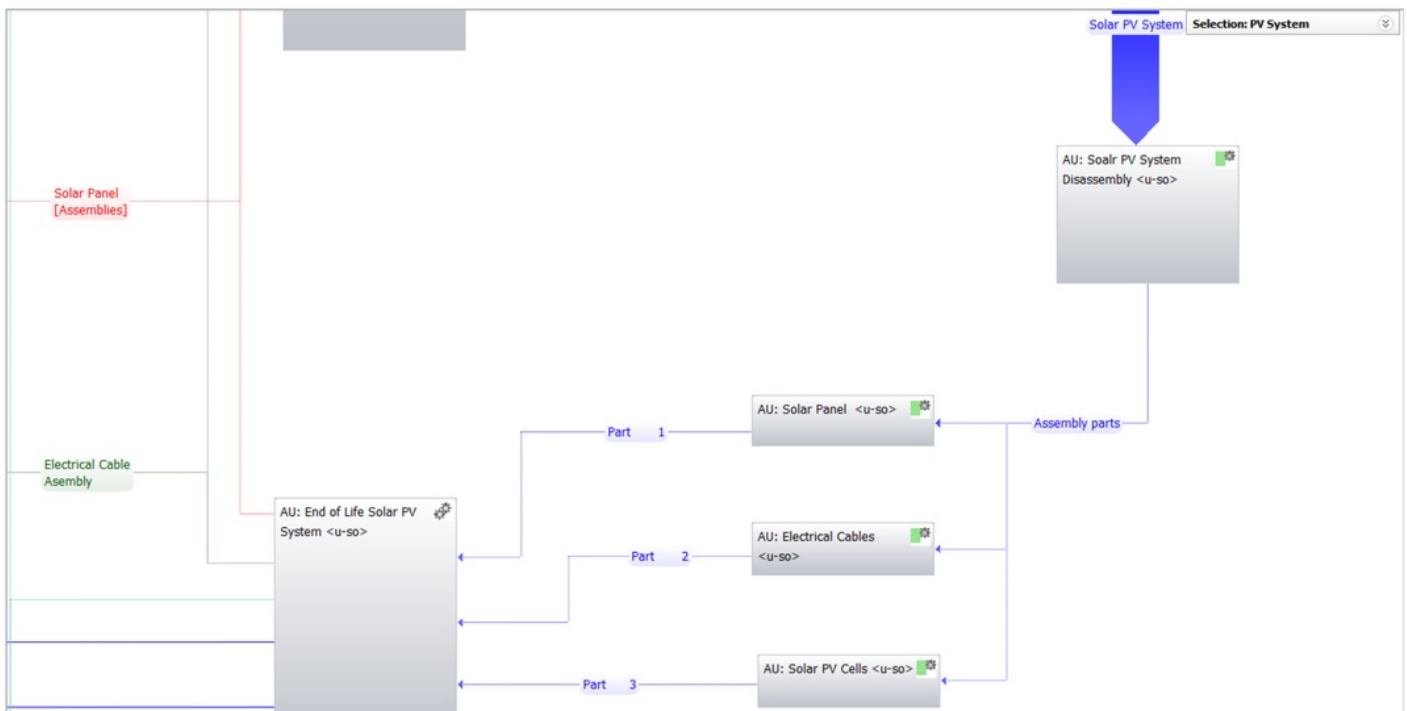
Figure 55: Life Cycle Plan Model of Solar PV System (Part 4)

67
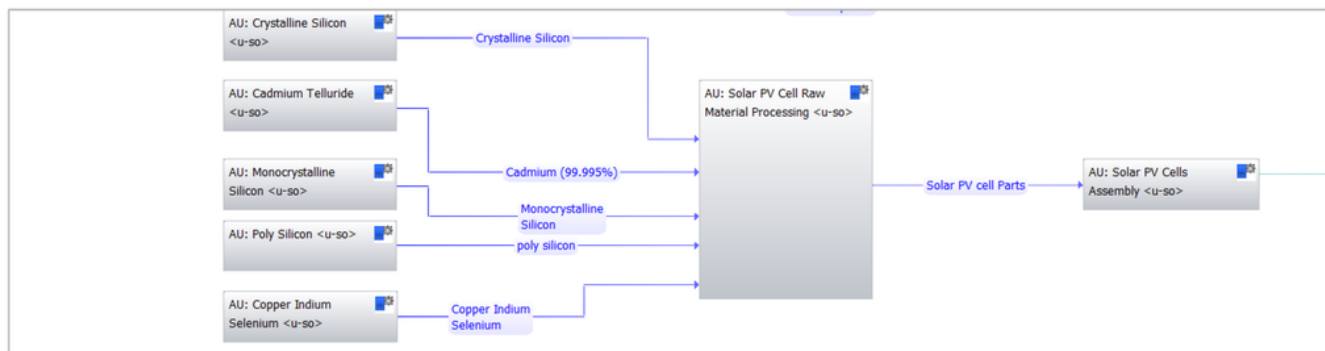
Figure 56: Life Cycle Plan Model of Solar PV System (Part 5)

Figure 57: Life Cycle Plan Model of Solar PV System (Part 6)

3.7 Comparison Between PV/T System and PV System

There are many differences between the solar PV system and the solar PV/T hybrid system. For instance, the amount of the greenhouse gas (GHG) emissions that generated by the PV system is less than the amount of GHG emissions generated by the hybrid PV/T system. Likewise, the solar PV/T hybrid system generated more electrical energy than the solar PV system. In addition, the environmental impact assessment was determined for both PV and PV/T systems, according to the CML 2001

to January 2016 assessment methodology. The environmental impact categories are: Global Warming Potential, Primary Energy Demand (Non Renewable and Renewable Resources), Acidification Potential, Eutrophication Potential, Eco toxicity Potential, Human Toxicity Potential and Photochemical Ozone Creation Potential. Moreover, the concepts of all these Potentials were explained in section 3.5.

3.7.1 Scenarios Interface and Reference Process

By using Gabi software, it is possible to consider different scenarios for a particular system. In this project, these scenarios are regarding the transportation and electricity processes associated with the solar hybrid PV/T system. Additionally, in Gabi, each life cycle plan model for any particular system should have one fixed process (reference process) so this will allow the software to calculate all the results in relation to this fixed process. Likewise, some parameters or codes must be added to the fixed process in order to activate the scenarios. For example, the fixed process of the life cycle plan model of the PV/T system was the (Solar PV/T Hybrid System Assembly Process). The figure below displays the fixed process of the solar hybrid PV/T system [42].

AU: Solar PV/T Hybrid System Assembly <u-so>   pX
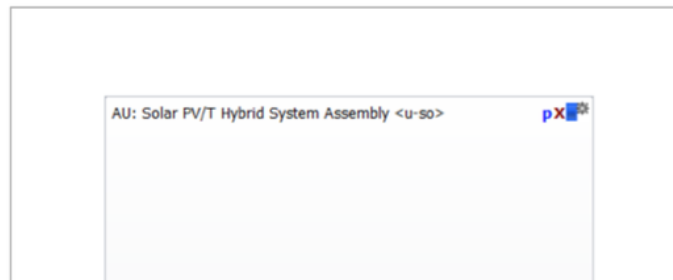
Figure 58: Fixed Process (Reference Process) of the Solar Hybrid PV/T System [42].

In fixed process the parameters must be defined clearly after defining the input and output flows of this process. For the solar hybrid PV/T system, the parameters of electricity process and for system mass were defined.

The figure below shows the dashboard of the fixed process of the solar hybrid PV/T system.
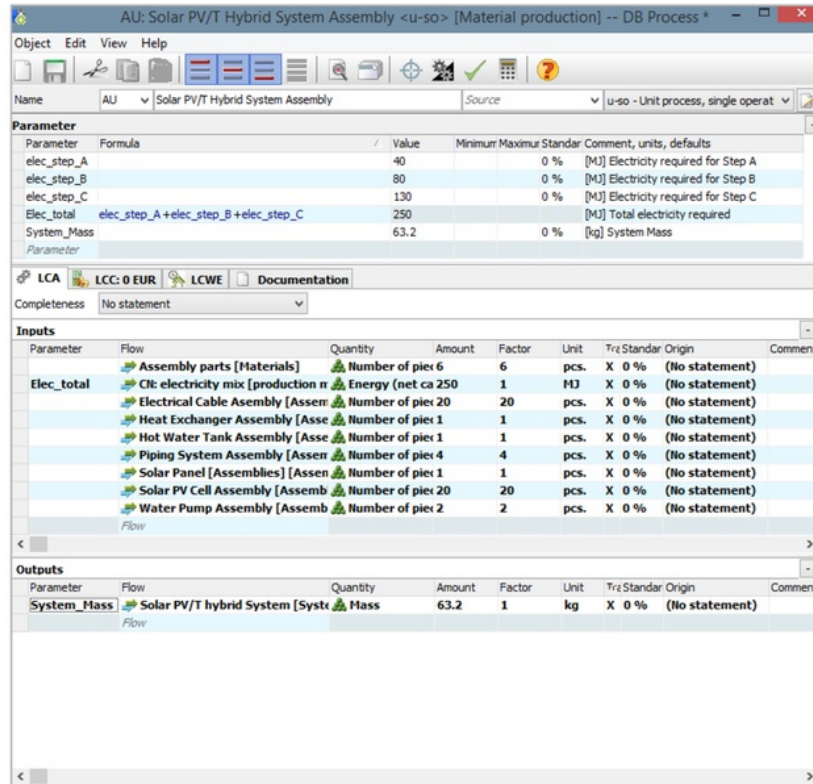
Figure 59: Dashboard of Fixed Process of Solar Hybrid PV/T System [42].

The next 2 figures show the fixed process of the solar PV system and the dashboard of the fixed process or the reference process.
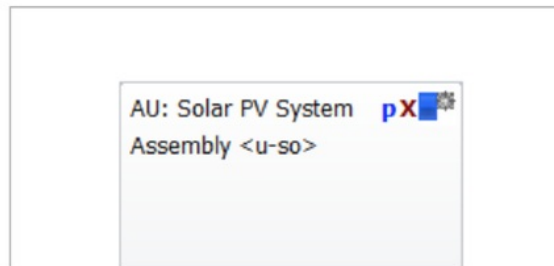
Figure 60: Fixed Process (Reference Process) of the Solar PV System [42].
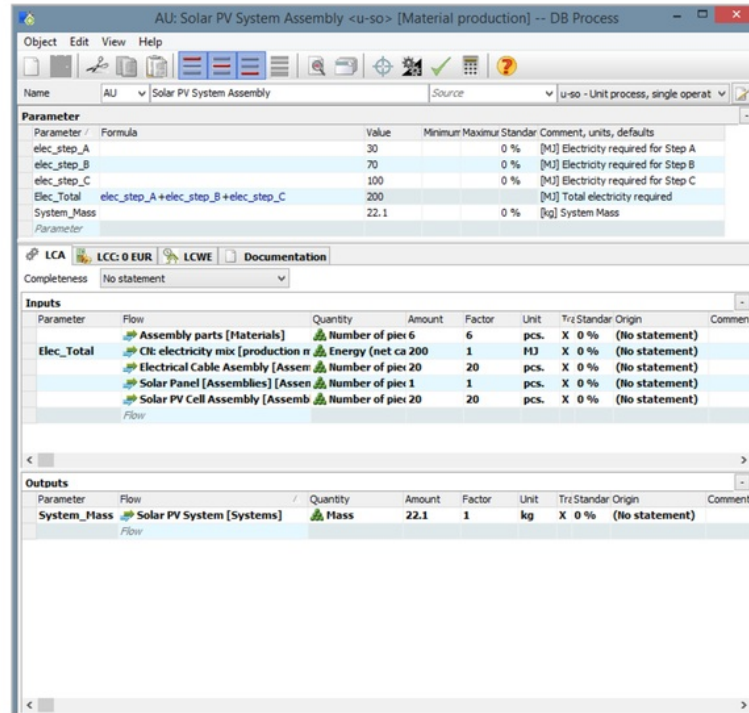
Figure 61: Dashboard of Fixed Process of Solar Hybrid PV/T System [42]

In addition, after defining the required parameters in the fixed process for both PV/T and PV systems, then the subset and scenarios settings must be created. The next four tables below shows how to create the subset and the required scenarios as well as shows the required values for each scenario. Tables 26 and 27 show the subset table and scenarios table for the solar hybrid PV/T system respectively. Likewise, tables 28 and 29 display the subset table and the scenarios table for the PV system respectively.

				Scenarios		
Alias	**Object**	**Parameter**	**Small**	**Medium**	**Large**	**Comments and Units**
System Type	AU[28]: Solar PV/T Hybrid System Assembly <u-so>[29]	System_Mass	43	63.2	72	[kg] System Mass

Table 26: Subset Results of Solar Hybrid PV/T System [42]

---

[28] Australia
[29] <u-so>: Unit Process Single Operation

71

			Scenarios				
Alias	**Object**	**Parameter**	**Benchmark**	**Alternative 1**	**Alternative 2**	**Alternative 3**	**Comments and Units**
PV/T Hybrid System Mass							
System Type	Subset	System_Mass	Medium	Medium	Small	Large	[kg] Mass of the System
Electricity Output							
elec_step_A	AU: Solar PV/T Hybrid System Assembly <u-so>	elec_step_A	30	50	60	30	[MJ] Electricity required for Step A
elec_step_B	AU: Solar PV/T Hybrid System Assembly <u-so>	elec_step_B	70	65	55	70	[MJ] Electricity required for Step B
elec_step_C	AU: Solar PV/T Hybrid System Assembly <u-so>	elec_step_C	100	90	88	100	[MJ] Electricity required for Step C
Transport Settings							
Truck Parameters							
Truck Distance	GLO[30]: Truck, Euro 3, 20-26t gross weight / 17,3t payload capacity <u-so>	Distance	100	50	37	0	[km] distance start - end, default = 100 km
Truck Utilisation	GLO: Truck, Euro 3, 20-26t gross weight / 17,3t payload capacity <u-so>	Utilisation	0.85	0.85	0.85	0.85	[-] utilisation by mass, default = 0,85
Plane Parameters							
Plane Distance	GLO: Cargo plane, 65 t payload <u-so>	Distance	0	1250	2500	2500	[003] [km] distance travelled [max 7408 km]
Plane Utilisation	GLO: Cargo plane, 65 t payload <u-so>	Utilisation	0.66	0.66	0.90	0.66	[002] [-] capacity utilisation, default = 66%

Table 27: Scenarios Results of Solar Hybrid PV/T System [42]

Moreover, the alias column defined the name of the parameters of the transportation and electricity process. The object column defined the processes associated with the PV/T and PV systems. The parameter column represented the codes and parameters associated with the PV/T and PV systems. In addition, benchmark, alternatives 1,2 and 3 are the main scenarios of the PV/T and PV systems.

---

[30] Global.

			Scenarios			
Alias	**Object**	**Parameter**	**Small**	**Medium**	**Large**	**Comments and Units**
System Type	AU: Solar PV System Assembly <u-so>	System_Mass	19	22.1	25	[kg] System Mass

Table 28: Subset Results of Solar PV System [42]

			Scenarios				
Alias	**Object**	**Parameter**	**Benchmark**	**Alternative 1**	**Alternative 2**	**Alternative 3**	**Comments and Units**
PV System Mass							
System Type	Subset	System_Mas s	Medium	Medium	Small	Large	[kg] Mass of the System
Electricity Output							
elec_step_A	AU: Solar PV System Assembly <u-so>	elec_step_A	30	50	60	30	[MJ] Electricity required for Step A
elec_step_B	AU: Solar PV System Assembly <u-so>	elec_step_B	70	65	55	70	[MJ] Electricity required for Step B
elec_step_C	AU: Solar PV System Assembly <u-so>	elec_step_C	100	90	88	100	[MJ] Electricity required for Step C
Transport Settings							
Truck Parameters							
Truck Distance	GLO: Truck, Euro 3, 20-26t gross weight / 17,3t payload capacity <u-so>	Distance	100	50	37	0	[km] distance start - end, default = 100 km
Truck Utilisation	GLO: Truck, Euro 3, 20-26t gross weight / 17,3t payload capacity <u-so>	Utilisation	0.85	0.85	0.85	0.85	[-] utilisation by mass, default = 0,85
Plane Parameters							
Plane Distance	GLO: Cargo plane, 65 t payload <u-so>	Distance	0	1250	2500	2500	[003] [km] distance travelled [max 7408 km]
Plane Utilisation	GLO: Cargo plane, 65 t payload <u-so>	Utilisation	0.66	0.66	0.90	0.66	[002] [-] capacity utilisation, default = 66%

Table 29: Scenarios Results of Solar PV System [42]

3.7.2 Environmental Impact Assessment of PV/T and PV Systems

After creating the subset settings and scenarios settings for both PV/T and PV system, it will be easy to display the results for any environmental impact category for both PV/T and PV systems. Then these results can be compared to each other to examine which system generates more emissions than the other system. Also, the results can be compared according to different scenarios. Moreover, the PV/T and PV systems were compared to each other in terms of the selected impact categories.

3.7.2.1 Global Warming Potential (GWP)

Figure 62 and 63 show the global warming potential results of PV and PV/T systems according to the CML 2001 to January 2016 assessment. The results in each chart are displayed for 4 different scenarios: benchmark, alternatives 1, 2 and 3. Likewise, the results of these scenarios are in table 27 for PV/T system and in table 29 for PV system. The electricity output and transport settings of all the scenarios of both PV/T and PV are identical except for the mass of the systems as shown in table 27 and 29. Furthermore, according to figure 62 and 63, the values of (benchmark) scenarios of PV/T system and PV system were 175 and 138 [Kg CO_2 − Equiv.] respectively.
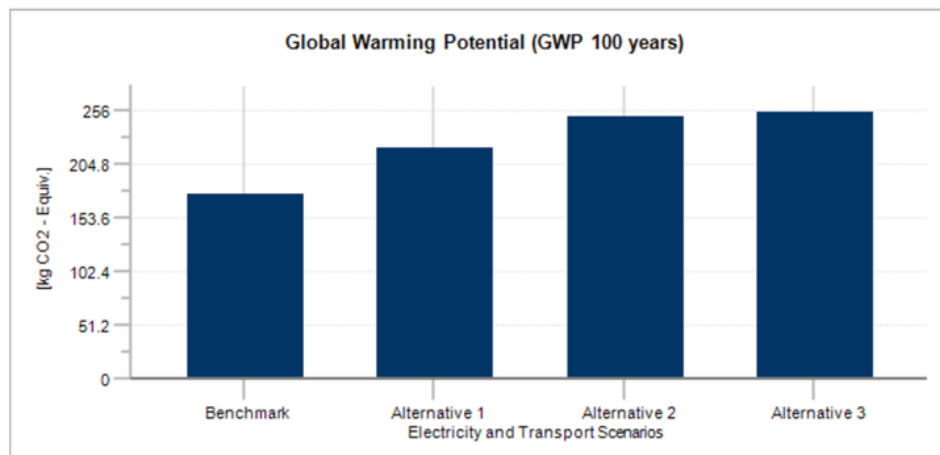
Figure 62: Global Warming Potential of Solar Hybrid PV/T System Scenarios

74

Also, the amount of carbon dioxide generated from (alternative 1) scenarios of PV/T and PV systems were 220 and 154 [Kg CO_2 – Equiv.] respectively. Additionally, the highest amount of carbon dioxide that generated from PV/T system and PV system were 254 and 169 [Kg CO_2 – Equiv.] respectively and both of them were from (alternative 3) scenario. Therefore, the hybrid PV/T system generates more carbon dioxide emissions than the PV system.
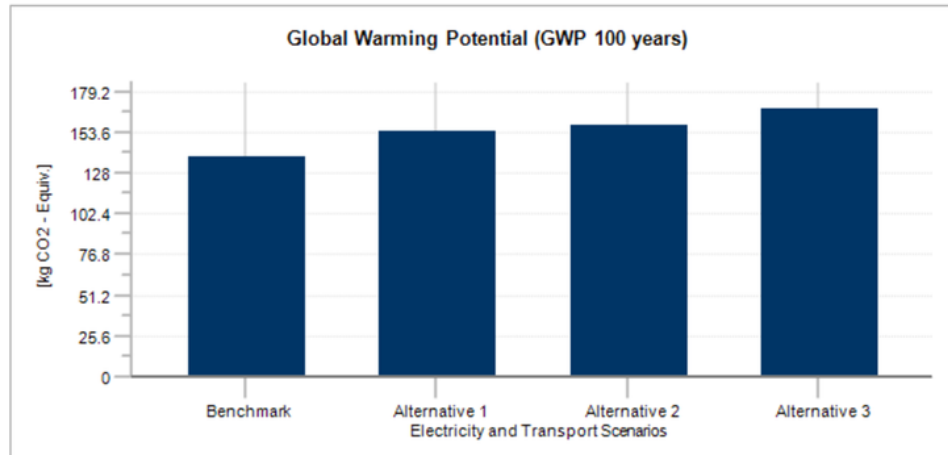
Figure 63: Global Warming Potential of Solar PV System Scenarios

	Scenarios			
	Benchmark	Alternative 1	Alternative 2	Alternative 3
Flows	176	220.25	249.71	254
Resources	-4.7	-4.75	-6.29	-4
Emissions to Air	180.7	225	256	258
Inorganic Emissions to Air	167	210	240	243
Organic Emissions to Air	13.7	15	16	15
Heavy Metals to Air	0	0	0	0

Table 30: Global Warming Potential of Solar PV/T System Flows Category [kg CO_2 – Equivalent]

	Scenarios			
	Benchmark	Alternative 1	Alternative 2	Alternative 3
Flows	138	154	158	168
Resources	-3	-3	-3	-3
Emissions to Air	141	157	161	171
Inorganic Emissions to Air	130	146	150	160
Organic Emissions to Air	11	11	11	11
Heavy Metals to Air	0	0	0	0

Table 31: Global Warming Potential of Solar PV System Flows Category [kg CO_2 − Equivalent]

Moreover, tables 30 and 31 show the input and output flows including the resources, and emissions to air of both PV/T and PV systems that contributes to the global warming potential, according to CML 2001 to January 2016 assessment methodology. These results are for 4 scenarios: benchmark, alternatives 1, 2 and 3. The negative values of the resources category indicate that there was input of the carbon dioxide (CO_2) in the input side (input flows). Additionally, the flows and emissions to air can be calculated as shown below. Likewise, all these values are in [kg CO_2-Equivalent].

$$Flows = Resources + Emissions\ to\ Air$$

$$Emissions\ to\ Air = Inorganic\ Emissions\ to\ Air + Organic\ Emissions\ to\ Air + Heavy\ Metals\ to\ Air$$

3.7.2.2 Primary Energy Demand

The primary energy is considered the form of energy that can be found in the nature. This particular energy has not been exposed to human engineered transformation or to

any conversion process. The primary energy can be divided into two types, the renewable energy, and the non-renewable energy. Each of these energies has various sources [64].

Renewable sources:

- Solar energy
- Biomass sources
- Geothermal energy

Non-Renewable sources:

- Fossil fuels such as, coals and natural gas
- Oil and petroleum
- Nuclear Energy

Moreover, figures 64 and 65 display the results of the primary energy sources for both PV/T and PV systems. These results also for 4 different scenarios: benchmark, alternatives 1, 2 and 3. This category can be measured in mega joule (MJ). In addition, table 32 compares the results of both PV/T and PV systems based on the four scenarios as shown in figure 64 and 65.

System	Scenario	Renewable Resource (MJ)	Non-Renewable Resource (MJ)
Hybrid PV/T System	Benchmark	320	2,365
	Alternative 1	323	2,976
	Alternative 2	450	3,387
	Alternative 3	267	3,454
PV System	Benchmark	317	1873
	Alternative 1	319	2096
	Alternative 2	330	2153
	Alternative 3	307	2292

Table 32: Primary Energy Sources (PV/T Against PV)
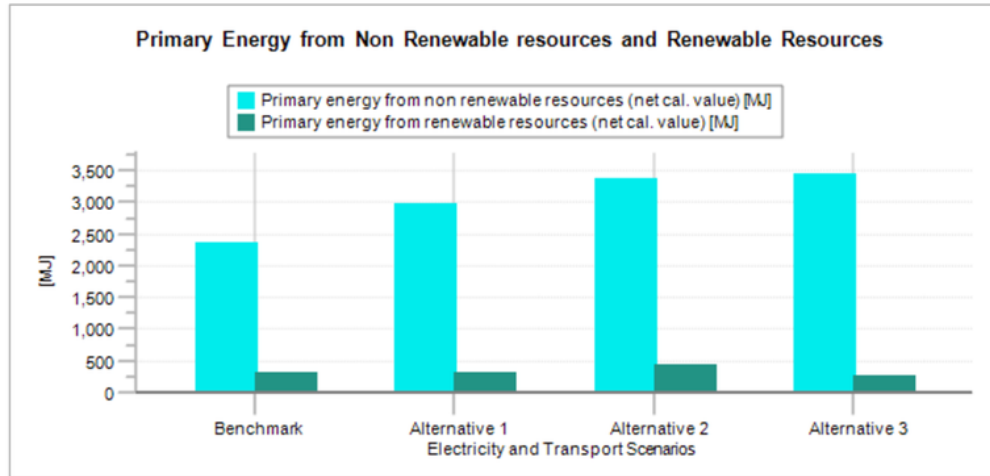
Figure 64: Primary Energy For Renewable and Non Renewable Resources of Hybrid PV/T System
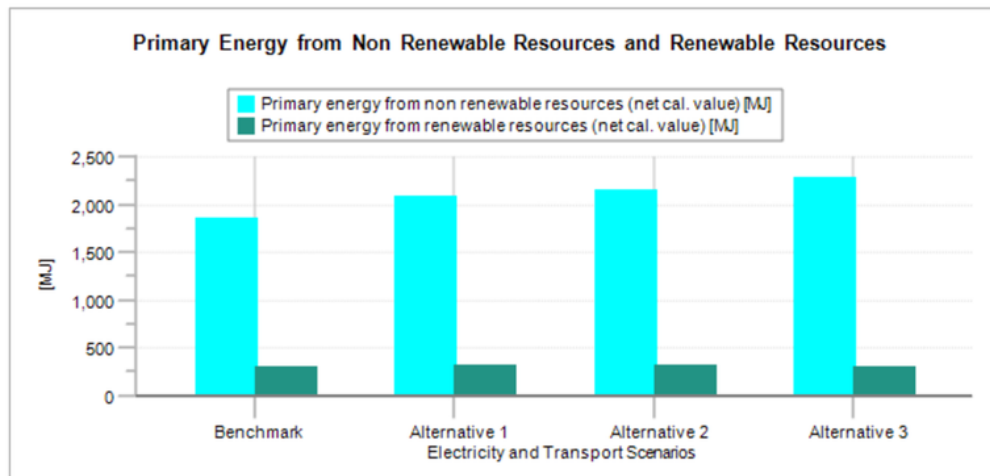
Figure 65: Primary Energy For Renewable and Non Renewable Resources of PV System

It is clear that, the amount of energy that produced from the non-renewable resources for both PV/T and PV systems are very high comparing that with the energy that produced from the renewable resources. Also, the fossil fuels, which is one of the non-renewable resources can generate very large amount of electricity. Therefore, non-renewable resources generate more energy than the renewable resources. In addition, the solar hybrid PV/T system generates more energy than the PV system as shown in figures 64 and 65 for all the scenarios except for (alternative 3) scenario. The

alternative 3 scenario of the PV system generates more energy from the renewable resources than the PV/T system as shown in table 30.

3.7.2.3 Acidification Potential (AP)

The charts in figures 66 and 67 display the acidification potential results for both PV/T and PV systems, according to the CML 2001 to January 2016 assessment methodology. The results in each chart are also displayed for four scenarios: benchmark, alternatives 1, 2 and 3. As mentioned before, this potential can be measured by (mole of H+ equivalent) or by (kg SO2 equivalent). Furthermore, alternative 2 of solar hybrid PV/T system generated the highest amount of sulfur dioxide emissions comparing that with the other scenarios of the system. Likewise, the lowest amount of emissions was generated from the (benchmark) scenario of the PV/T system, which was 0.83 kg SO2. For PV system, (alternative 2) scenario generated 0.7 kg SO2 that is lower than alternative 2 of the PV/T system. Consequently, the summary of the results of both figures 66 and 67 is that the hybrid PV/T system generated more sulfur dioxide emissions than the PV system. Table 33 summarizes all the results of the acidification potential for the scenarios of both systems.

System	Scenario	Acidification Potential (kg SO2 Equivalent)
Hybrid PV/T System	Benchmark	0.83
	Alternative 1	0.97
	Alternative 2	1.15
	Alternative 3	1.03
PV System	Benchmark	0.63
	Alternative 1	0.69
	Alternative 2	0.7
	Alternative 3	0.72

Table 33: Acidification Potential (PV/T Against PV)
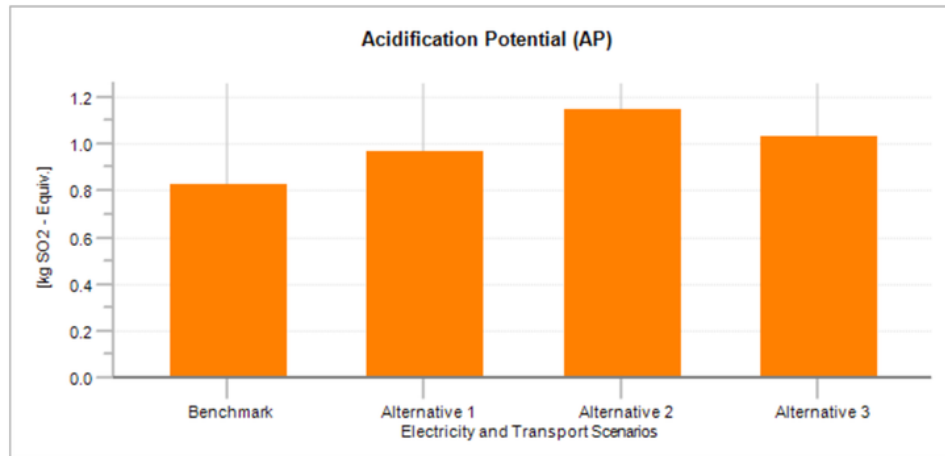
Figure 66: Acidification Potential of Solar Hybrid PV/T System Scenarios
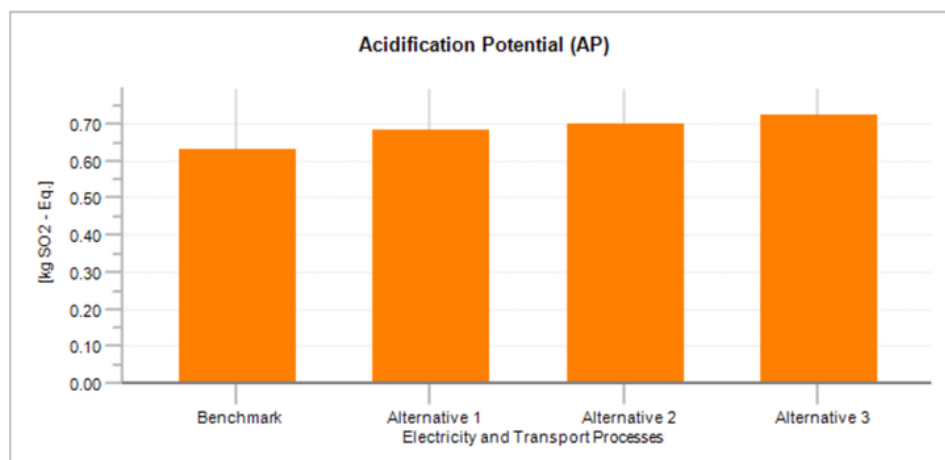
Figure 67: Acidification Potential of Solar PV System Scenarios

3.7.2.4 Eutrophication Potential (EP)

The comparison of the fresh water eutrophication potential results for the PV/T and PV systems are displayed in figures 68 and 69 respectively, according to the CML 2001 to January 2016 assessment methodology. The values of fresh water eutrophication potential of PV/T system are slightly higher than the values of PV system. Likewise, all the values are measured in kg of phosphorus equivalent.
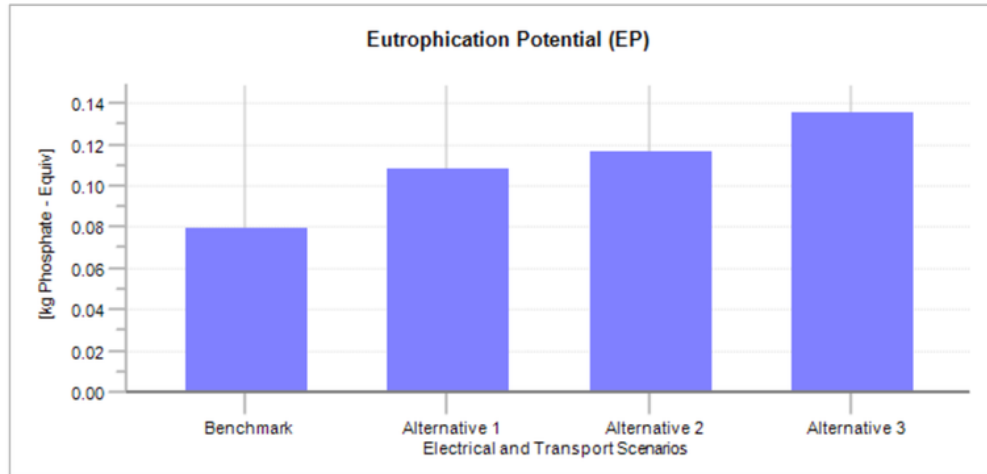
Figure 68: Eutrophication Potential of Solar Hybrid PV/T System Scenarios [kg PO_4^{-3} Equiv.]
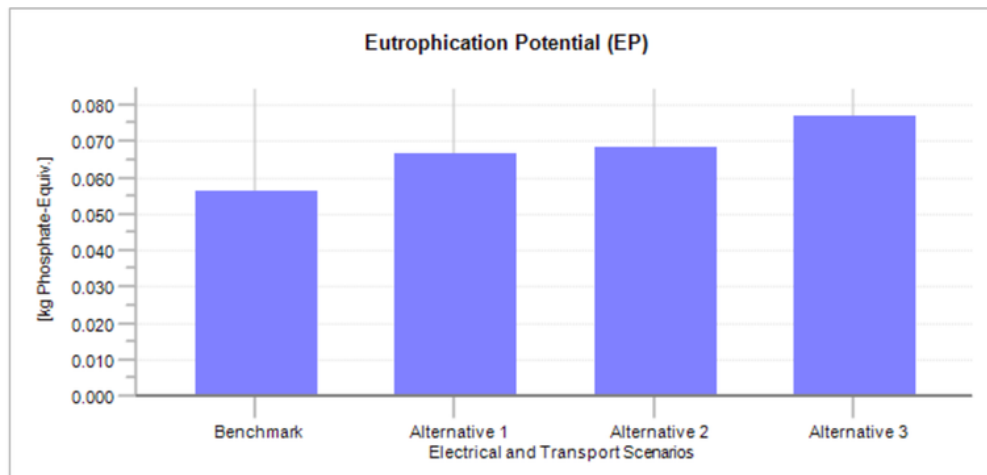
Figure 69: Eutrophication Potential of Solar PV System Scenarios [kg PO_4^{-3} Equiv.]

The value of (benchmark) scenario of the PV/T system is similar to the value of (alternative 3) scenario of PV system 0.08 kg PO_4^{-3} Equivalent. However, the other values of PV/T scenarios are higher that the values of PV as shown in table 34. The values of (Alterative 1 and 2) scenarios of PV system are exactly the same despite their

81

different electricity output and transport settings such as, the truck parameters and plane parameters, as shown in table 29.

System	Scenario	Eutrophication Potential [kg PO_4^{-3} Equiv.]
Hybrid PV/T System	Benchmark	0.08
	Alternative 1	0.11
	Alternative 2	0.12
	Alternative 3	0.14
PV System	Benchmark	0.06
	Alternative 1	0.07
	Alternative 2	0.07
	Alternative 3	0.08

Table 34: Eutrophication Potential (PV/T Against PV)

Furthermore, tables 35 and 36 show the results of input and output flows that contribute to the eutrophication potential of the both PV/T and PV systems respectively. The flows include the emissions to air, fresh water, sea water and industrial soil and agricultural soil.

	Scenarios			
	Benchmark	Alternative 1	Alternative 2	Alternative 3
Flows	0.0796	0.108	0.116	0.136
Emissions to Air	0.0589	0.0873	0.0935	0.116
Emissions to Fresh Water	0.0181	0.0182	0.021	0.017
Emissions to Sea Water	3.52×10^{-5}	5.75×10^{-5}	6.82×10^{-5}	7.8×10^{-5}
Emissions to Industrial Soil	0.0026	0.0026	0.00178	0.00296
Emissions to Agricultural Soil	0	0	0	0

Table 35: Eutrophication Potential of Solar PV/T System Flows Category [kg PO_4^{-3} Equiv.]

	Scenarios			
	Benchmark	Alternative 1	Alternative 2	Alternative 3
Flows	0.0563	0.0666	0.0683	0.077
Emissions to Air	0.0439	0.0542	0.0557	0.0647
Emissions to Fresh Water	0.0121	0.0121	0.0123	0.012
Emissions to Sea Water	1.88×10^{-5}	2.66×10^{-5}	2.82×10^{-5}	3.52×10^{-5}
Emissions to Industrial Soil	0.000226	0.000226	0.000195	0.000256
Emissions to Agricultural Soil	0	0	0	0

Table 36: Eutrophication Potential of Solar PV System Flows Category [kg PO_4^{-3} Equiv.]

3.7.2.5 Eco Toxicity Potential

The eco toxicity potential can be divided into two main potentials, the aquatic, and terrestrial potentials. Figures 70 and 71 display the result of both PV/T and PV system scenarios in [kg DCB equivalent]. The aquatic, and terrestrial potentials must be measured separately for the effects of the toxic substances on the terrestrial and aquatic ecosystems. Likewise, these potentials can be measured in [CTUe] and [kg DCB[31] equivalent] [65].

System	Scenario	Fresh Water Aquatic Eco Toxicity Potential [kg DCB Equiv.]	Terrestric Eco Toxicity Potential [kg DCB Equiv.]
Hybrid PV/T System	Benchmark	2.35	0.41
	Alternative 1	2.43	0.41
	Alternative 2	3.33	0.62
	Alternative 3	2.13	0.32
PV System	Benchmark	0.63	0.24
	Alternative 1	0.66	0.24
	Alternative 2	0.70	0.24
	Alternative 3	0.67	0.23

Table 37: Eco Toxicity Potential (PV/T Against PV)

---

[31] Dichlorobenzene
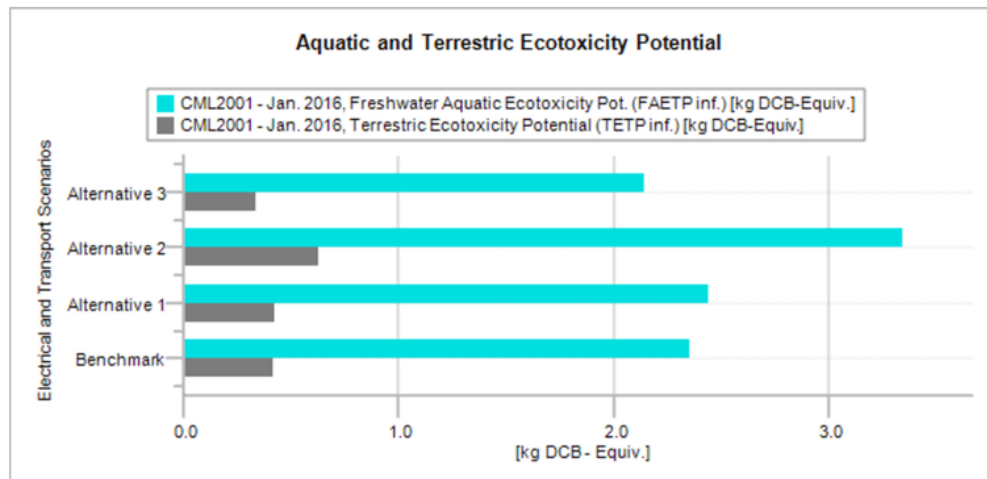
Figure 70: Eco Toxicity Potential of Solar Hybrid PV/T System Scenarios [kg DCB Equiv.]
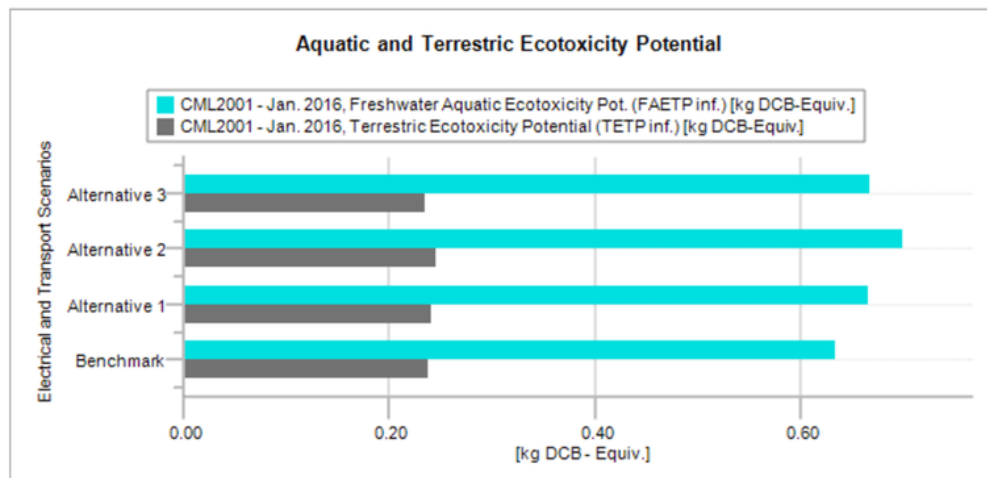
Figure 71: Eco Toxicity Potential of Solar PV System Scenarios [kg DCB Equiv.]

3.7.2.6 Human Toxicity Potential (HTP)

The comparison of human toxicity potential of both PV/T and PV system are displays in figures 72 and 73 respectively. It worth mentions that for this particular potential the scenarios values of PV system have higher values than the scenarios values of

84

hybrid PV/T system except for (alternative 2) scenarios. (Alternative 2) of PV/T system the value is 236.71 kg DBC equivalent and for PV/system is 187.91 kg DBC equivalent. As shown in these figures this potential also can be measured in (kg DBC equivalent). Table 38 summarizes the results of these two figures below.
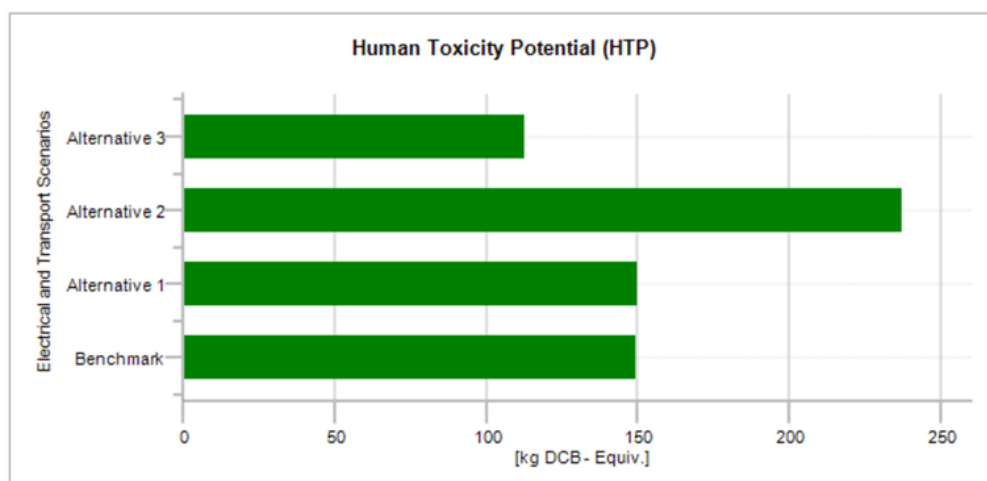
Figure 72: Human Toxicity Potential of Solar Hybrid PV/T System Scenarios [kg DCB Equiv.]
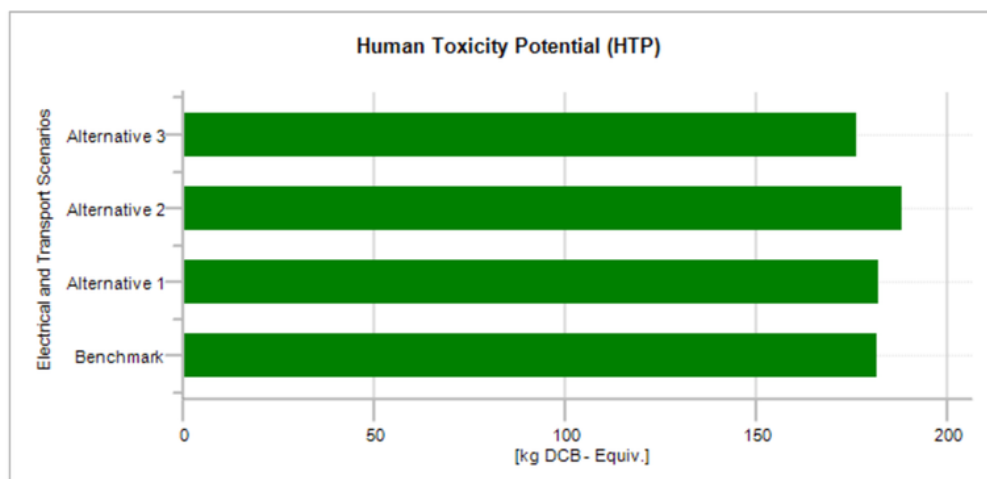
Figure 73: Human Toxicity Potential of Solar PV System Scenarios [kg DCB Equiv.]

System	Scenario	Human Toxicity Potential [kg DCB Equiv.]
Hybrid PV/T System	Benchmark	148.67
	Alternative 1	149.47
	Alternative 2	**236.71**
	Alternative 3	112.06
PV System	Benchmark	181.27
	Alternative 1	181.64
	Alternative 2	**187.91**
	Alternative 3	175.88

Table 38: Human Toxicity Potential (PV/T Against PV)

In addition, tables 42 and 43 in appendix A display the results of input and output flows that contribute to the human toxicity potential of the PV/T and PV systems respectively.

3.7.2.7 Photochemical Ozone Creation Potential (POCP)

The charts in figures 74 and 75 show the photochemical ozone creation potential results for hybrid PV/T and PV systems. The values were measured in kg ethene equivalent. As shown, the scenarios values of PV/T system are also higher than the PV system values.
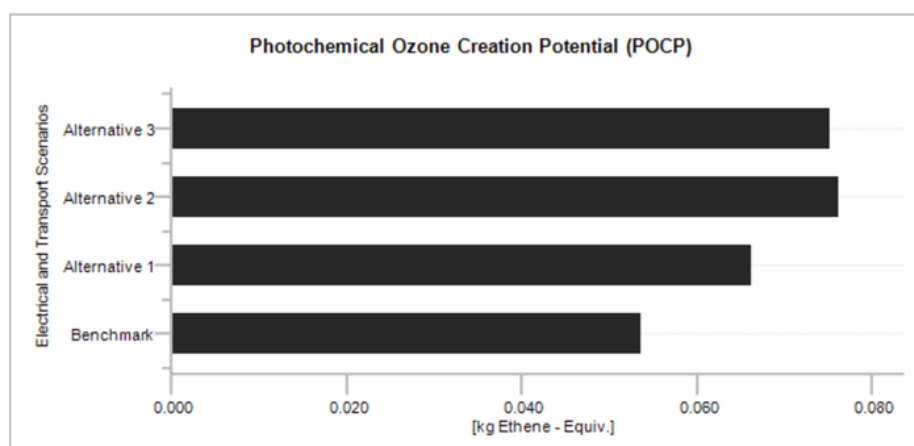
Figure 74: POCP of Solar Hybrid PV/T System Scenarios [kg Ethene Equiv.]
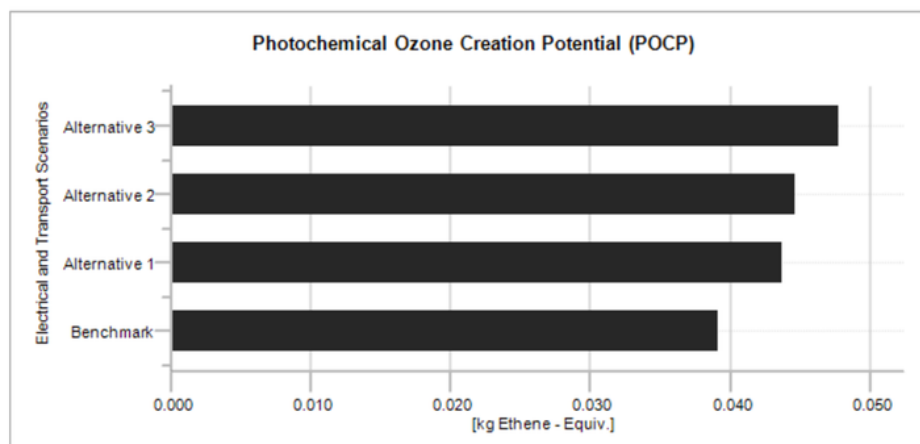
Figure 75: POCP of Solar PV System Scenarios [kg Ethene Equiv.]

Moreover, table 39 summarizes the results of Photochemical Ozone Creation Potential for 4 different scenarios for both hybrid PV/T and PV systems. Therefore, the PV/T system generated more emissions that the PV system for all the scenarios. Additionally, in appendix A, tables 44 and 45 show the results of input and output flows that contribute to Photochemical Ozone Creation Potential of the PV/T and PV systems.

System	Scenario	Photochemical Ozone Creation Potential [kg Ethene Equiv.]
Hybrid PV/T System	Benchmark	0.052
	Alternative 1	0.067
	Alternative 2	0.079
	Alternative 3	0.078
PV System	Benchmark	0.039
	Alternative 1	0.044
	Alternative 2	0.045
	Alternative 3	0.048

Table 39: Photochemical Ozone Creation Potential (PV/T Against PV)

87

Chapter 4: Energy Modeling and Experimental Modeling of PV/T System

4.1 Introduction

The achievement of the renewable energy is growing dramatically in various countries especially in developed countries. Some developed countries implemented new energy approaches in order to reduce the amount of carbon emissions as mush as possible. Recently, the hybrid renewable inventions systems such as the solar hybrid PV/T systems are very popular due to the high overall efficiency of these systems.

In addition, in the area of collectors design, there are various approaches ranged from simple approaches to complex approaches. One of the simple approaches of the solar systems is the simple mounting of photovoltaic cells on the absorber plate of the thermal collector. Likewise, the complex approaches aims to overcome the thermal efficiency as well as the electrical efficiency losses of the simple solar systems [66].

Moreover, the simple approaches of solar systems have some defects in the thermal efficiency of the solar systems. For example, the heat is not transferred properly through the photovoltaic cells to the absorber plate of the collector. Also, the long wavelength radiation that reflected on the metallic rear surface of the photovoltaic cells can reduce the thermal efficiency of the collector [67].

According to Erik Alsema [68], the solar hybrid PV/T system that produce both thermal energy and electrical energy better and more efficient than the thermal solar system. Erik assumed that the electrical efficiency of the solar hybrid PV/T collector would be between 5% and 12% when the temperature of the PV panel of the collector is between 25 °C or 77 °F and 30 °C or 86 °F. Also the average thermal efficiency would be

60% when the temperature of the PV panel is 25 °C or 77 °F. According to Gangwar et al. [69], a study by the General Electric Company in United States of America showed that there are some transmission losses in the photovoltaic output of the solar hybrid PV/T collector due to the high temperature in the collector that. This high temperature can reduce the overall efficiency of the PV/T collector.

Furthermore, the main sections that were discussed in this chapter are:

1. Solar hybrid PV/T system development.

2. Mathematical analysis of thermal and electrical energy of flat plate PV/T collector.

    -   Analysis of the flat plate PV/T collectors that includes its advantages, disadvantages, classifications, and equations of total efficiency, useful energy gain and heat removal factor.
    -   Calculations of heat removal rate and overall efficiency of the flat plate PV/T collector.

3. Energy modeling of solar hybrid PV/T system and TRNSYS tool.

    -   Simulation model of the hybrid PV/T system for Sydney and Melbourne, Australia.
    -   Simulation model of the hybrid PV/T system for Nicosia, Cyprus.
    -   Simulation model of the hybrid PV/T system for Taiwan.

4.2 Development of Solar Hybrid PV/T System

According to Bergene et al [70], the side-by-side photovoltaic and thermal collector arrays are more cost effective than the combined PV/T collector. Likewise, PV/T collector requires more space than the side-by-side photovoltaic and thermal collector in order to install it. In addition, there are some engineering problems associated with the solar PV/T system. For instance, heating of solar PV module that caused by the reflective index of the surface of the module and by the energy band level of the photovoltaic cells in the PV module. Also, increasing the heat of the PV module can be because of the absorption of low wavelength rays (infrared) rays. However, according to Gangwar et al. [69], there are many methods to improve the overall efficiency of the solar hybrid PV/T system. The first method is to develop the technology of solar photovoltaic cells in the PV/T system. For example, using the dye-sensitized solar PV cells, which can convert sunlight into electrical energy in a better way than any other types of solar photovoltaic cells. Also it can generate the electrical energy at low cost and with high overall efficiency. Likewise, the incremental cost of the PV/T collectors are less than the incremental cost of the side-by-side photovoltaic and thermal collector [71].

Figure 76: Dye-Sensitized Solar PV Cells [72]

The second method to improve the efficiency of the solar hybrid PV/T system is to cool the PV modules by air or water in order to reduce the temperature of the PV modules.

90

When the PV cells heat up, the operating voltage decreases. Therefore, the best temperature to test the solar PV panel is 25°C. This temperature is referred to the standard temperature conditions (STC). Likewise, the natural conversion is the most effective way to cool the PV panels also; this way is very cost effective. However, this way will be less effective when the ambient temperature is less than 20°C [73]. Additionally, using heat extraction device or heat exchanger is also one of the best methods to cool the PV module however; this method is expensive comparing that with other methods.

Moreover, there are many ways to increase the electrical and thermal efficiency of the solar hybrid PV/T system in order to optimize the energy outputs of this system. This can be by developing a dynamic 3D[32] and 2D models for the solar PV/T prototypes with heat exchanger. Also, it is feasible to improve the performance of the solar hybrid PV/T system and this can be achieved by using the flat or curved reflectors [74]. In addition, Y. Tripanagnostopoulos et al. [12] developed some design concepts for water type PV/T collectors and air type PV/T collectors. This study involved the solar hybrid PV/T collectors with glazing and without glazing. These collectors with glazing and without glazing can be analyzed in order to calculate the total electrical energy and thermal energy output of these collectors by using heat exchanger (heat extraction device) using the water or air as the working fluid for these collectors. Figure 77 shows the cross section of the glazed and unglazed PV/T collectors.

PV/T UNGLAZED
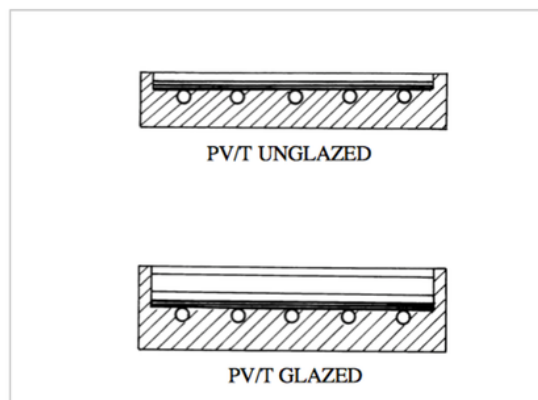
PV/T GLAZED

Figure 77: Cross Sections of PV/T Systems With and Without Glazing [75]

---

32 Three-Dimensional

In addition, there are three types of glazed air-type PV/T collectors; the single air PV/T module, the double glazed air PV/T module, and the double pass glazed air PV/T module. In the single glazed air PV/T module there is only one glass and the air enters the collector from one inlet. While, in the double glazed air PV/T module, there are two glasses and also the air enters the collector from one inlet. However, the double pass glazed air PV/T module consists of one glass and air enters the collectors from 2 inlets. Additionally, All these collectors contain polyurethane layers (insulation layer) [76]. Figure 78 displays all the types of glazed and unglazed air PV/T collectors.
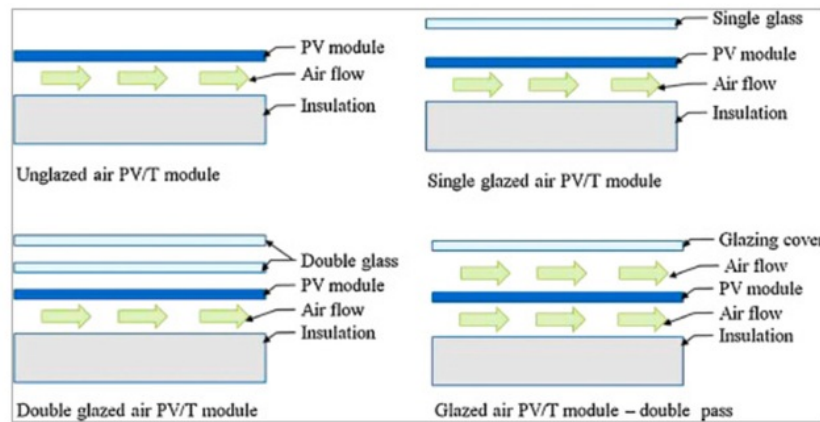
Figure 78: Types of Glazed and Unglazed Air-Based PV/T Collectors [76]

Moreover, both glazed and unglazed PV/T collectors are used for water heating especially, the unglazed, low temperature PV/T collector that used for swimming pool heating [75, 77].
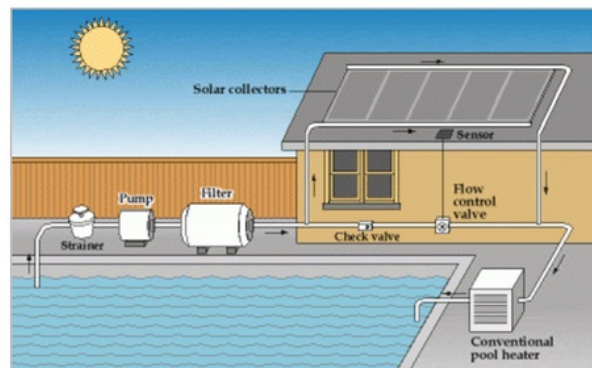
Figure 79: Solar Swimming Pool Heaters [78]

92

4.3 Mathematical Analysis of Thermal and Electrical Energy of Flat Plate PV/T Collector

4.3.1 Analysis of Flat Plate Solar PV/T Collector

The flat plate PV/T collector is also one of the water PV/T collectors that can produce heat and electrical energy simultaneously. This particular system has some of advantages and disadvantages [79]. The advantages are:

1. Very low maintenance system.
2. This system does not produce toxic waste or toxic materials.
3. The expected life span of this system approximately 25 years.

The disadvantages of the system are:
1. Very expensive system (Installation Cost).
2. The total efficiency of these collectors is low.
3. The cooling system of these collectors is not uniform.
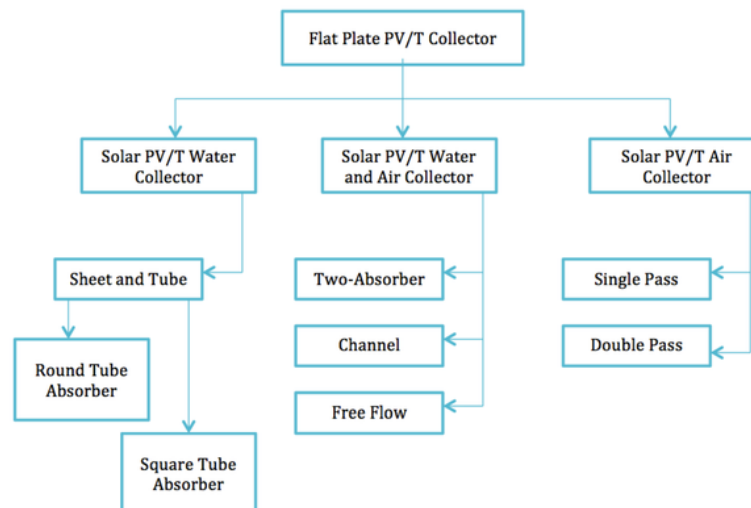
Figure 80: Classification of Flat Plate PV/T Collector [79]

In addition, the general classification of the flat plate PV/T collector is shows in figure 80. Furthermore, the solar thermal energy of the flat plate PV/T collector can be used in many ways such as; it can be used as solar swimming pool heaters, and as solar water heating system. For this particular collector there are many parameters must be taken into account and must be calculated in order to determine the thermal performance, thermal energy as well as the efficiency of the collector. These parameters are the heat input of the collector Q_i, the heat loss of the collector Q_o, the solar radiation intensity I and the useful energy gain Q_u [80]. Q_u is also known as the heat removal rate or the rate of extraction heat. Figure 81 displays the scheme of the solar energy collection system that employs the flat plate collector and tank system.
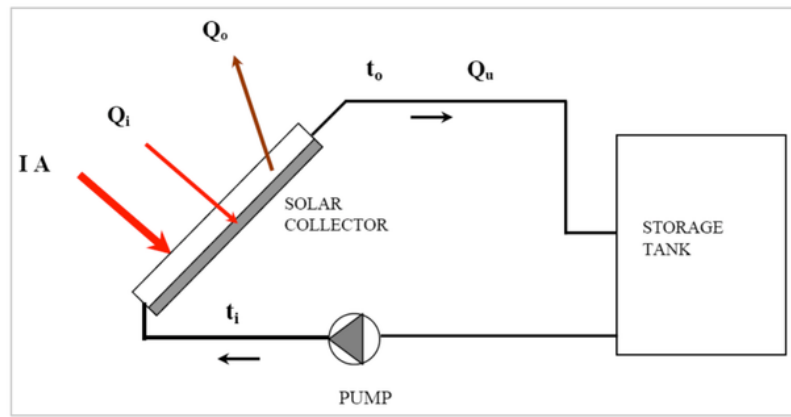
Figure 81: Solar Energy Collection System with Flat Plate and Tank System [80]

The amount of solar radiation that received by the flat plate PV/T collector or the heat input can be calculated by the formula below. Where I is the intensity of the radiation and it can be measured in W/m^2 and A is the surface area of the PV/T collector in m^2.

$$Q_i = I \times A$$

Additionally, a portion of the solar radiation is reflected to the sky, the glazing absorbed another component likewise; the other portion of the solar radiation is transmitted through the glazing to reach the absorber plate. Consequently, the solar rays percentage that enters the cover of the system and the percentage that being

absorbed are essentially the consequence of transmission rate (τ) of the collector cover and the absorption rate (α) of the absorber of the collector. Therefore, the collector heat input can be calculated as shown below. The unit of heat input is watt (W) [80].

$$Q_i = I \times (\alpha \times \tau) \times A$$

Moreover, generally when the collector absorbs the heat, its temperature increases gradually and the heat will be lost by radiation and by convection. Likewise, the heat loss can be calculated by the equation below. Where U_L is the overall heat transfer coefficient, T_c is the average temperature of the PV/T collector and T_a is the ambient temperature.

$$Q_o = U_L \times A \times (T_c - T_a)$$

Therefore, the useful energy gain Q_u is:

$$Q_u = Q_i - Q_o$$

$$Q_u = [I \times \alpha \times \tau \times A] - [U_L \times A \times (T_c - T_a)]$$

In addition, Q_u is also known as the heat extraction rate and it can be measured by the formula below. Where T_o and T_i are the outlet and inlet fluid temperatures respectively. (m) [kg/s] is the mass flow rate of the fluid that pass through the collector and C_p is the specific heat [79].

$$Q_u = m \times C_p \times (T_o - T_i)$$

The quantity that relates useful gain to the actual useful energy gain of the collector when the collector surface at the inlet fluid temperature T_i is the heat removal factor quantity. The heat removal factor F_R of the collector can be calculated by using the formula below.

95

$$F_R = \frac{m \times C_p \times (T_o - T_i)}{[I \times \alpha \times \tau \times A] - [U_L \times A \times (T_i - T_a)]}$$

Likewise, actual useful energy gain Q_u in the collector can be calculated as shown below. This equation below is known as the Hottel Whillier Bliss Equation [80, 81].

$$Q_u = F_R \times A \times ([I \times \alpha \times \tau] - [U_L \times (T_i - T_a)])$$

In order to measure the performance of the flat plate PV/T collector, it is required to calculate the total efficiency of the collector η.

$$\eta = \frac{Q_u}{A \times I} = \frac{F_R \times A \times ([I \times \alpha \times \tau] - [U_L \times (T_i - T_a)])}{A \times I}$$

$$\eta = F_R \times \alpha \times \tau - F_R \times U_L \times \frac{(T_i - T_a)}{I}$$

Moreover, the electrical energy U of the flat plate PV/T collector can be calculated by using this equation below. Where η_a and η_r are the PV array efficiencies at ambient and reference temperatures respectively. Also, B_r is the temperature coefficient of cell efficiency and τ is the glazing transmissivity [82].

$$U = I \times A \times \tau \times \eta = I \times A \times \tau \times [\eta_a - \eta_r \times B_r \times (T_i - T_a)]$$

4.3.2 Example of Heat Removal Rate and Efficiency of Flat Plate Collector

Assumption: A flat plate solar collector without cover plate, its emissivity ε, and solar absorptivity α are 0.1 and 0.95 respectively. This collector has selective absorber surface and the temperature of this surface is T_s = 393 K likewise this surface is diffuse. The effective sky temperature T_{SKY} = 263 K if the solar irradiation G_s = 750 W/m^2. Assuming that the ambient temperature in Sydney, Australia is T_a = 303 K. Likewise, the heat transfer convection coefficient is $\bar{h} = 0.22 \times (T_s - T_a)^{\frac{1}{3}}$.
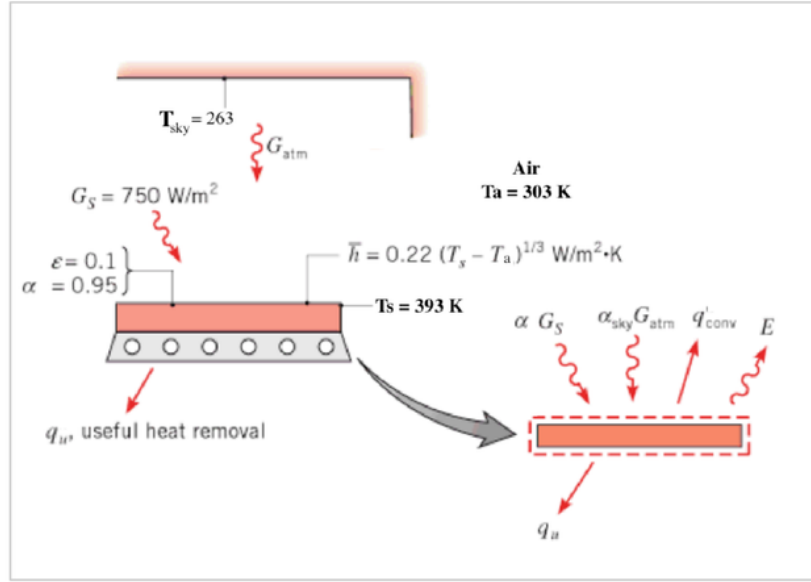
Figure 82: Flat Plate Solar Collector Diagram [83]

In order to calculate the useful heat removal rate per unit area q_u from the flat plate collector, it is necessary to use the energy balance equation on the selective absorber. Where G_{ATM} is the atmospheric irradiation and σ is Stefan's constant, which equal to 5.67×10^{-8} $(W/m^2 . K^4)$. The calculations of useful heat removal rate per unit area q_u and the efficiency η of the flat plate collector are shown below [83].

$$\dot{E}_{in} - \dot{E}_{out} = 0$$

Then

$$\alpha \times G_s + \alpha_{SKY} \times G_{ATM} - q_{CONV} - E - q_u = 0$$

$$\alpha \times G_s + \alpha_{SKY} \times (\sigma \times T_{SKY}^4) - q_{CONV} - E - q_u = 0$$

$$\alpha \times G_s + \alpha_{SKY} \times (\sigma \times T_{SKY}^4) - [0.22 \times (T_s - T_a)^{\frac{4}{3}}] - E - q_u = 0$$

$$\alpha \times G_s + \alpha_{SKY} \times (\sigma \times T_{SKY}^4) - [0.22 \times (T_s - T_a)^{\frac{4}{3}}] - (\varepsilon \times \sigma \times T_s^4) - q_u = 0$$

Assuming that $\alpha_{SKY} = \varepsilon = 0.1$

So

$$\alpha \times G_s + \varepsilon \times (\sigma \times T_{SKY}^4) - [0.22 \times (T_s - T_a)^{\frac{4}{3}}] - (\varepsilon \times \sigma \times T_s^4) - q_u = 0$$

$$q_u = \alpha \times G_s + \varepsilon \times (\sigma \times T_{SKY}^4) - [0.22 \times (T_s - T_a)^{\frac{4}{3}}] - (\varepsilon \times \sigma \times T_s^4)$$

$$q_u = \alpha \times G_s - \left[0.22 \times (T_s - T_a)^{\frac{4}{3}}\right] - \varepsilon \times \sigma(T_s^4 - T_{SKY}^4)$$

$$q_u = 0.95 \times 750 - \left[0.22 \times (393 - 303)^{\frac{4}{3}}\right] - 0.1 \times 5.67 \times 10^{-8} (393^4 - 263^4)$$

$$q_u = 515.64 \, W/m^2$$

In addition, the collector efficiency can be calculated by using the formula below.

$$\eta = \frac{q_u}{G_s} = \frac{515.64}{750} = 0.6875 = 68.75\%$$

4.4 Energy Modeling and TRNSYS Tool

4.4.1 Introduction

Energy modeling is a computer simulations process to analysis the energy of the system. This process established some models such as the LEAP [33] and MARKAL[34]/TIMES[35]. The TIMES is considered the advancement of the MARKAL as they are similar in many ways. Furthermore, technically the energy modeling of the

---

[33] Long range Energy Alternatives Planning System
[34] Market Allocation
[35] The Integrated MARKAL_EFOM System

solar hybrid PV/T system can be investigated by using TRNSYS[36] software. This software is a simulation program that was available since 1970s and was developed in Wisconsin University in United States of America. It can be used in the renewable energy fields such as activating a solar system design. The aim of TRNSYS is to model the systems such as solar system as well as assess the performance of the thermal energy and electrical energy of a particular system. In addition, generally TRNSYS is consists of 2 essential parts, the first one is the engine (kernel) and the second is the (ELOC[37]). The function of the first part is to process the input file as well as plot the variables of the system. While the second part ELOC can be used to model the performance of single part of system and this extensive library can include around 140 models [84, 85].

Generally, in order to develop simulations for any system by using TRNSYS tool, it is required to add several components that are not typically a part of the system for instance the output producing devices and the utility subroutines. In addition, the purpose of the TYPE number in each component is to relate a particular component to the Fortran subroutine that models the particular component [85]. The Fortran subroutines collections can be divided into 5 main categories. Kernel category that required some subroutines in order to run the TRNSYS simulation and every routine must be linked to TRNSYS DLL. There are many files were designed as Kernel routines files such as, (TRNSYS.FOR), (SOLVER.FOR), (TYPECK.FOR), (SYSTEM.FOR), (PRINT.FOR), (MYSTOP.FOR) and (ONLINE.FOR). The second category is Types category, which considered the actual component subroutines in TRNSYS software. Third is Option category, the Option subroutines are called by the certain component routines, and the files that were designed as Option routines files are: (HPLOT.FOR) [TYPE 27], (PLOTER.FOR) [TYPE 26] and (SUMARY.FOR) [TYPE 24 and 28]. Fourth category is Utility, and the Utility routines are called by plenty of the component Type routines. The files were designed as Utility routines files are: (DFIT.FOR) [TYPEs 51 and 53], (INVERT.FOR) [TYPES 19 and 37], (TABLE.FOR) [TYPE 19), (VIEW.FOR)

---

[36] Transient Systems
[37] Extensive Library Of Components

[TYPES 1 and 20], (FLUIDS.FOR) [TYPE 58]. The fifth category is Dummy category. Many Fortran compilers require this particular category [84, 86].

Moreover, There are many components in TRNSTS software library such as solar flat plate PV/T collector, hot water tanks, pumps, fans, weather data generator, and auxiliary heaters [87]. Therefore, this software is very useful for modeling the energy of the solar hybrid PV/T system.

Worldwide users of TRNSYS Software [88]:

- National Renewable Energy Lab (NREL)
- Trane company
- BMW[38] company
- NASA[39]
- Electricitie de France company
- More than 200 Universities
- Bechtel Corporation

4.4.2 Simulation Model of Solar Hybrid PV/T Systems For Australia

The annual simulations of two steady state photovoltaic/thermal water models were simulated in TRNSYS software by Jose Bilbao et al [89, 90] in Australia. The PV/T models are flat plate PV/T collectors (Type 850) and the standard PV/T model (Type 50). These two models were compared to each other based on the yearly electrical and thermal outputs of the solar PV/T residential hot water system for Sydney and Melbourne weathers using TMY2[40] data. TMY data is a weather data collection for a particular location and TMY2 is the second edition of the TMY.

---

[38] (Bayerische Motoren Werke) In English: Bavarian Motor Works
[39] National Aeronautic and Space Administration
[40] Typical Meteorological Year 2

4.4.2.1 Description of the Models

Model 1: Flat plate PV/T Collectors, TYPE 850

This model is called the single iteration model. For this model, Akhtar et al [91] developed an empirical relations in order to estimate the flat plate PV/T collector's cover temperature. One of the advantages of these relations is to use the sky temperature and thus it will be possible to get correct calculation for the radiation losses. Likewise, the equations and the algorithm that were used in this model are shown below [90].

The total losses of PV/T module equation:

$$U_{With\ Cover} = \left[\frac{1}{U_{RPC}+U_{CPC)}} + \frac{1}{U_{RCS}+U_{W)}}\right]^{-1} + U_{BE}$$

Where
U_{RPC}: The radioactive loss between the cover and the plate.
U_{CPC}: The convective loss between the cover and the plate.
U_{RCS}: The radioactive loss of the top cover of the collector.
U_W: The Convection loss of the top cover of the collector.
U_{BE}: The back and edges losses.
h_f: The total thermal conductance between the plate of the collector and the liquid.

The thermal efficiency factor equation:

$$\acute{F} = \frac{1}{1 + \dfrac{U_{L,With\ Cover}}{h_f}}$$

Where
h_f: The total thermal conductance between the plate of the collector and the liquid.

101

Electrical energy rate per unit area equation:

$$q_e = \tau \times G_t \times \eta_r [1 - \beta_r (T_p - T_r)]$$

Where

τ: Total transmittance.

G_t: Total incident irradiance.

η_r: Efficiency of the PV cell.

β_r: Coefficient of PV cell temperature.

T_p: Temperature of plate.

T_r: Reference temperature

Thermal energy rate per unit are equation:

$$q_t = F_r [\dot{S} - q_e - U_{L,With\ Cover}(T_{in} - T_{amb})]$$

Where

F_r: Heat removal factor

T_{in}: Inlet temperature

T_{amb}: Ambient temperature

Moreover, all these parameters above are considered the parameters (inputs and outputs) of Type 850.

Model 2: Standard PV/T model, Type 50

The Type 50 contains 4 operation modes for the solar PV/T flat plate collectors [89]:

- Mode 1: Both total losses ($U_{With\ Cover}$) and total transmittance (τ) must be constant and should be considered as parameters of the model.

- Mode 2: Total losses ($U_{With\ Cover}$) must be calculated by Florschuetz equations and the total transmittance (τ) must be constant.
- Mode 3: Total losses ($U_{With\ Cover}$) should be constant and the transmittance angular dependence is unstable.
- Mode 4: This mode is the combination of both Mode 2 and 3.

In addition, the mode that was used in this work was mode 2 because this mode was the most stable model comparing that with the other modes of the model likewise, the total transmittance of the cover of mode 2 is constant. Consequently, the modifications were introduced to the solar irradiance in order to compare the models together. Also, Type 50 used the single iteration process in order to solar the equations of the heat transfer and also Klein's equations were used to calculate the collector's top cover losses (U_{Top}). The equations are shown below [89, 90].

$$U_{Top} = \cfrac{1}{\left(\cfrac{N}{(C/T_{mf}) \times \left[\frac{T_{mf}-T_{amb}}{N+f}\right]^{0.33}}\right) + \cfrac{1}{U_W}} + \cfrac{\sigma\left(T_{mf}^2 + T_{amb}^2\right) \times (T_{mf} + T_{amb})}{\left(\cfrac{1}{\varepsilon_p + 0.05 \times N\,(1-\varepsilon_p)}\right) + \left(\cfrac{2 \times N + f - 1}{\varepsilon_g}\right) - N}$$

Where

N: is the number of covers.

U_W: The convection loss factor because of the wind.

ε_p: The emissivity of collector plate.

ε_g: The emissivity of glass cover.

T_{amb}: Ambient temperature.

f and C: is the correction factors.

T_{mf}: Mean water temperature (this temperature was used instead of the mean plate temperature).

$$C = 365.9 - 3.2309\beta + 0.0474\beta^2$$

Where

C: is the correction factor.

β: PV panel tilt or the slope of the PV panel (in degrees).

$$f = (1 - 0.04U_W + 0.0005U_W^2) \times (0.091N + 1)$$

f is the correction factor (f is equal to 1 if the number of covers N smaller than 0.5). Additionally, in the PV/T module if the quality of the heat transfer is high, the errors will be low. Likewise, the error percentage will be very high if the PV/T modules have low heat thermal transfer [89].

4.4.2.2 Results of Annual Outputs Comparison in TRNSYS Software

The yearly electrical and thermal outputs of the domestic PV/T system were presented for Sydney and Melbourne climates. The simulation of PV/T system was developed in TRNSYS software with two models, model 1 and 2 (Type 850 and Type 50) respectively. The yearly hot water energy consumption for 4 persons house in Sydney is approximately 2,700 kWh, which is 7.4 kWh per day. Likewise, the annual electrical energy consumption for 4 persons residence in the same location is 8,249 kWh, which is 30 kWh per one day [92, 93]. The solar PV/T system that designed by Jose Bilbao was connected to 300 L with set point temperature of 333 K. The electrical energy output of the photovoltaic array was expected to be at the highest power point. Additionally, the area of the solar PV/T module for both models of 1 and 2 is 1.28 m^2 and the efficient of electrical energy is 14% at the standard test conditions. The PV/T system of 3.2 kWp contains 18 PV panels was selected in order to simulate a standard system. This standard system is very similar to the system that can be installed in the residential houses [90].

There are two scenarios were used in order to compare the two models. These two scenarios are the system with cover and system without cover. Also, all the parameters of both models 1 (Type 850) and model 2 (Type 50) and for both scenarios (with cover and without cover) are kept equivalent. In addition, the results of percentage errors of

auxiliary energy, PV energy, and net energy between model 1 and model 2 are displayed in the next 3 figures below. Figure 83 shows the results of the percentage error of the auxiliary energy (Q_{AUX}) between model 1 (Type 850) and model 2 (Type 50) for Sydney and Melbourne climates.
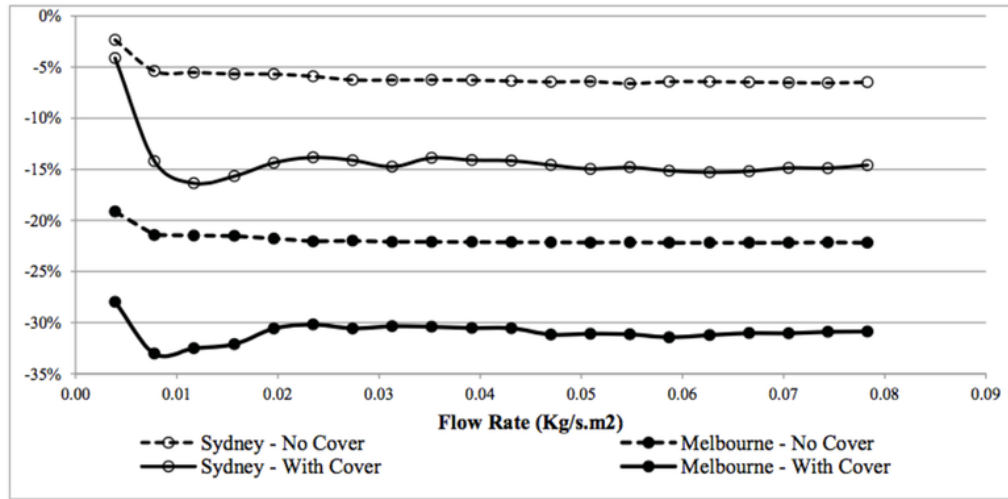
Figure 83: Annual Percentage Error of Auxiliary Energy (Q_{AUX}), (Model 1 Against Model 2) [90]

Model 2 over predicts the thermal energy output; as a result, model 1 under predicts the thermal energy output or the auxiliary energy. For Sydney climate, the annual errors of the auxiliary energy (Q_{AUX}) are approximately 15% for PV panels with cover while the errors of the panels without cover are 6%. For Melbourne climate, the errors for the panels with cover and without covers are around 31% and 21.5% respectively. For the electrical output or the PV energy (Q_{PV}), model 2 with the cover under predicts the yearly output by approximately 7% likewise; it over predicts it without the cover by around 3% as shown in figure 84. As a result, model 2 with the cover runs hotter than model 1 also, model 2 without the cover runs cooler than model 1. Moreover, according to figure 85 for Sydney climate, the percentage errors for the annual net energy for the PV panels without cover and with cover are approximately 5% and 3% respectively. However, for Melbourne weather the errors of yearly amount of the net energy are around 3% for PV panels without cover and 7% with the cover. The net energy can be calculated by using this equation: $Q_{net} = Q_{PV} + (Q_{Load} - Q_{AUX}) - Q_{PUMP}$.

105
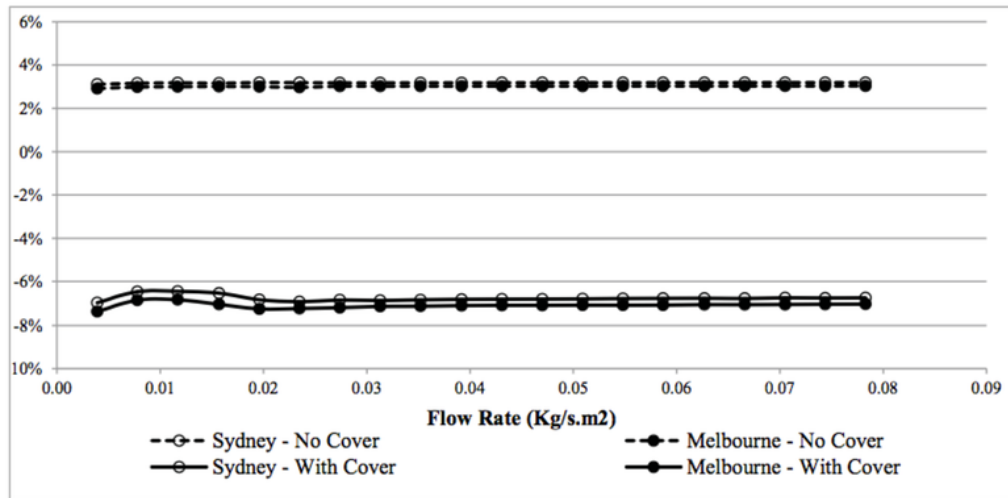
Figure 84: Annual Percentage Error of Electrical Energy (Q_{PV}), (Model 1 Against Model 2) [90]
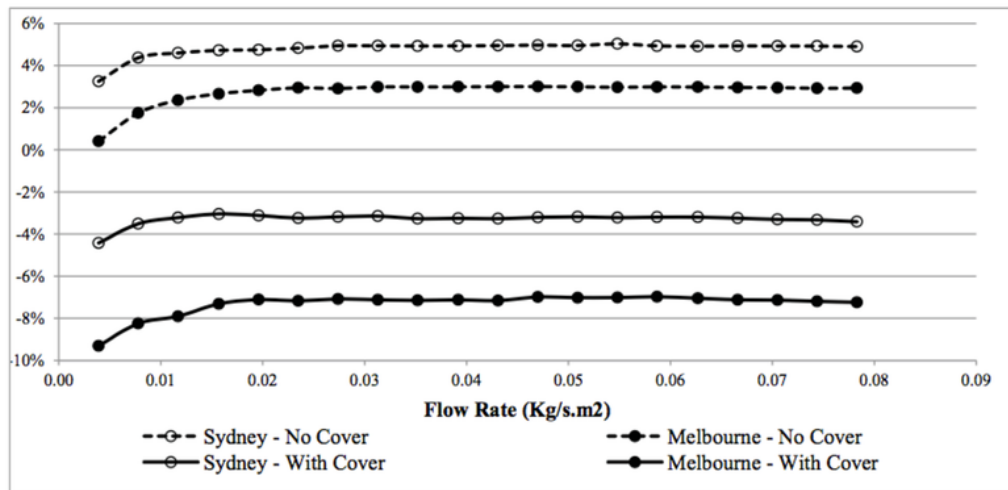
Figure 85: Annual Percentage Error of Net Energy (Q_{net}), (Model 1 Against Model 2) [90]

The results of the 3 figures (figures 83, 84 and 85) are seem to be contradictory however, actually the results reflect how the performance of the solar hybrid PV/T system varies depending on the system's size as well as the operation [90].

106

4.4.3 Simulation Model of Solar Hybrid PV/T System For Cyprus

A simulation model of solar hybrid PV/T system was developed by Soteris Kalogirou in Nicosia, Cyprus [85]. This particular system consists of photovoltaic panel, inventor, battery, hot water tank, hot water pump, and thermostat as shown in figure 86.
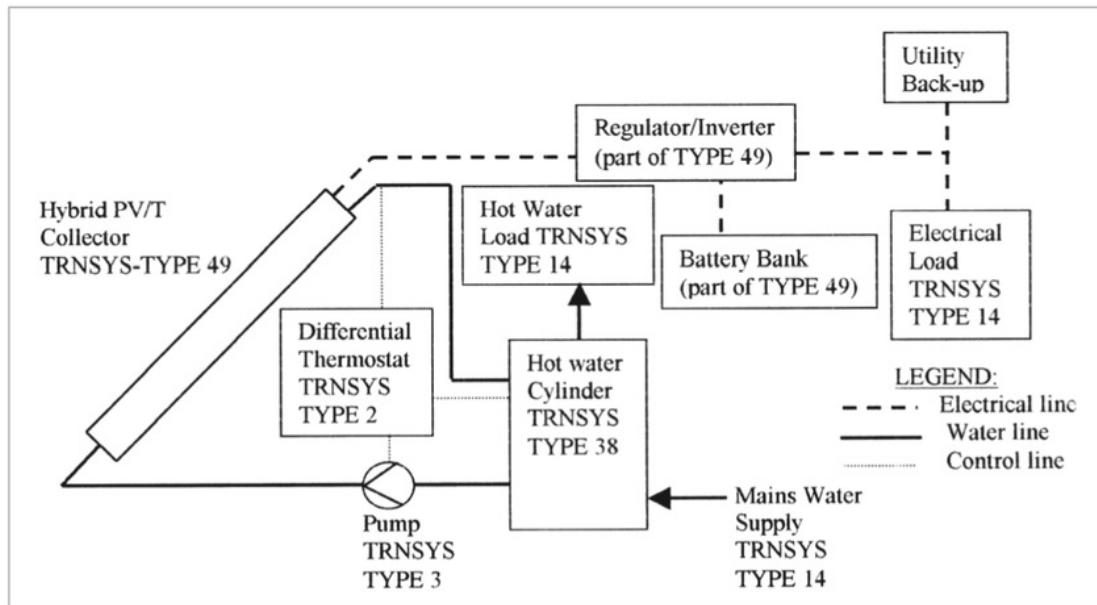
Figure 86: Solar Hybrid PV/T System Diagram [85]

The main component of the TRNSYS deck file is TYPE 49 that includes the solar hybrid PV/T collector, the battery bank, and the inverter. Likewise, the TRNSYS types that were used in the solar hybrid PV/T system that developed by Kalogirou are shown below.

A. **Type 16**: For the radiation processor
B. **Type 3:** For hot water pump
C. **Type 9:** For data reader
D. **Type 2:** For the differential controller
E. **Type 14:** For the load (electrical load demand), (hot water demand)
F. **Type 11:** For the diverter

G. **Type 38:** For hot water tank

In addition, Type 14 was used in the deck file 3 separate times; the first time was used in order to define the monthly temperatures of water. The second time was used to define the necessary electrical load in the system and the third time to define the flow rate. The flow rate that was used for each day is 120 liters which is enough for 4 persons [85]. Figure 87 displays the flow diagram of the solar hybrid PV/T system.
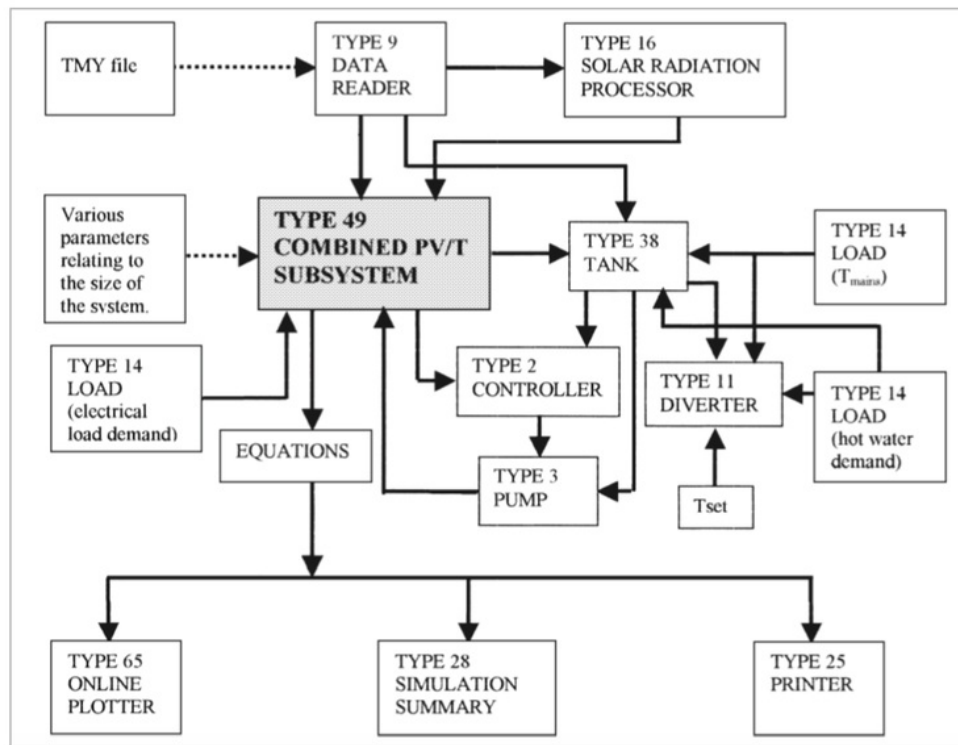
Figure 87: Solar Hybrid PV/T System Flow Diagram [85]

This diagram shows the deck file for the solar hybrid PV/T system. This file must contain all the required information including the weather data file as well as the output format. Every component in the system has a specific TYPE number as shown in figure 87. Likewise, unit number can be used in order identify every component in the deck file. It is possible for 2 or more components to have same number of TYPE such as TYPE 14 Load but different unit number as displayed in figure 87. In addition

108

the deck file can read the information that provided by the typical meteorological year weather data (TMY) for any country around the world. However, Kalogirou [85] used the TMY weather data for Cyprus and this data were made by Petrakis et al [94]. Therefore, in order to model the solar hybrid PV/T system it is necessary to use both TRNSYS software and TMY conditions.

4.4.3.1 Results

The main parameters of TYPE 49 system that were developed by Kalogirou [85, 95] are:

- Area of Collector A_c (5.1 m^2)
- Fluid thermal capacitance C_p (4200 J/kg.°C)
- The inventor's output power capacity $P_{L,max}$ (0.83 KW)
- Maximum current I_{max} and minimum current I_{min} (30 A[41] and -30 A respectively)
- High and low limit on F[42] (0.95 and 1 respectively)
- The absorptance of the collector plate α (0.9)
- Loss coefficient U_b(1 W/m^2. °C)
- Regulator efficiency η_1 (100%)
- Efficiency of inventor η_2 (90%)

In addition, the output results on a daily, monthly and yearly basis can be provided by using TRNSYS tool. The results of specific day can be chosen randomly; likewise, the results must be correlated to the design parameters of the particular system. Kalogirou [85], plotted graphs that shows the daily consumption of electricity and hot water. The day was chosen randomly and it was on 21 of April 2001. According to figure 88, the hybrid PV/T system consumed the largest amount of electricity 2 MJ at 9 AM and between 12:30 PM and 1:30 PM. The consumption of electricity gradually decreased from 1.59 MJ to 0 MJ between 7 PM and 12 AM. Then it increased again between 5 AM

---

[41] Ampere
[42] Fractional State of Charge

and 9 AM and reached 2 MJ. Additionally, between 3 PM and 4 PM the electricity consumption was 1.21 MJ and then increased again to 1.59 MJ between 6 PM and 7 PM. At 6 AM the electricity consumption increased dramatically from 0.60 MJ to 1.4 MJ. Furthermore, figure 89 displays the results of the daily hot water consumption of the solar hybrid PV/T system.
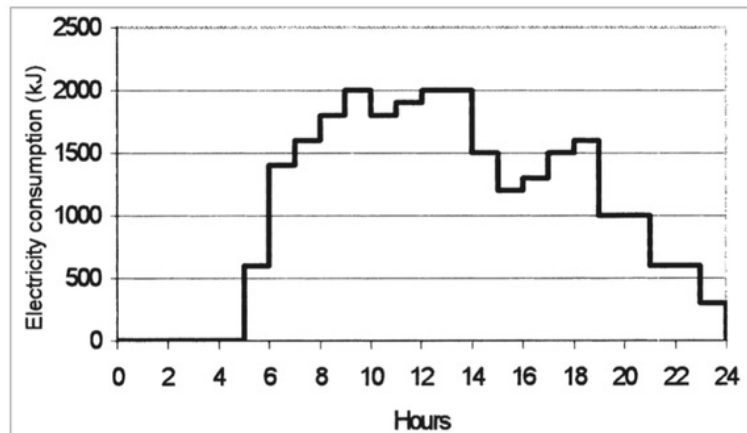
Figure 88: Daily Consumption of Electricity [85]
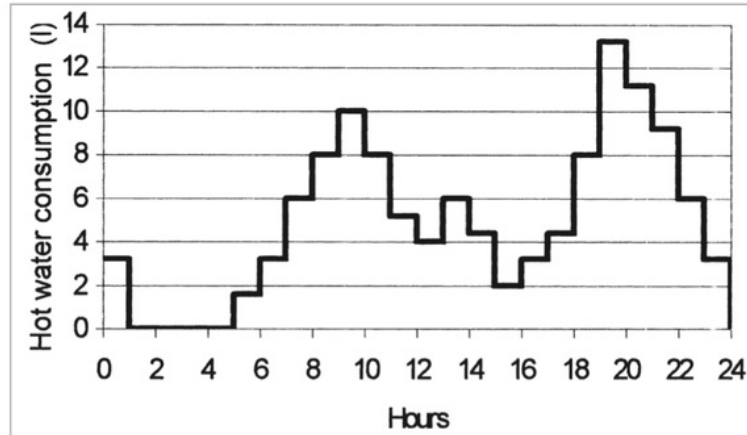
Figure 89: Daily Consumption of Hot Water [85]

The system consumed 13.4 liters between 7 PM to 8 PM, which considered the largest quantity that were consumed by this system. There was no consumption between 1 AM to 4:30 AM. Additionally, between 5 AM and 9 AM the daily consumption of hot water

110

increased from 1.8 liters to 10 liters and then decreased from 10 liters to 2 liters between 10 AM and 3 PM. After that, the consumption increased again from 2 liters to 13.4 liters between 4 PM and 7 PM. Finally, it decreased again from 13.4 liters to 3.3 liters between 8 PM and 11 PM, then decreased from 3.3 liters to zero at 12 AM.

Moreover, to determine the water flow rate $\dot{Q}$ or to optimize it, it is is necessary to use the yearly output of TRNSYS tool. If the PV panel worked at low temperature, then both the electrical energy output and the flow rate will increase simultaneously. However, the thermal energy put will increase to reach specific limit then it will decrease. Likewise, the electrical energy that required from the utility in order to cover the load Q_{UTIL} and the thermal auxiliary energy that needed to cover the load of hot water Q_{AUX} are used to specify the additional energy that needed to cover the thermal and electrical loads. In addition, Q_U is the output of the thermal energy from the PV/T hybrid system and Q_E is the output of electrical energy from PV/T hybrid system [85].
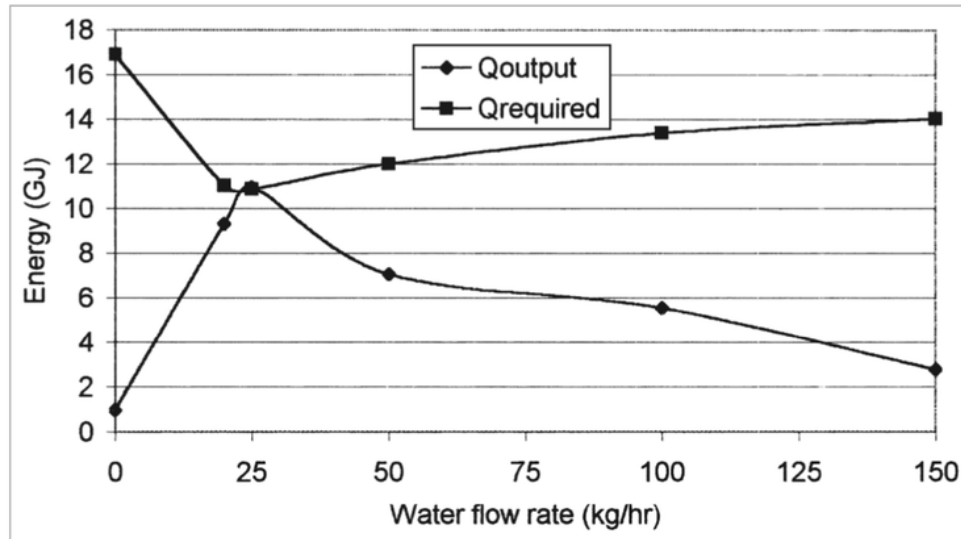
Figure 90: Water Flow Rate of Solar Hybrid PV/T System [85]

As a result, the optimum value of the water flow rate can be determined by adding the values of Q_U and Q_E together ($Q_U + Q_E$) as well as adding the values of Q_{UTIL} and Q_{AUX}

111

together ($Q_{UTIL} + Q_{AUX}$). Then, these values must be plotted against water flow rate $\dot{Q}$ as shown in figure 90.

According to the chart above, Q_{output} represent the total values of ($Q_U + Q_E$) and $Q_{required}$ the total values of ($Q_{UTIL} + Q_{AUX}$). Both Q_{output} and $Q_{required}$ were 11 GJ while the water flow rate was 25 kg/hr or l/hr. This low value of the water flow rate $\dot{Q}$ indicates that it is possible to use the solar hybrid PV/T system in a thermo syphon mode, which means using the system without hot water pump and thermostat. Consequently, this will improve the economic viability of the solar hybrid PV/T system. In addition, while the $Q_{required}$ increased from 11 GJ to 14 GJ, the water flow rate $\dot{Q}$ also increased from 25 l/hr to 150 l/hr however, Q_{output} decreased from 11 GJ to 2.8 GJ. Likewise, the values of $Q_{required}$ and Q_{output} are 17 GJ and 1 GJ respectively when the flow rate is zero l/hr.
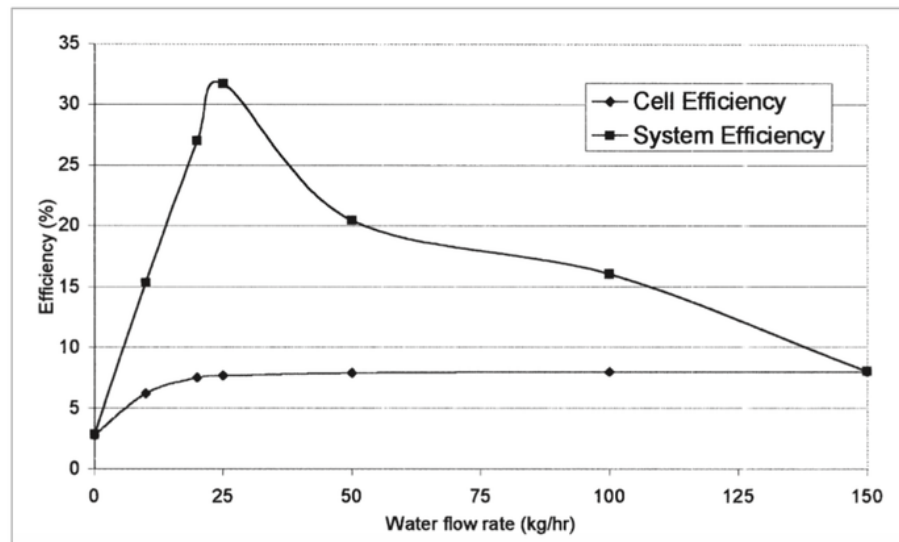
Figure 91: System Efficiency and PV Cell Efficiency Against Water Flow Rate $\dot{Q}$ [85]

Furthermore, the graph in figure 91 plotted the values of PV cell efficiency, hybrid PV/T system efficiency against the water flow rate $\dot{Q}$. The solar hybrid PV/T system

112

operated at the best flow rate $\dot{Q}$ value, which was 25 l/hr when the PV efficiency was 7.7% and the PV/T system efficient was 31.75%. The maximum value of PV cell efficiency was 8% at higher flow rate values than 25 l/hr. In addition, the PV cell efficiency and PV/T system efficiency were 6% and 15.25% respectively while the flow rate was 10 l/hr. Also, the efficiency of the PV/T system decreased gradually from 371.7% to 8% when the water flow rates values were ranging from 26 l/hr to 150 l/hr. Likewise, the PV cell efficiency stabilized at 8% when the flow rate values were between 55 l/hr to 150 l/hr. It worth mentioning that, the corresponding value of the PV system efficiency (without cooling) was 2.8%.

4.4.4 Simulation Model of Solar Hybrid PV/T System For Taiwan

According to Huang et al [14], the components that used in TRNSYS in order to develop the solar hybrid PV/T system are unglazed flat plate PV/T collector, hot water tank, hot water pump, and temperature controller. Likewise, the local weather data is required to perform the energy modeling in TRNSYS tool. In addition, in TRNSYS the aim of the PV/T model is to create power source from photovoltaic module and then it can provide heat to the liquid that can pass though a tube of copper. The photovoltaic module can be cooled by the heat recycle that comes from the photovoltaic module. This will provide the electricity as well as hot water that can be used in home heating and swimming pool. Moreover, TRNSYS has plenty of types and each component of the solar hybrid PV/T system must have specific type [14]. According to Huang, the TRNSYS types that were used in the solar hybrid PV/T system simulation are:

A. **Type 4**: For hot water tank (storage tank)
B. **Type 3**: For hot water pump
C. **Type 109:** For Weather data
D. **Type 2:** For the temperature differential Controller
E. **Type 563:** For the flat plate PV/T collector (unglazed)

Figure 92 displays the solar hybrid PV/T system in TRNSYS tool developed by Huang.

113
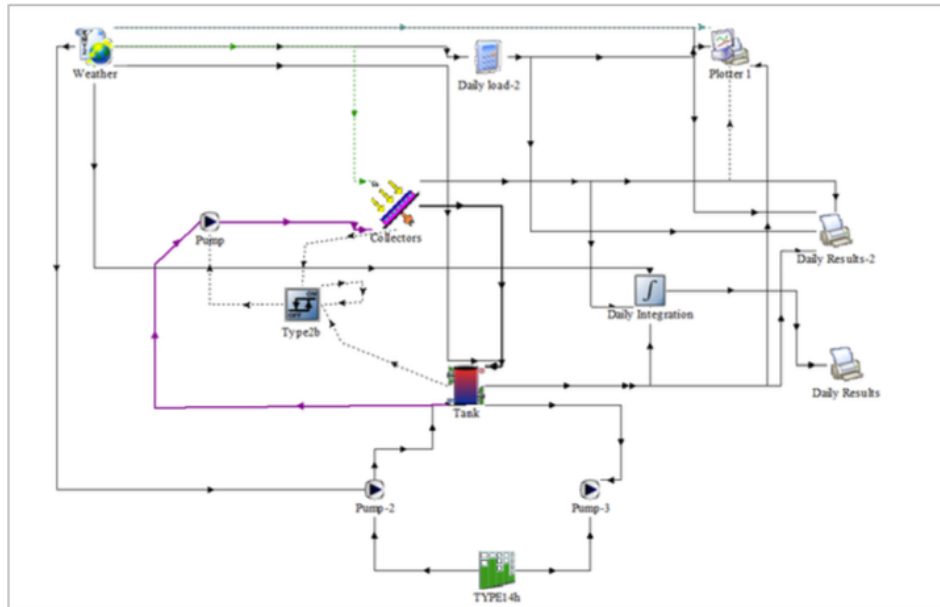
Figure 92: Solar Hybrid PV/T system in software TRNSYS [14]

4.4.4.1 Parameters in TRNSYS Software

Huang et al [14] outlined some design parameters in TRNSYS software for solar hybrid PV/T system. These parameters are important to create the simulation model of the PV/T system. Each component of the PV/T system has some parameters in TRNSYS and each parameter has specific value. The parameters are for 3 components of the solar hybrid PV/T system, the PV/T Module, hot water pump, and hot water tank. The values below are related to the solar hybrid PV/T system that were developed by Huang [14].

The parameters of the PV/T module are:
- Area of the module ($9.78\ m^2$)
- Packing factor (1)
- Reference temperature of PV cell (25°C)
- Reference radiation of PV cell 1000 (W/m^2)
- Specific heat of the fluid (4180 J/kg.°C)

- The efficiency of PV at reference condition (14.7%)
- Temperature coefficient of the efficiency of the solar cell (0.004/°C)
- The absorber's thermal conductivities (200 $W/m.°C$)

The hot water pump and hot water tank parameters:
- Maximum value of the power of the pump (300 W)
- The Maximum flow rate of the pump (4 LPM[43])
- Volume of the tank (500 L)

In addition, the calculations of the performance of the solar hybrid PV/T system can be done by using the 2 two formula below. Where η_{EL} and η_{TH} are the electrical efficiency and thermal efficiency respectively and H is the solar radiation measured in (kWh/m^2), Q is the thermal capacity of the water at simulation period of time, and P is the electrical power and can be measured in kWh. A is the module area (m^2).

PV Efficiency

$$\eta_{EL} = \frac{P}{A \times H}$$

Thermal Efficiency

$$\eta_{TH} = \frac{Q}{A \times H}$$

4.4.4.2 Simulation Model Verification

According to Huang et al [14], the best method to verify the simulation model of the solar hybrid PV/T system is to use real experimental data. Figure 93 shows the relation of water temperature T_W with simulation and experiment. Likewise, T_a is the ambient temperature.

_____

[43] Liters per Minute
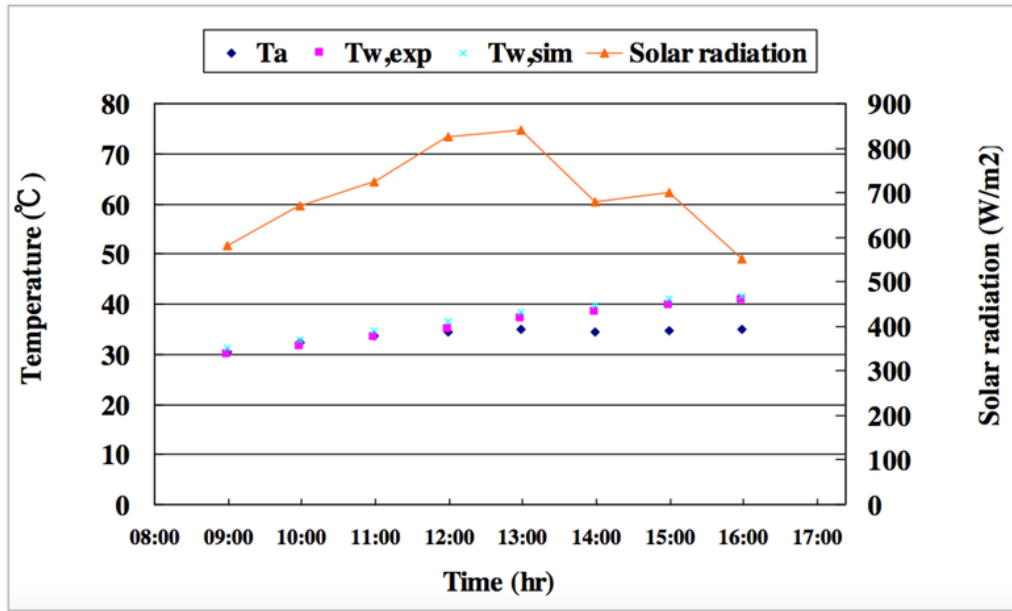
Figure 93: Water Temperature (Experiment) and Water Temperature (Simulation) [14]

At 9 AM all the temperatures, the ambient temperature T_a, and water temperatures T_W with experiment and simulation are approximately 30 °C and 31 °C . These temperatures are increasing gradually between 9:30 AM to 4 PM. There are simple differences between the water temperature (experiment) and water temperature (simulation) during the day. For example, the temperatures of water with experiment and simulation are 38.5 °C and 40 °C respectively at 2 PM. Likewise, the temperatures of water with experiment and simulation at 12 PM are 35 °C and 37.5 °C respectively. The ambient temperature is slightly different from water temperatures only between 1:30 PM to 4 PM. In addition, the solar radiation is increasing dramatically between 9 PM to 1 PM however, it gradually decreasing between 1 PM to 4 PM. For example, at 11 PM, the temperatures of water with experiment and simulation are 34 °C and 35 °C respectively and the solar radiation of the system is 725 W/m^2. Also, at 4 PM when both of the temperatures of water became 41°C, the solar radiation decreased to 550 W/m^2. The highest value of the solar radiation in the chart is 838 W/m^2 at 1 PM.

116

Chapter 5: Performance and Design of Solar PV/T Collectors

5.1 Introduction

There are many types of solar hybrid PV/T systems as shown in figure 6 in chapter 2 such as, concentrator PV/T collectors, water PV/T collectors, and air PV/T collectors. The water PV/T and air PV/T collectors are the most popular types of solar hybrid PV/T collectors. These types are often used in buildings and some houses, which can be installed in the roofs in order to use its electricity and the heat as well. Moreover, this chapter is regarding the performance, design, and the thermal and electrical efficiencies of water PV/T collector and air PV/T collector. In addition, these collectors were compared to each other in terms of the types, costs, thermal and electrical efficiencies, overall efficiency, heat conductivity and heat transfer.

5.2 Performance and Design of Solar PV/T Water Collector

The solar water based collector is considered one of the most common types of the solar hybrid PV/T system. For liquid-based collector the working fluids that can be used are water or mineral oil or glycol. For solar PV/T water collector, the water is used in order to cool the photovoltaic panel or module [75]. Generally, when the sunlight reaches the PV panel not all the solar energy will be converted to electricity however, some of it will heat the PV panel and then this will increase the temperature of this panel. Therefore, it is necessary to reduce the temperature of the PV cells and this can be by cooling the PV module [24]. The essential aim of cooling the PV module is to increase the performance and efficiency of the PV/T water collector and to

increase the amount of electricity that generated by the collector or to raise electrical efficiency of the photovoltaic module of the collector. In addition, there are several steps must be taken into account to cool the PV module of the PV/T collector [96]. The steps are:

A. The cold water must be pumped from the water tank to the heat extraction device (Heat exchanger). This device must be installed at the back surface of the PV panel.
B. The Heat exchanger circulates the working fluid (water) likewise; the temperature of working fluid (water) must be lower than the temperature of the PV cells in order to cool the PV module properly.
C. The heat then will be extracted from the back surface of the PV panel by using the heat exchanger.
D. Finally, the hot water will return to the water tank.

Figure 94: Solar Hybrid PV/T system in Macquarie University [97]

Furthermore, figure 94 shows the picture of the solar hybrid PV/T system designed by Dr Nazmul Huda in Macquarie University. This system can be installed in different ways as long as the system is working properly. According to the PV/T system in figure 94, the system was designed by using several components, such as: photovoltaic

system that includes the PV panel, metal frame, PV cells, electrical cables, and battery. The inclination angle between the table and the PV panel is approximately between 30° to 35°. In addition, the thermal system consists of water tank, pipes, water pump, and heat exchanger. The exchanger was installed at the rear surface of the PV panel and water pump was installed between the black pipe and the water tank as shown in figure 95. The water pump was used to pump the cold water up to the PV panel in order to cool the panel.
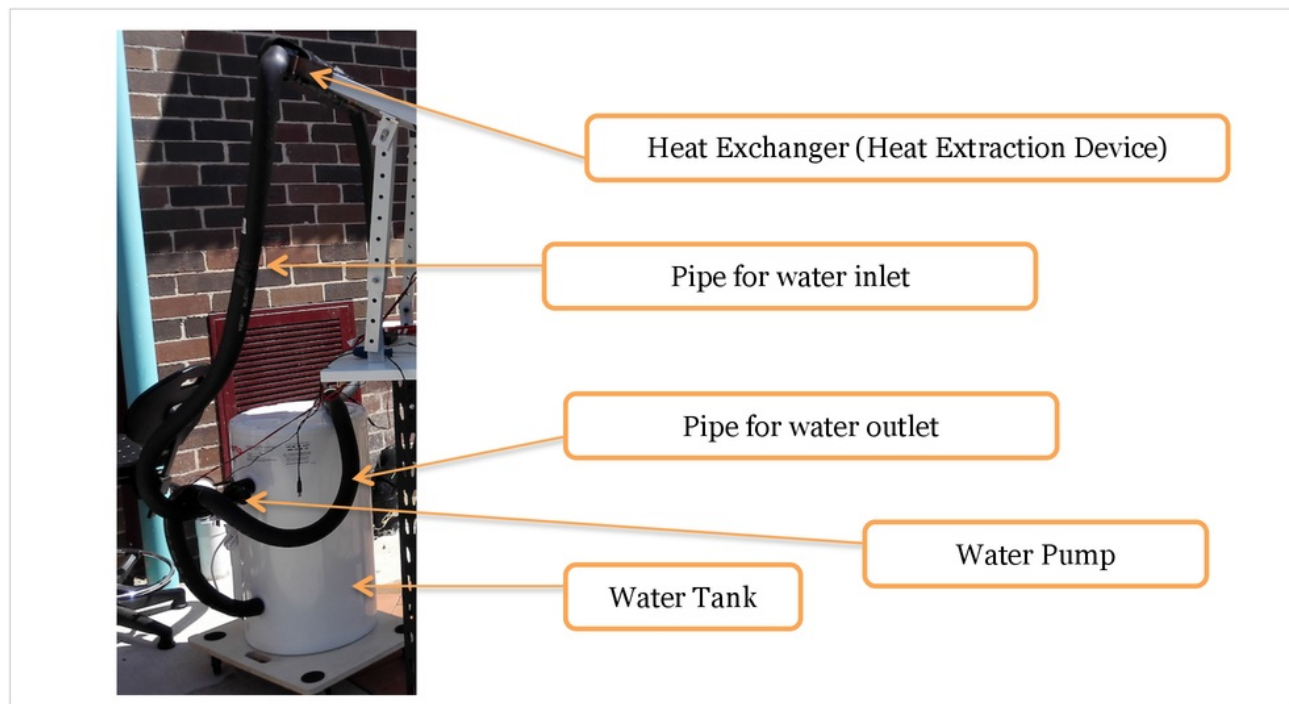
Figure 95: Solar Hybrid PV/T system in Macquarie University [97]

Consequently, when the waste heat is extracted from the PV panel by the heat exchanger, the temperature of the PV panel will decrease then its efficiency will increase dramatically and then the collector will produce more electrical energy. Therefore, the overall efficiency of PV/T collector is higher than the efficiency of PV collector. According to Othman et al [37], the total efficiency that can be achieved by the solar hybrid PV/T system is between 39% to 70%. Additionally, Chow [4] indicated that the electrical and thermal efficiencies of solar water PV/T collector are 9.39% and

37.5% respectively. Likewise, according to Abu Baker et al [16], the average electrical and thermal efficiencies of their water PV/T system are 10.92% and 40.57% respectively, also the total efficiency of the overall PV/T system increases with the increase of the water flow rate ($\dot{Q}$). According to Fudholi et al [98], electrical and thermal efficiencies of the water PV/T collector under 800 W/m^2 solar radiation are 13.8% and 54.6% respectively

5.3 Performance and Design of Solar PV/T Air Collector

The PV/T air collector is also called the air-based PV/T collector that uses the air to cool the PV panel. For this type of collectors, to have great performance and high overall efficiency, it is necessary to extract the heat from the collector in the form of hot air so to reduce its temperature. This extracted heat can be used as a heat source for houses and buildings. Likewise, this collector requires a very high volume of air flow in order to get high thermal efficiency [17]. Air PV/T collectors has two types; the single pass and double pass PV/T collectors. According to Sopian et al [99], the performance of the double pass collector is better than the performance of the single pass collector because the double pass collectors cools the photovoltaic cells in a better than the single pass collector. In addition, performance for air PV/T collectors are based on design and climatic parameters [17]. These parameters are:

A. Solar radiation intensity (I)
B. Ambient Temperature (T_{amb})
C. Inlet and outlet Temperatures (T_{in}) and (T_{out})
D. Speed of wind
E. Temperature of PV Cell
F. Inlet air velocity
G. Length of the PV module
H. Width of the PV module
I. Rear surface temperature of the PV module

5.3.1 Design of Air PV/T Collector

Figure 96 shows the air PV/T collector designed by Kim and park [17]. The inclination angle of the PV panel is 35° and mono crystalline silicone cells are used to manufacture the PV cells. The PV panel dimensions are $165 \times 98 \times 4$ cm and the diameter of the exhaust air pipes is 10 cm. These pipes were used in order to extract the hot air and to cool the back surface of the PV laminate. Likewise, the maximum voltage and power of the PV module are 31.9 voltages and 250 watts respectively.
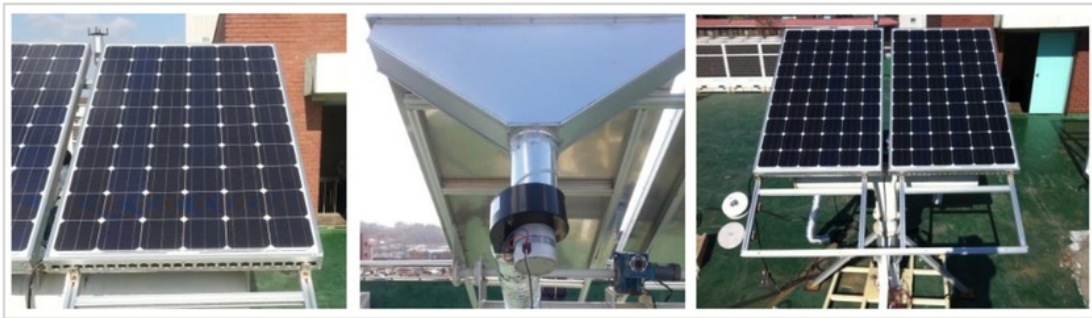
Figure 96: Solar Air PV/T Collector [17]

5.3.2 Thermal and Electrical Performance of Air PV/T Collector

The results of the thermal and electrical performance of the PV/T air collector are displayed in figures 97 to 99. The performance was measured outdoor at ambient temperature. Kim et al [17] shows that the temperatures of the back of PV laminate is ranging from 12°C to 32°C from 9 AM to 12:30 PM. Likewise, at ambient temperature the temperatures of exhaust air were ranging approximately from -2°C to 10°C. Additionally, the maximum value of the solar radiation was 910 W/m^2 as shown in figure 97. Consequently, the temperature of the PV module was low because of the hot air that exhausted from the PVT collector while the solar radiation is high.
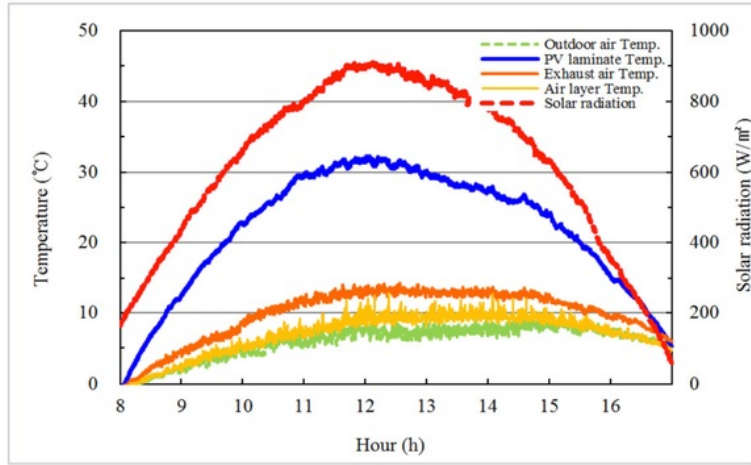
Figure 97: Solar Radiation and Temperatures of PV Module and Exhaust air of Air PV/T Collector [17]

Moreover, the thermal efficiency of the air PV/T collector can be calculated by using the formula below. Where $\dot{m}$ is the mass flow rate in m^3/h, C_p is the specific heat, G is the irradiance on the surface of air PV/T collector, A is the collector are, T_o and T_i are the outlet and inlet temperatures of the collector respectively. η_o is the efficiency at zero temperature and α is the heat loss coefficient which equal to $19.2\ W/m^2K$.

$$\eta_{TH} = \frac{\dot{m} \times C_p \times (T_o - T_i)}{A \times G}$$

The rational expression of thermal efficiency of the air PV/T collector is:

$$\eta_{TH} = \eta_0 - \alpha \times \left(\frac{(T_o - T_i)}{G}\right)$$

$$\eta_{TH} = 0.29 - 19.2 \times \left(\frac{(T_o - T_i)}{G}\right)$$

As a result, the thermal efficiency at 0°C is 29% that indicates a great performance. Therefore, the average thermal efficiency of the air collector is 22% at ambient

temperature likewise; figure 98 displays the results of thermal efficiency of the collector where X is the axis coefficients $[(T_o - T_i)/G]$.

Figure 98: Thermal Efficiency of Air PV/T Collector [17]

Furthermore, the electrical efficiency of the air PV/T collector can be calculated by using the equation below. Where V and I are the voltage and current of the photovoltaic panel.

$$\eta_{ELEC} = \frac{I \times V}{A \times G}$$

Figure 99: Electrical Efficiency of Air PV/T Collector [17]
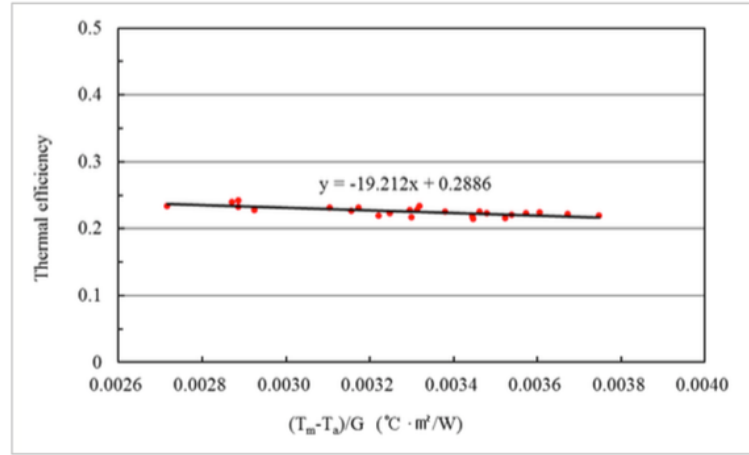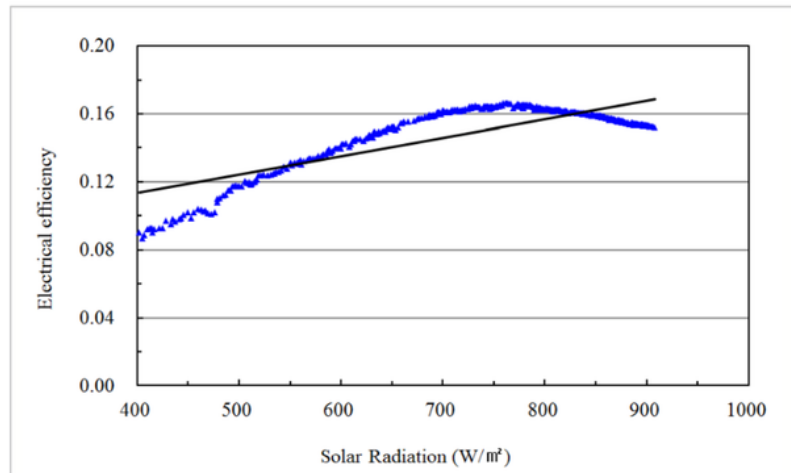
123

Figure 99 shows the results of the electrical efficiency and solar radiation of the air PV/T collector. It indicates that electrical efficiency increased gradually when the solar radiation was between $400\ W/m^2$ to $748\ W/m^2$. Then the efficiency decreased when the solar radiation was higher than $750\ W/m^2$. So the highest electrical efficiency of air PV/T collector is 16.5% and the average electrical efficiency is 15% [17]. According to Slimani et al [100], average electrical efficiency of the double pass water PV/T collector is 10.5%.

5.4 Comparison Between Air and Water PV/T Collectors

Tables 40 and 41 show the comparison between water and air PV/T collectors according to Abu Baker et al [16], Chow [4] Othman et al [37], Kim and park [17], Taygi et al [101] ,Tripanagnostopoulos et al [75] and Fudholi et al [98].

	Solar Hybrid PV/T System	
Classification	**Water-Based PV/T Collector**	**Air-Based PV/T Collector**
Working Fluid	Water	Air
Circulation (Natural / Forced)	Forced circulation	Both natural and forced circulations
Cost	More expensive than air PV/T collector	Cheaper than water PV/T collector
Types	Sheet and tube absorbers such as: 1. Round tube absorber. 2. Square tube absorber. 3. Rectangular tube absorber.	1. Glazed air PV/T module (single glass and single pass). 2. Glazed air PV/T module (double pass and single glass). 3. Unglazed air PV/T module (single pass and double glass). 4. Unglazed air PV/T module (single pass and single glass).

Table 40: Water PV/T Collector Against Air PV/T Collector (Table A)

124

Classification	Solar Hybrid PV/T System	
	Water-Based PV/T Collector	**Air-Based PV/T Collector**
Heat Conductivity	High	Low
Heat Capacity	High	Low
Heat Transfer	High	Low
Scheme of Collector (Covered or Uncovered)[44]		
Average Electrical Efficiency	11.5%	12%
Average Thermal Efficiency	44.5%	22%
Overall Efficiency	Higher than air PV/T collector	Lower than water PV/T collector
Performance	Better than Air type	Worse than Water type

Table 41: Water PV/T Collector Against Air PV/T Collector (Table B)

---

[44] Blue arrows represent the cold (water or air) inlet and red arrows represent the hot (water or air) output.

Chapter 6:Conclusions

In conclusion, the main aim of this project was to perform a life cycle assessment for the solar hybrid PV/T system (water PV/T system). There are some essential steps must be taken into considerations when performing the Life cycle assessment by using GABI software. Specifying all the raw materials of all the components of the solar hybrid PV/T system was the first step to perform the LCA for this system. The hybrid PV/T system consists of two main systems the electrical and thermal systems. Second step was to specify all the seven phases of the life cycle of solar hybrid PV/T system starting from the raw material acquisition phase until the last phase, which is the end of life phase of the system as described in chapter 3 sections 3.3 to 3.4.

After performing the life cycle of the solar hybrid PV/T system the results of environmental impact assessment of system were obtained by GABI Software. The total amount of carbon dioxide emissions generated from solar hybrid PV/T system was 215 [kg CO_2-Equivalent] and this amount contributes to the global warming potential. Likewise, the total amount of emissions that contributes to the ozone depletion potential and produced by the PV/T system was 1.8×10^{-7} [kg R11-Equiavalent] or [kg of Trichlorofluoromethane]. Also, the total amount to toxic emissions that generated for the PV/T system that cause cancer was 3.97×10^{-6} CTUh and the non-cancer emissions produced by the system was 3.2×10^{-5} CTUh. Also, the radiations that generated from PV/T system were 4 Uranium-235 equivalent. The amount of emission that contributes to acidification potential and produced by the PV/T system was 1.12 mole of H+. Additionally, the results of terrestrial, marine, and fresh water eutrophication potential for the whole PV/T system were 2.8 mole of nitrogen, 0.26 kg of nitrogen and 2.002×10^{-3} kg of phosphorus respectively. Likewise, the total aquatic eco toxicity emissions that generated from solar hybrid PV/T system were 132 CTUe.

Furthermore, the life cycle assessment of the PV system was also implemented and the purpose was only to compare the results of the environmental impact assessment of both PV with the PV/T systems. As that, the PV system only contains the electrical system without the thermal part. Likewise, the results of the selected impact categories for both systems were compared to each other according to different scenarios as described in chapter 3, section 3.7. Therefore, the results indicated that all results of the GWP, Primary Energy, AP, EP, Eco Toxicity, and POCP for PV/T were higher than the results of PV system except for the human toxicity potential (HTP) as the results of scenarios of HTP of PV system was higher than the scenarios results of PV/T system.

In addition, the other aim of this project was to investigate the energy modeling of the solar hybrid PV/T system. The mathematical analysis of electrical and thermal energy of the flat plate PV/T collectors was analyzed. Likewise, the energy modeling was investigated for 3 countries: Australia, Cyprus, and Taiwan as described in chapter 4, section 4.5. According to Sydney climate, the annual percentage error of the auxiliary energy for PV panels with cover and without cover were 15% and 6% respectively also the yearly percentage error of the net energy for PV panels with cover and without cover were 3% and 5% respectively for Sydney climate.

Finally, this project also investigated the performance and design of two PV/T collectors: water PV/T collector and air PV/T collector as shown in chapter 5. These two collectors were compared to each other in terms of the electrical and thermal efficiencies, heat transfer, working fluid, and overall efficiency. Likewise, the water-based PV/T collector has better performance and overall efficiency than the air PV/T collector.

Chapter 7: Future Work

7.1 LCA and Solar Systems

In this project, the Life cycle assessment for both water type PV/T system and PV system was performed. As mentioned in chapter 3, the aim of that was to assess the environmental impacts of the two systems and to compare the results against each other. Also, the second aim was to predict the costs and future marketing of the system's components. However, it is possible to perform the LCA for other types of PV/T systems such as, air PV/T collectors, PV/T concentrator collectors, and water-air PV/T collectors in GABI software. Likewise, the LCA is also to be performed for other types of solar systems such as, the thermal systems for example, the solar evacuated tube collector and parabolic through collector. The benefit of performing the LCA for all these systems is to obtain its environmental impacts results and calculations throughout its life cycle from first phase (raw material acquisition) to the final phase (end of life of the system). The thermal system's components different from the PV/T system's components therefore, the result of environmental impacts and costs will be completely different.

7.2 Future Research and Solar PV/T System

As discussed in chapter 5, there are several methods to improve and develop the performance of solar hybrid PV/T system. For instance, increasing the overall efficiency by extracting the waste heat from the collector and cooling the PV panel by using appropriate working fluid with high heat conductivity and high density. Moreover, further research in this area need to be occurred in order to improve the performance and reduce the costs of the PV/T system. For example, one of the ways to reduce the costs of the PV/T system is to use the transparent amorphous silicone PV cells for the PV module. This type of solar hybrid PV/T system is very suitable for

consumers and users because the cost of this type of cells is low and cheaper than the monocrystalline silicon PV cells. However, large amounts of space are required to install the PV/T system when using this type of PV cells. Likewise, the overall efficiency of this system is approximately between 30 to 45%. Therefore, further research can be done on this particular system.

In addition, as was mentioned previously, the PV/T system produces both electricity and heat and this allows the system to have high exergy. Consequently, the total efficiency of this system will be higher than the photovoltaic system and the thermal system. Therefore, it is possible to study the exergy analysis of the solar hybrid PV/T system.

7.3 Final Words

In Australia and the world, the demand of energy in rising dramatically and the majority of people in Australia and in the world started to install the solar systems with output power between of 1000 and 1500 Wp. These systems are considered large and if the system is large it means that the system generates less GHG emissions than the small system. Therefore, further analysis is required in order to investigate the environmental impacts such as, the GHG emissions for large PV/T hybrid systems.

Chapter 8: Abbreviations

UN	United Nations
MTOE	Million Tones of Oil Equivalent
EIA	Energy Information Administration
BTU	British Thermal Units
PV	Photovoltaic
PV/T	Photovoltaic/ Thermal
LCA	Life Cycle Assessment
LCC	Life Cycle Cost
LCI	Life Cycle Inventory
LCIA	Life Cycle Inventory Assessment
KWP	Kilo Watt Peak
GHG	Green House Gases
GW	Giga Watt
IEN	International Energy Agency
MJ	Multi Junction
CPC	Compound Parabolic Collector
PUR	Polyurethane
PVF	Polyvinyl Fluoride
PPS	Polyphenylene Sulphide
İ	Irreversibility
MANIT	Maulana Azad National Institute of Technology
GABI	Ganzheitliche Bilanz (Holistic Balance)
PELD	Polyethylene Low Density Granulate
GWP	Global Warming Potential
CML	Chain Management Life Cycle Assessment
ODP	Ozone Depletion Potential
CFC 11	Trichlorofluoromethane
R 11	Trichlorofluoromethane

|	
UV	Ultraviolet
HTP	Human Toxicity Potential
TRI	Toxic Release Inventory
CTUH	Comparative Toxic Units for Human
U235	Uranium-235
VOC	Volatile Organic Components
NMVOC	Non Methanic Volatile Organic Components
AP	Acidification Potential
EP	Eutrophication Potential
STC	Standard Temperature Conditions
3D	Three-Dimensional
LPM	Liters Per Minute
NREL	National Renewable Energy Lab
BMW	Bayerische Motoren Werke (Bavarian Motor Works)
NASA	National Aeronautic and Space Administration
DCB	Dichlorobenzene
POCP	Photochemical Ozone Creation Potential

Appendix A: Related Figures and Tables
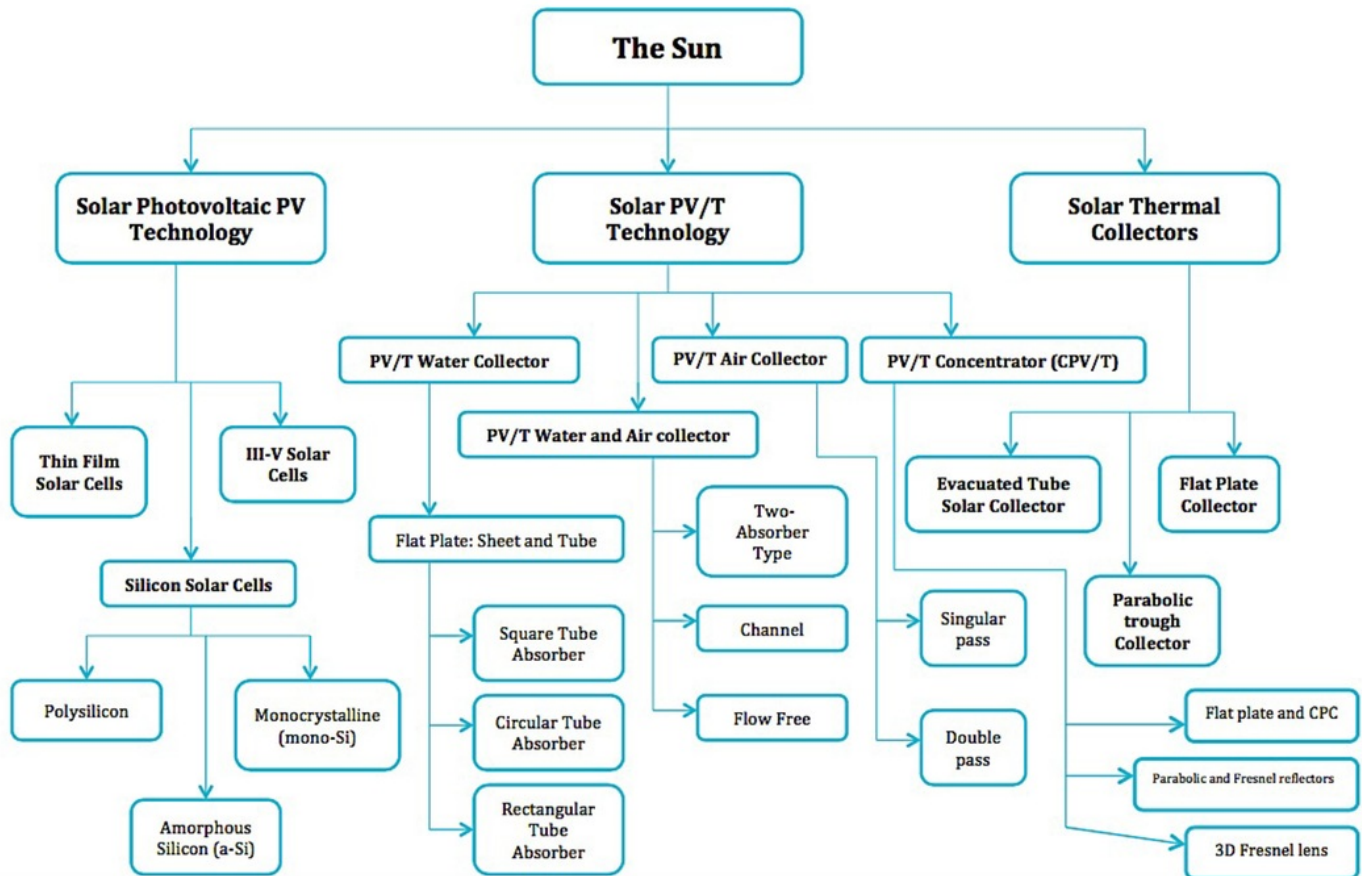
Figure 100: Classification of Solar Systems [24, 79, 101]

	Scenarios			
	Benchmark	Alternative 1	Alternative 2	Alternative 3
Flows	149	149	237	112
Emissions to Air	147	148	233	11
Emissions to Fresh Water	1.37	1.53	3.08	1.05
Emissions to Sea Water	0.119	0.21	0.232	0.304
Heavy Metals to Sea Water	0.0331	0.0581	0.0659	0.083
Inorganic Emissions to Sea Water	0.0785	0.139	0.151	0.201
Organic Emissions to Sea Water	0.0076	0.013	0.015	0.0197
Radioactive Emissions to Sea Water	0	0	0	0
Emissions to Agricultural Soil	0.00342	0.00348	0.00579	0.00266
Emissions to Industrial Soil	0.0002	0.000208	0.000154	0.000231

Table 42: Human Toxicity Potential of Solar PV/T System Flows Category [kg DCB Equiv.]

	Scenarios			
	Benchmark	Alternative 1	Alternative 2	Alternative 3
Flows	181	182	188	176
Emissions to Air	180	180	187	175
Emissions to Fresh Water	1	2	1	1
Emissions to Sea Water	0.04	0.072	0.077	0.109
Heavy Metals to Sea Water	0.0113	0.02	0.0214	0.03
Inorganic Emissions to Sea Water	0.0269	0.048	0.0513	0.0721
Organic Emissions to Sea Water	0.00264	0.0047	0.00502	0.00706
Radioactive Emissions to Sea Water	0	0	0	0
Emissions to Agricultural Soil	-0.00264	-0.00265	-0.00271	-0.00247
Emissions to Industrial Soil	0.000146	0.000146	0.000127	0.000164

Table 43: Human Toxicity Potential of Solar PV System Flows Category [kg DCB Equiv.]

	Scenarios			
	Benchmark	Alternative 1	Alternative 2	Alternative 3
Flows	0.0535	0.066	0.076	0.0751
Emissions to Air	0.0535	0.066	0.076	0.0751
Inorganic Emissions to Air	0.0382	0.0468	0.0547	0.0524
Organic Emissions to Air	0.0153	0.0192	0.0213	0.0227
Heavy Metals to Air	0	0	0	0

Table 44: POCP of Solar Hybrid PV/T System Flows Category [kg Ethene Equiv.]

	Scenarios			
	Benchmark	Alternative 1	Alternative 2	Alternative 3
Flows	0.039	0.0435	0.0445	0.0476
Emissions to Air	0.039	0.0435	0.0445	0.0476
Inorganic Emissions to Air	0.0291	0.0322	0.0329	0.0349
Organic Emissions to Air	0.00991	0.0113	0.0116	0.0127
Heavy Metals to Air	0	0	0	0
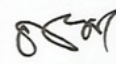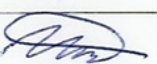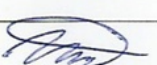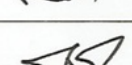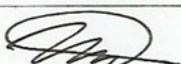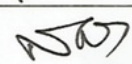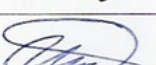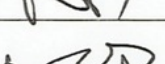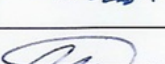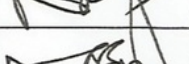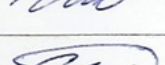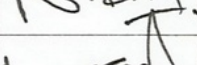
Table 45: POCP of Solar PV System Flows Category [kg Ethene Equiv.]

Appendix B: Project Plan and Attendance Form

Week	Date	Project Activity	Deliverables
Week 1 to Week 12	**31/7/2017 to 5/11/2017**	**Editing and Writing Project Document**	
Week 1	**31/7/2017 to 6/8/2017**	**Background Research**	
Week 1	**31/7/2017 to 6/8/2017**	**Literature Review**	
Week 2 to Second Week of Mid Semester Break	**7/8/2017 to 1/10/2017**	**LCA for Solar PV/T System**	
Week 2 to Week 4	7/8/2017 to 27/8/2017	System Inventory and Data Analysis	Results and calculations
Week 5 to Week 6	28/8/2017 to 10/9/2017	Results and Data From GABI Software	Results, data, tables, charts and diagrams
Week 5 to Week 7	28/8/2017 to 17/9/2017	Environmental Impact Assessment	Results, data, tables and charts
First Week of Mid Semester Break	18/9/2017 to 24/9/2017	LCA for PV System	Diagrams
Second Week of Mid Semester Break	25/9/2017 to 1/10/2017	Comparison Between PV/T and PV Systems	Results, data, tables and charts
Week 8 to Week 10	**2/10/2017 to 22/10/2017**	**Energy Modeling Investigation**	
Week 8	2/10/2017	Development of Solar Hybrid PV/T System	
Week 8	3/10/2017 to 8/10/2017	Mathematical Analysis of Thermal and Electrical Energy	Results and calculations
Week 9 to Week 10	9/10/2017 to 22/10/2017	Energy Modeling and TRNSYS Tool	Results, graphs and charts
Week 11	**23/11/2017 to 29/10/2017**	**Performance and Design of PV/T Collectors**	Results and tables
Week 12	**30/10/2017 to 5/11/2017**	**Finalise Thesis Document**	Final Report
Week 13 to Week 15	**6/11/2017 to 21/11/2017**	**Poster, Abstract and Presentation**	

Table 46: Project Schedule

Consultation Meetings Attendance Form

Week	Date	Comments (if applicable)	Student's Signature	Supervisor's Signature
2	8/8/2017	Gabi software and progress report		
3	15/8/2017	Gabi software and progress report		
4	22/8/2017	Gabi software and LCA analysis		
5	29/8/2017	Life cycle impact assessment of PV/T		
6	5/9/2017	Progress Report		
7	12/9/2017	Progress Report		
8	3/10/2017	Final Report		
9	10/10/2017	Final Report		
10	17/10/2017	Final Report		
11	24/10/2017	Final Report		
12	31/10/2017	Finalising final report		

136

List of References

1. Ortiz-Ospina, b.M.R.a.E. *World Population Growth*. 2017; Available from: https://ourworldindata.org/world-population-growth/.

2. *World energy demand and economic outlook*. U.S Energy Information Administration 2017.

3. Alex Chadwick, *National Science Foundation*. An Energy Journal 2012.

4. Chow, T., *A review on photovoltaic/thermal hybrid solar technology*. Applied Energy, 2010. 87(2): p. 365-379.

5. Besheer, A., Smyth, M., Zacharopoulos, A., Mondol, J., & Pugsley, A, *Review on recent approaches for hybrid PV/T solar technology*. International Journal of Energy Research, 2016. 40(15): p. 2038-2053.

6. Leon, N.D., *Design & fabrication of hybrid energy production system*. 2015.

7. *ECOLOGICAL LIFE CYCLE ASSESSMENT*, in *Life Cycle Engineering Experts GMBH*. 2006, LCEE: Germany. p. 16.

8. Ernesto Macías Galán, G.W., Yongping Zhai and Li Junfeng, *Global Status Report*. 2016, REN 21. p. 271.

9. Gaëtan Masson, M.B.a.R.H., *SNAPSHOT OF GLOBAL PHOTOVOLTAIC MARKETS*. 2016, IEA International Energy Agency.

10. Carlos A.F.Fernandes, J.P.N.T., P.J Costa Branco, *Cell string layout in solar photovoltaic collectors*. Energy Conversion and Management, 2017. 149: p. 997-1009.

11. Good, C., *Environmental impact assessments of hybrid photovoltaic–thermal (PV/T) systems – A review*. Renewable and Sustainable Energy Reviews, 2016. 55: p. 234-239.

12. Tripanagnostopoulos, Y., Souliotis, M., Battisti, R., & Corrado, A, *Energy, cost and LCA results of PV and hybrid PV/T solar systems*. Progress in Photovoltaics: Research and Applications, 2005. 13(3): p. 235-250.

13. Engin, D., & Çolak, M, *Modeling and performance optimization of photovoltaic and thermal collector hybrid system*. TURKISH JOURNAL OF ELECTRICAL ENGINEERING & COMPUTER SCIENCES, 2016. 24(5): p. 3524-3542.

14. Chao-Yang Huang, C.-J.H., *A study of photovoltaic thermal (PV/T) hybrid system with computer modeling*. International Journal of Smart Grid and Clean Energy. 195: p. 75-79.

15. S.S.S. Baljit, H.-Y.C., V.A.A Audwinto, S.A Hamid, Ahmad Fudholi, S.H Zaida, m.Y. Othman, K. Sopian, *Mathematical modelling of a dual-fluid concentrating photovoltaic-thermal (PV-T) solar collector*. Renewable Energy, 2017. 114: p. 1258-1271.

16. Abu Bakar, O., Hj Din, Manaf, & Jarimi. , *Design concept and mathematical model of a bi-fluid photovoltaic/thermal (PV/T) solar collector*. Renewable Energy, (2014. 67: p. 153-164.

17. Jin-Hee Kim, S.-H.P., and Jun-Tae Kim, *Experimental performance of a photovoltaic-thermal air collector*. Energy Procedia, 2014. 48: p. 888 - 894.

18. Sarhaddi, F., Ajam, Behzadmehr, & Mahdavi Adeli, *An improved thermal and electrical model for a solar photovoltaic thermal (PV/T) air collector*. Applied Energy, 2010. 87(7): p. 2328-2339.

19. Mtunzi, B., & Meyer, E, *Design and implementation of a directly cooled PV/T*. Journal of Engineering, Design and Technology, 2015. 13(3): p. 369-379.

20. Martin Treberspurg, M.D., BOKU Heimo Staller, *Photovoltaic/Thermal Systems (PV/T)*. 2011, SCI-Network, Sustainable Construction & Innovation through Procurement.

21. Robert A Taylor, T.O.a.G.R., *Nanofluid-based optical filter optimization for PV/T systems*. Light: Science & Applications 2012.

22. Eduardo F. Fernández, F.A., J.A. Ruiz-Arias, A. Soria-Moya *Analysis of the spectral variations on the performance of high concentrator photovoltaic modules operating under different real climate conditions*. 2014. 127: p. 179-187.

23. FabioFamoso, R.l., Simone Maeza and Pier Francesco Scandura, *Performance Comparison between Low Concentration Photovoltaic and Fixed Angle PV Systems*. Energy Procedia, 2015. 81: p. 516-525.

24. Ali H.A Al-Waeli, M.T.C., *Photovoltaic/Thermal (PV/T) systems: Status and future prospects* Renewable and Sustainable Energy Reviews, 2017. 77: p. 109 - 130.

25. Niels Jungbluth, M.S., Karin Flury, Rolf Frischknecht, Sybille Büsser, *Life Cycle Inventories of Photovoltaics.* 2012, Swiss Federal Office of Energy SFOE.

26. Höök, S.D.a.M., *Material requirements and availability for multi-terawatt deployment of photovoltaics.* Energy Policy, 2017. 108: p. 574-582.

27. *Weight of UIP Polyurethane Insulation.* 2017; Available from: http://www.urecon.com/documents/documents_weight.html.

28. Witoon Chingtuaythong, P.P., Chinaruk Thianpong, Monsak Pimsarn, *Heat transfer characterization in a tubular heat exchanger with V-shaped rings.* Heat transfer characterization in a tubular heat exchanger with V-shaped rings, 2017. 110: p. 1164-1171.

29. Tripanagnostopoulos, Y., Tzavellas, D., Zoulia, I., Chortatou, M, *Hybrid PV/T systems with dual heat extraction operation.* 2001, Berlin, Germany: ResearchGate.

30. Moradi, A.E., & Lin. , *A review of PV/T technologies: Effects of control parameters.* International Journal of Heat and Mass Transfer, 2013. 64: p. 483-500.

31. Ban-Weiss, W., Delp, Ly, Akbari, & Levinson. , *Electricity production and cooling energy savings from installation of a building-integrated photovoltaic roof on an office building.* Energy & Buildings, 2013. 56(210-220).

32. Carnevale, L., & Zanchi. , *Life Cycle Assessment of solar energy systems: Comparison of photovoltaic and water thermal heater at domestic scale.* Renewable Energy, 2014. 77: p. 434-446.

33. Dubey, S., & Seshadri, *Temperature Dependent Photovoltaic (PV) Efficiency and Its Effect on PV Production in the World – A Review. .* Energy Procedia, 2013. 33: p. 311-321.

34. Hassani, S., Mekhilef, & Taylor, *Environmental and exergy benefit of nanofluid-based hybrid PV/T systems.* Energy Conversion and Management, 2016. 123: p. 431-444.

35. Sobhnamayan, S., Alavi, Farahat, & Yazdanpanahi, *Optimization of a solar photovoltaic thermal (PV/T) water collector based on exergy concept.* Renewable Energy. 68: p. 356-365.

36. Herrando, M., & Hellgardt. , *A UK-based assessment of hybrid PV and solar-thermal systems for domestic heating and power: System performance.* Applied Energy, 2014. 122: p. 288-309.

37. Othman, I., Jin, Ruslan, Sopian, & Othman, Mohd, *Photovoltaic-thermal (PV/T) technology a The future energy technology.* Renewable Energy, 2013. 49: p. 171-174.

38. Rawat, P., Debbarma, M., Mehrotra, S., & K. S, *DESIGN, DEVELOPMENT AND EXPERIMENTAL INVESTIGATION OF SOLAR PHOTOVOLTAIC/THERMAL (PV/T) WATER COLLECTOR SYSTEM.* Renewable Energy, 2016. 154.

39. Zhang, Z., Smith, Xu, & Yu. , *Review of R&D progress and practical application of the solar photovoltaic/thermal (PV/T) technologies.* Renewable and Sustainable Energy Reviews, Renewable and Sustainable Energy Reviews., 2011.

40. Zogou, O., & Stapountzis, Herricos, *Flow and heat transfer inside a PV/T collector for building application.* Applied Energy, 2012. 91(1): p. 103-115.

41. Yin, H., Yang, D., Kelly, G., & Garant, J, *Design and performance of a novel building integrated PV/thermal system for energy efficiency of buildings.* Solar Energy, 2013. 87: p. 184-195.

42. *Gabi Software.* 2017 [cited 2017; Available from: http://www.gabi-software.com/international/support/gabi-learning-center/gabi-6-learning-center/part-1-lca-and-introduction-to-gabi/.

43. Haloui, T., Zaabat, Hocine, & Khelifa., *The Copper Indium Selenium (CuInSe2) thin Films Solar Cells for Hybrid Photovoltaic Thermal Collectors (PVT).* Energy Procedia, 2015. 74: p. 1213-1219.

44. *Brining renewable technology down to earth!* Solar Direct 2016; Available from: http://www.solardirect.com/pv/systems/systems.htm.

45. *Rainbow Power Company.* 2017; Available from: http://www.rpc.com.au/catalog/solar-panels-sale-c-2_260.html.

46.   *Panel   Specification.*   2017;   Available   from: http://site.dyd.com.ph/main/3000/index.asp?pageid=131313&t=panel-specification.

47.   *Aluminium   Org.*   2016;   Available   from: http://www.aluminum.org/industries/production

48.   Thomas R. Karl, A.A., Boyin Huang, Jay H. Lawrimore, James R. McMahon, Matthew J. Menne, *Possible artifacts of data biases in the recent global surface warming hiatus.* Science Journal, 2015. 384(6242): p. 1469 - 1472.

49.   Aditya Akundi, *GREEN ENERGY MANUFACTURING CLASS.* 2013, UNIVERSITY OF TEXAS, EL PASO.

50.   L., D.A.F.C.H.H.a.D., *Ozone Depletion Potentials.* Ozone Depletion Potentials: p. 299-377.

51.   Edgar G. Hertwich, S.F.M., William S. Pease, homas E. McKone, *Human toxicity potentials for life-cycle assessment and toxics release inventory risk screening.* Enviromental toxicology and chemistry, 2001. 20: p. 928-939.

52.   *Ionizing radiation, health effects and protective measures.* 2016.

53.   Eric Labouze Cécile Honoré, L.M., Bénédicte Couffignal, Matthias Beekmann., *Photochemical ozone creation potentials.* The International Journal of Life Cycle Assessment, 2004. 9: p. 187-195.

54.   Heijungs, R., *Environmental Life Cycle Assessment of Products.* Guide, Ed. CML (Center of Environmental Science), 1992.

55.   Pidwirny, M., *"Acid Precipitation".* Fundamentals of Physical Geography, 2nd Edition. 2006.

56.   Smith, R., *Cemical Process, Design and Integration.* Second Edition ed. 2016, United Kingdom: School of Chemical Engineering and Analytical Science, The University of Manchester

57.   *Agriculture: Nutrient Management and Fertilizer.* 2017   [cited 2017 5 September]; Available from: EPA.gov.

58.   Kümmel, K.a. *POLLUTION CATEGORIES - Eutrophication Potential – "Overfertilization".* 1999; Available from: http://www.stiftung-mehrweg.de/calculator/PollutionCategoryDescription_en.html.

59. *Eutrophication* 2013 [cited 2017; Available from: https://www.sciencelearn.org.nz/system/images/images/000/001/023/full/Eutrophication20160428-23313-1cf3q9o.jpg?1461804920.

60. David L. Correll, J.E.a.Q.U., *The Role of Phosphorus in the Eutrophication of Receiving Waters: A Review*. PHOSPHORUS ROLE IN THE EUTROPHICATION OF RECEIVING WATERS, 1998. 27: p. 261 - 266.

61. Truhaut, R., *Ecotoxicology: Objectives, principles and perspectives*. Ecotoxicology and Environmental Safety, 1977. 1(2): p. 151 -173.

62. *Kuwait battles oil spill in Persian Gulf waters*. 2017; Available from: http://www.cbc.ca/news/world/kuwait-battles-oil-spill-in-persian-gulf-waters-1.4245702.

63. Rush, J. *Australia oil spill: 'dolphins, emaciated and starving, unable to feed in the toxic waters'*. 2009 [cited 2017].

64. Birol, F., *Key World Energy Statistics*. 2017, International Energy Agency.

65. Huijbregts, M.A.J., *Periority Assessment of Toxic Substances in the frame of LCA*. 1999, Interfaculty Department of Environmental Science, Faculty of Enviromental Sciences, University of Amsterdam: Netherlands.

66. Raghuraman, P., *Analytical prediction of liquid photovoltaic/thermal flat-plate collector performance*. DOE COO-4094-66, 1979.

67. Alsema E.A., F.P., Kato K., *Energy payback time of photovoltaic energy systems:*

Present status and prospects. Solar Energy Convers, 1998: p. 2125-2130.

68. Alsema, E., *V-2 – Energy Pay-Back Time and CO2 Emissions of PV Systems*. 2003.

69. Gangwar S., B.D., & Biswas A, *Cost, reliability, and sensitivity of a stand-alone hybrid renewable energy system—A case study on a lecture building with low load factor*. Journal of Renewable and Sustainable Energy, 2015. 7(1).

70. Bergene T., a.L.O.M., *Model calculations on a flat-plate solar heat collector with integrated solar cells*. Solar Energy 1995. 55: p. 453-462.

71. Brogren M., K.B., Werner A. and Roos A., *Design and evaluation of low concentrating, stationary, parabolic reflectors for wall-integration of water-*

cooled photovoltaic-thermal hybrid modules. In Proc. Int. Conf, 2002: p. 551-555.

72. Treacy, M. *Liquid-to-Solid Material Leads to Cheaper, More Environmentally-Friendly Solar Cell.* 2012 [cited 2017.

73. Karlsson B., B.M.L.S., Svensson L., Hellstrom B. and Sarif Y., *A large bifacial photovoltaic-thermal low-concentrating module.* Photov. Solar Energy Conference, 2001: p. 808-811.

74. AlBaali, A., *Improving the power of a solar panel by cooling and light concentrating.* Solar & Wind Technology, 1986. 3: p. 241-245.

75. Tripanagnostopoulos, Y., Souliotis, M., Battisti, R., and Corrado, A., *APPLICATION ASPECTS OF HYBRID PV/T SOLAR SYSTEMS.* 2003.

76. Adham Makki, S.O.a.H.S., *Advancements in hybrid photovoltaic systems for enhanced solar cells performance.* Renewable and Sustainable Energy Reviews, 2015. 41: p. 658-684.

77. Florschuetz, L.W., *Extension of the Hottel-Whillier model to the analysis of combined photovoltaic/thermal flat plate collectors.* Solar Energy, 1979. 22: p. 361-366.

78. *Solar Swimming Pool Heaters.* 2017; Available from: https://energy.gov/energysaver/solar-swimming-pool-heaters.

79. Adnan Ibrahim, M.Y.O., Mohd Hafidz Ruslan, Sohif Mat, Kamaruzzaman Sopian, *Recent advances in flat plate photovoltaic/thermal (PV/T) solar collectors.* Renewable and Sustainable Energy Reviews, 2011. 15: p. 352–365.

80. Struckmann, F., *Analysis of a Flat-plate Solar Collector.* 2008, Dept. of Energy Sciences, Faculty of Engineering, Lund University: Lund, Sweden. p. 4.

81. A.Weiss, C.C.S.a.T., *Design application of the Hottel-Whillier-Bliss equation.* Solar Energy, 1977. 19(2): p. 109 - 113.

82. D. Hendrie, S., *Evaluation of combined photovoltaic/thermal collectors.* 1979.

83. Theodore L. Bergman, A.S.L., Frank P. Incropera and David P. Dewitt, *Introduction To Heat Transfer.* Sixth Edition ed. 2011. 961.

84. *TRNSYS Software, Transient System Simulation Tool.* 2017 [cited 2017; Available from: http://www.trnsys.com.

85. Kalogirou, S., *Use of TRNSYS for modelling and simulation of a hybrid pv–thermal solar system for Cyprus.* Renewable Energy, 2001. 23(2): p. 247-260.

86. A. Frank Shi, A.F.a.A.N.P. *CHANGING THE TRNSYS FORTRAN DYNAMIC LINK LIBRARY AND USING TRNSYS OUTSIDE THE WINDOWS ENVIRONMENT.* 2017.

87. Kalogirou, S. *HYBRID PV/T SOLAR WATER HEATERS.* 2006; Available from: http://slideplayer.com/slide/5838286/.

88. Keilholz, N.B.a.W. *TRNSYS. Transient System Simulations.* 2004 [cited 2017; Available from: http://docplayer.net/30670867-Trnsys-transient-system-simulations.html.

89. Bilbao, J.I., *PHOTOVOLTAIC THERMAL WATER SYSTEMS*, in *School of Photovoltaic and Renewable Energy Engineering, Faculty of engineering.* 2012, The University of New South Wales: Australia. p. 86 - 110.

90. Bilbao, J., Sproul B, *ANALYSIS OF FLAT PLATE PHOTOVOLTAIC-THERMAL (PVT) MODELS.* 2012, School of Photovoltaic and Renewable Energy Engineering, University of New South Wales: Australia.

91. Akhtar, N.a.M., S. C., *Approximate Method For Computation of Glass Cover Temperature and Top Heat-Loss Coefficient of Solar Collectors with Single Glazing.* Solar Energy, 1999. 66(5): p. 349 -354.

92. Michael Keating, J.C., Sibylle Krieger, *Residential energy and water use in Sydney, the Blue Mountains and Illawarra.* 2007, Independent Pricing and Regulatory Tribunal of New South Wales: Australia.

93. *Energy Use in the Australian Residential Sector 1986 – 2020.* 2009, Department of the Environment, Water, Heritage and the Arts: Australia.

94. M.Petrakis, H.D.K., S.Lykoudis, A.D.Adamopoulos, P.Kassomenos, I.M.Michaelides, S.A.Kalogirou, G.Roditis, I.Chrysis and A.Hadjigianni, *Generation of a "typical meteorological year" for Nicosia, Cyprus.* Renewable Energy, 1998. 13(3): p. 381 - 388.

95. Bergene T, B.B., *Thermodynamic considerations concerning the efficiency and possible utilisation of combined quantum/thermal solar energy converters.* Proceedings of the ISES Solar World Congress, 1993. 4: p. 25 - 30.

96. Pierrick Haurant, C.M.n.z., Leon Gaillard, Patrick Dupeyrat, *A numerical model of a solar domestic hot water system integrating hybrid photovoltaic/thermal collectors.* Energy Procedia, 2015. 78: p. 1991 - 1997.

97. Huda, N., *Solar Hybrid PV/T System.* 2017, Nazmul Huda: Macquarie University, Sydney, Australia.

98. Ahmad Fudholi, K.S., Mohammad H. Yazdi, Mohd Hafidz Ruslan, and H.A.K. Adnan Ibrahim, *Performance analysis of photovoltaic thermal (PVT) water collectors.* Energy Conversion and Management, 2014. 78: p. 641 - 651.

99. K.Sopian, K.S.Y., H.T.Liu, S.Kakaç, T.N.Veziroglu, *Performance analysis of photovoltaic thermal air heaters.* Energy Conversion and Management, 1996. 37(11): p. 1657 - 1670.

100. Mohamed El Amine Slimani, M.A., Sofiane Bahria, IIdiko Kurucz and Rabah Sellami, *Study and modeling of energy performance of a hybrid photovoltaic/thermal solar collector: Configuration suitable for an indirect solar dryer.* Energy Conversion and Management, 2016. 125: p. 209 - 221.

101. V.V.Tyagi, S.C.K., S.K.Tyagi, *Advancement in solar photovoltaic/thermal (PV/T) hybrid collector technology.* Renewable and Sustainable Energy Reviews, 2012. 16(3): p. 1383 - 1398.